Appendix A. Photos from Jacobs Site Visit

Appendix A. Photos from Jacobs Site Visit

Picture A-1. Photographs of TSFs taken by Jacobs at site visit. Top – NTSF. Centre – STSF. Bottom – slump in embankment wall of NTSF.

Picture A-2. Photographs of VR8 vents taken by Jacobs at site visit

Picture A-3. Photograph showing undulating terrain to the northwest (foreground) and southeast (background) of Cadia, taken from Four Mile Creek Road 33.43372°S, 148.95607°E

Picture A-4. Photo of Ridgeway AWS taken during the Jacobs site visit.

Picture A-5. Photo of SLB AWS, in Zephyr (2022). This AWS could not be visited during the Jacobs site visit.

Picture A-6. Photo of Orange AQMS, taken by Jacobs.

Picture A-7. Photo of Bathurst AQMS, taken by Jacobs.

Picture A-8. Dust emissions from loading ore to stockpiles from conveyors.

Picture A-9. Dust emissions from vehicle carrying ore/rock on road near main stockpile.

Picture A-10. Water spray truck operating on road near main stockpile.

Appendix B. Vent Discharge Characteristics Sensitivity Testing

Appendix B. Vent Discharge Characteristics Sensitivity Testing

B.1 Model Options Tested

The various run options for the discharge characteristics from vents VR3A, VR5, VR7 and VR8 are shown in Table B-1. The stack parameters applied for each run are summarized in Table B-2. The vents were assumed to operate at constant flow and emission rate 24/7.

B.2 Model Results

The model results for each option are provided in the figures listed in the last column of Table B-1. The model results show the following:

1. Dispersion from all vents is moderately sensitive to the discharge temperature, with lower temperatures producing higher ground-level concentrations.

2. Dispersion from VR8 is slightly sensitive to inclusion of building downwash, with options using building downwash producing higher ground-level concentrations, but vents VR3A, VR5 and VR7 are insensitive to building downwash.

3. Dispersion from VR8 is slightly sensitive to defining the discharge as being from two vents, versus one vent with the diameter applied in TAS (2023a). Options using two vents produce higher ground-level concentrations than with one vent.

It is reiterated that the model results for VR8 are higher than is likely in reality due to the issues with measuring particulate concentrations in the discharge from VR8. However, the relative comparison between the options is still valid.

For vents VR3A, VR5 and VR7, the model results indicate the potential for 24-hour concentrations of 10 $\mu g/m^3$ impacting the Woodville monitor. Therefore, the ambient PM_{10} contribution from these three vents is not negligible. However, the discharge parameters and emission rates are based on only one round of testing in 2022. In addition, Jacobs is not aware of whether the emissions from vents VR3A, VR5 and VR7 suffer from the same measurement difficulties as VR8 which could reduce the potential impact from these sources.

Table B-1: Model runs for vent sensitivity tests (see Section Error! Reference source not found. **of main report for details)**

Run name	Source group	Results figure
Option 1 – Base case	VR3A, VR5 and VR7 VR8 (as one vent) All vents	Figure B-1(a) Figure B-1(b) Figure B-1(c)
Option 2 – Effect of splitting VR8 discharge into two vents	VR8 (as two vents)	Figure B-2
Option 3 – Effect of reducing discharge temperature	VR3A, VR5 and VR7 VR8 (as one vent) All vents	Figure B-3(a) Figure B-3(b) Figure B-3(c)
Option 4 – Effect of excluding building downwash	VR3A, VR5 and VR7 VR8 (as one vent) All vents	Figure B-4(a) Figure B-4(b) Figure B-4(c)

Table B-2. Vent flow rates and emission rates for models (blank cells = source not included in model run)

Vent	VR3A	VR5	VR7	VR8	
				Simulated as one combined vent	Per vent, simulated as two separate vents
All runs					
Flow rate, Sm^3/s	215	300	303	480	240
Vent equivalent diameter, m	5.0	5.4	6.2	10.2	5.3
PM_{10} emission rate, g/s	10.5	0.21	2.8	106	53
Run 1					
Flow rate, Am^3/s	265	365	370	581	
Temperature of discharge (K)	296.4	297.6	296.6	295.6	
Plume exit velocity, m/s	13.5	15.9	12.3	7.1	
Building downwash	Yes	Yes	Yes	Yes	
Run 2					
Flow rate, Am^3/s					290
Temperature of discharge (K)					295.6
Plume exit velocity, m/s					13.2
Building downwash					Yes
Run 3					
Flow rate, Am^3/s	259	356	362		285
Temperature of discharge (K)	290	290	290		290
Plume exit velocity, m/s	13.2	15.5	12.0		12.9
Building downwash	Yes	Yes	Yes		Yes
Run 4					
Flow rate, Am^3/s	259	356	362		285
Temperature of discharge (K)	290	290	290		290
Plume exit velocity, m/s	13.2	15.5	12.0		12.9
Building downwash	No	No	No		No

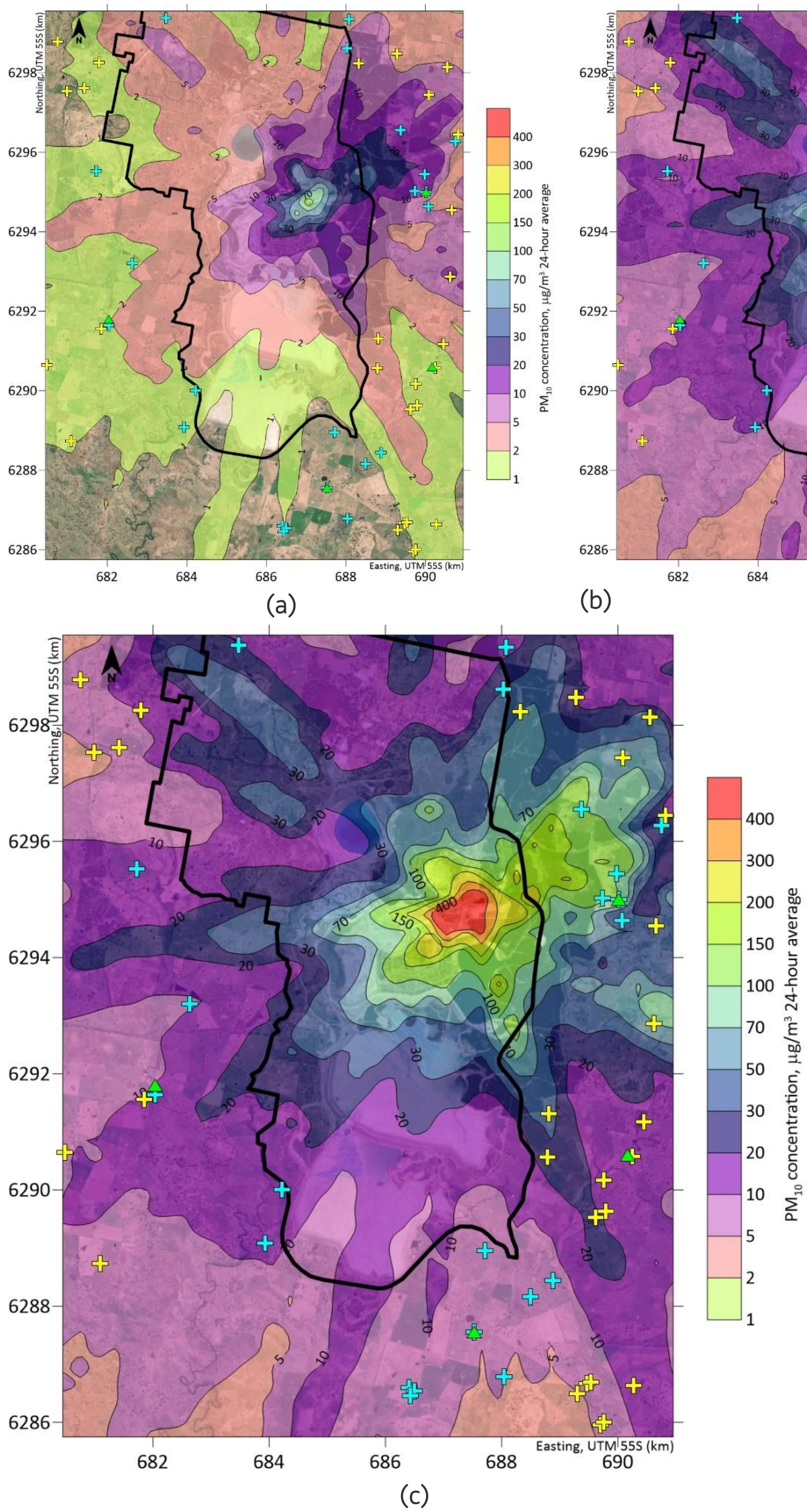

(a) VR3A, VR5 and VR7

(b) VR8

(c) All vents combined

Figure B-1: 24-hour average concentrations of PM_{10} due only to vent emissions, Option 1 Base Case.

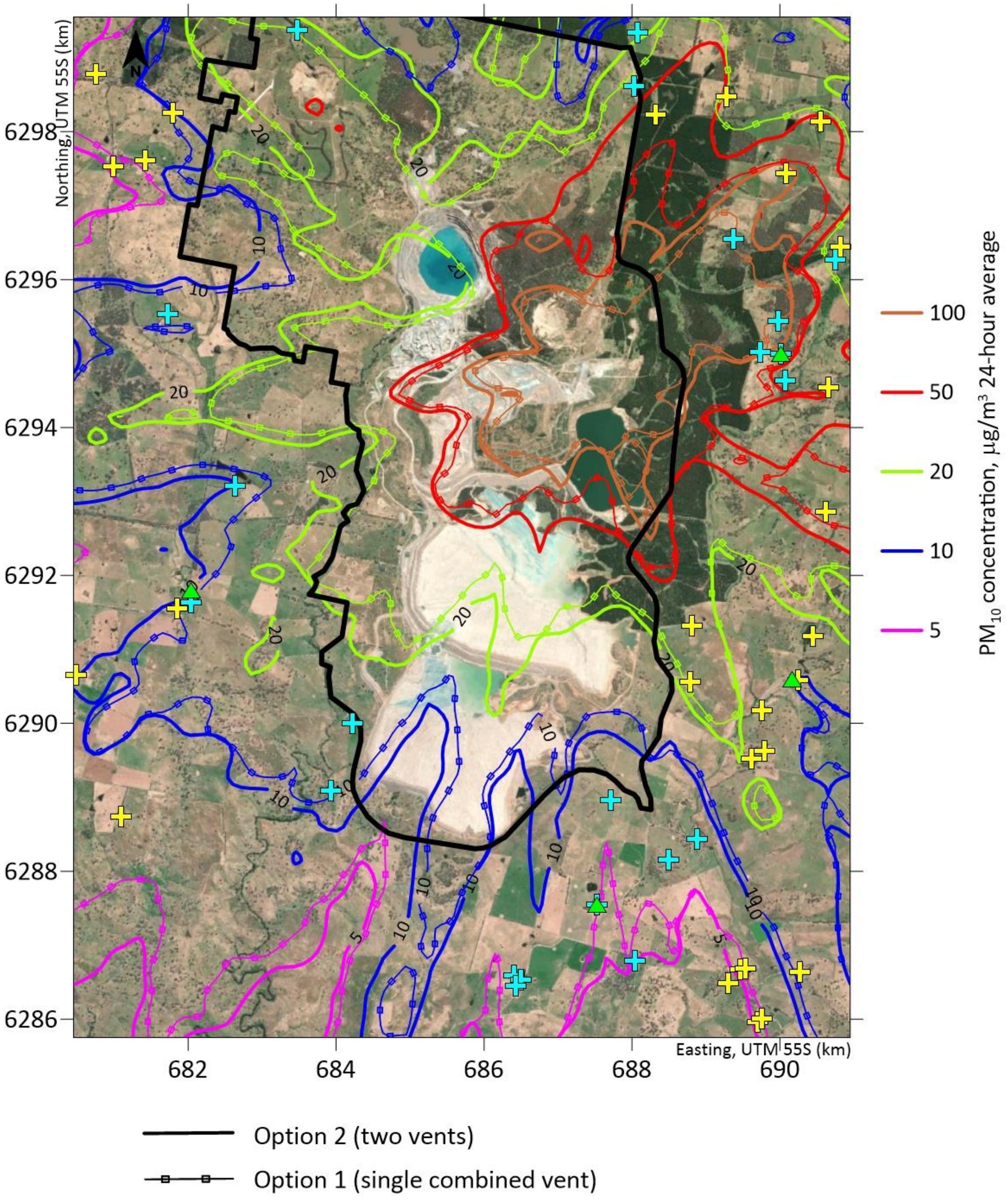

Figure B-2: 24-hour average concentrations of PM_{10} due only to vent emissions, comparing VR8 only for Option 1 versus Option 2 (modelling single combined vent versus two vents).

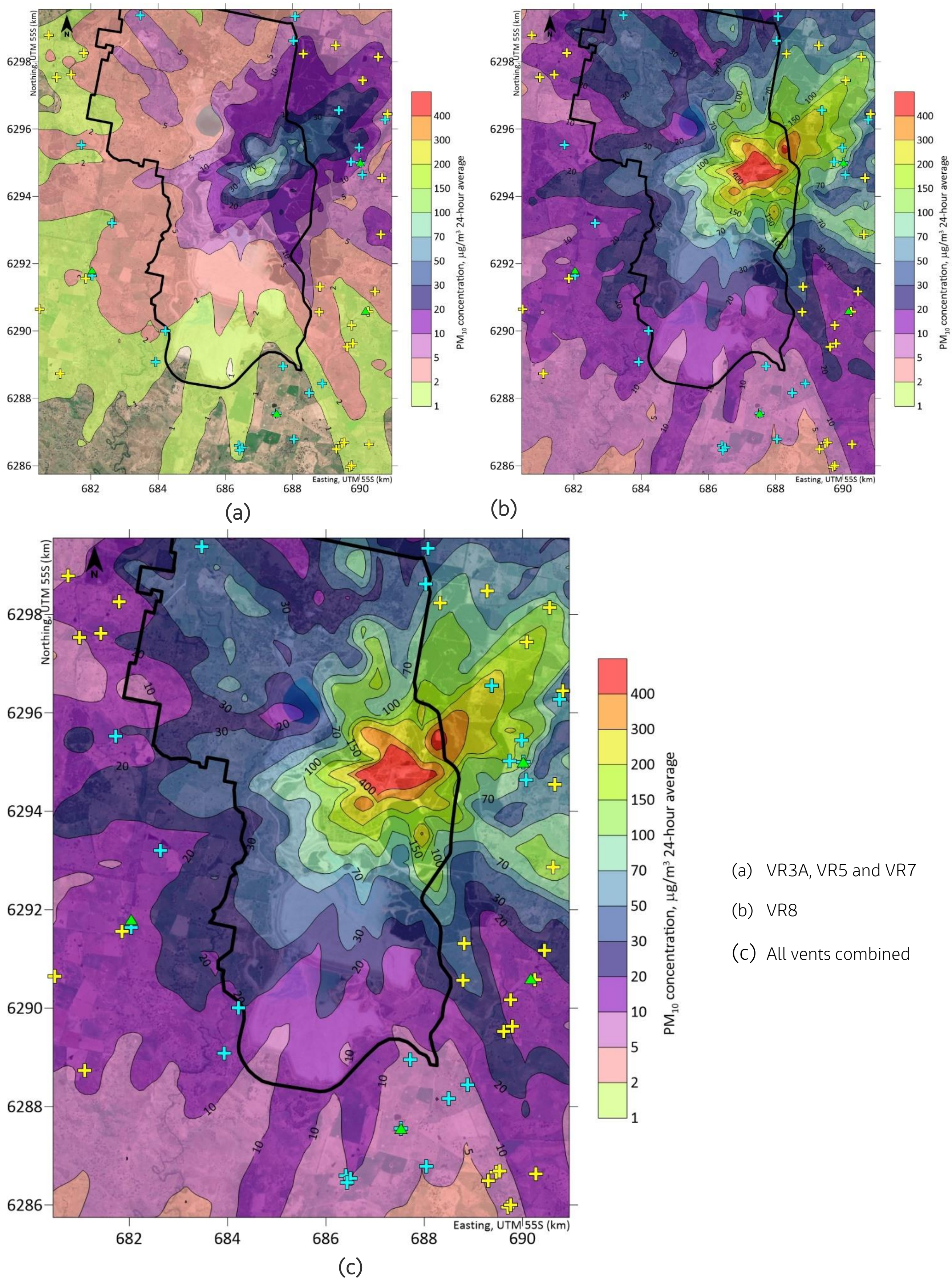

Figure B-3: 24-hour average concentrations of PM_{10} due only to vent emissions, Option 3 (effect of reducing discharge temperature).

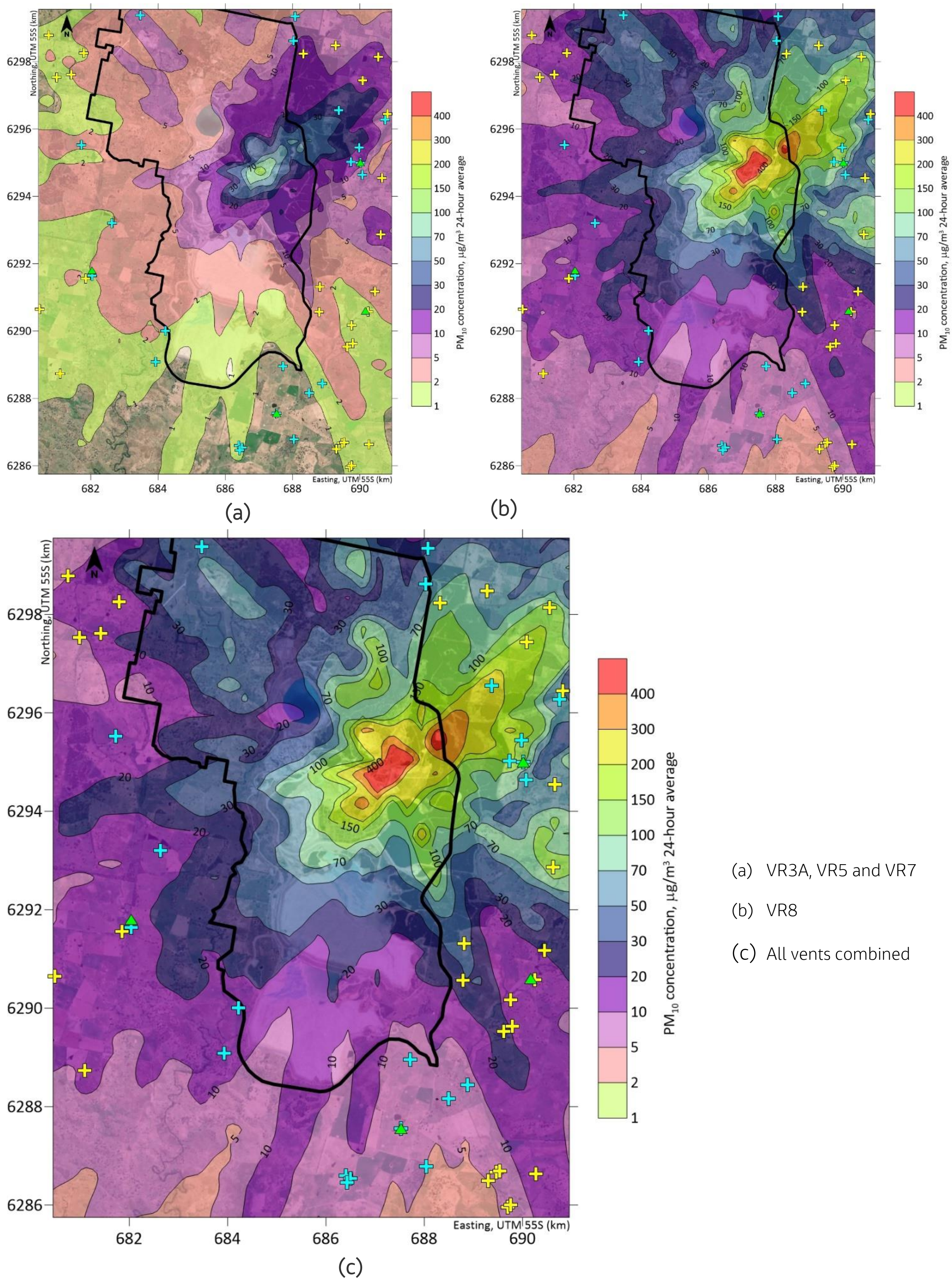

(a) VR3A, VR5 and VR7

(b) VR8

(c) All vents combined

Figure B-4: 24-hour average concentrations of PM$_{10}$ due only to vent emissions, Option 4 (effect of excluding building downwash).

Appendix C. Emission Sensitivity Testing – Crushing

Appendix C. Emission Sensitivity Testing – Crushing

C.1 Model Options and Results

The various sensitivity test runs for emissions from crushing activities are shown in Table C-1. These activities were assumed to operate 24/7.

The 24-hour PM_{10} concentrations for these test runs are displayed in the figures listed in Table C-1.

Table C-1. Model runs for crushing sensitivity tests

Run name	Results figure	Control efficiency	PM_{10} emission rate, kg/h
1. Base case	Figure C-1(a)	90%	5.07
2. Sensitivity test for EFs	Figure C-1(b)	90%	12.7
3. Sensitivity test for control efficiency	Figure C-1(c)	70%	15.2
4. Sensitivity test for both EFs and control efficiency	Figure C-1(d)	70%	38.0

The model results are moderately sensitive to the EFs and assumed control efficiency, with the predicted maximum 24-hour average PM_{10} at Woodville varying between 1.5 and 10 µg/m^3, and varying between 0.3 and 2.5 µg/m^{3}at Meribah.

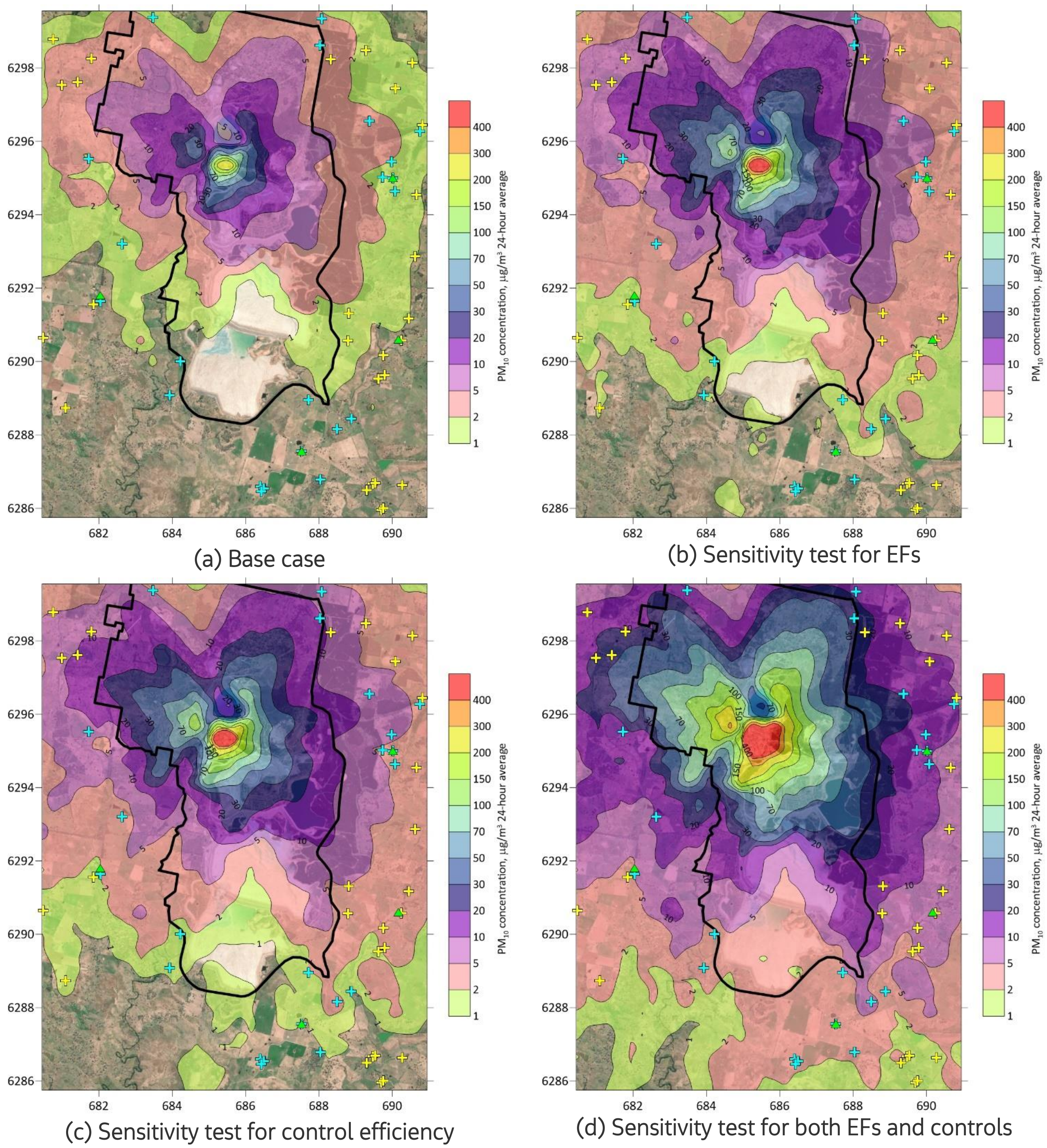

Figure C-1: 24-hour average concentrations of PM_{10} due to crushing emissions.

Appendix D. Emission Sensitivity Testing – Loading and Handling

Appendix D. Emission Sensitivity Testing – Loading and Handling

D.1 Model Options Tested

The various sensitivity test runs for emissions from loading and handling activities are shown in Table D-1. Short-haul and continuous activities were assumed to operate 24/7. Long haul handling activities were assumed to operation 11/7.

This activity group includes both batch loading activities and continuous loading activities as described in Section 4.3.5 of the main report. For the sensitivity testing, the "ore processing in mill" activity is excluded from the loading and handling emission inventory because the basis for definition of this source is unclear and the emission rates are very large relative to the other loading and handling sources. The model results for that source alone are provided in Appendix E instead.

Table D-1. Model runs for loading and handling sensitivity tests

Run name	Results figure	Description	Total PM_{10} emission rate (kg/h)	
			Day hours	Night hours
1. Base case	Figure D-1(a)	As TAS (2023) emission factor basis and activity intensity rates	2.60	0.78
2. Sensitivity test (i) for EFs	Figure D-1(b)	Sensitivity test for EFs from Equation 1, include activity of loading ore to and from main COS and storage location	7.20	4.43
3. Sensitivity test (ii) for EFs	Figure D-1(c)	NPI emission factors for batch loading operations, include activity of loading ore to and from main COS and storage location	49.5	16.1
4. Sensitivity test (iii) for EFs	Figure D-1(d)	NPI emission factors for handling low moisture content ore from metalliferous mines, include activity of loading ore to and from main COS and storage location	222	189
5. Sensitivity test for hour-by-hour wind speed adjustment	Figure D-2	Sensitivity test for hour-by-hour variation of emission rate with wind speed, with moisture content and activity rates as Option 2	Varies by hour	Varies by hour

D.2 Model Results

The 24-hour PM_{10} concentrations for these test runs are displayed in the following figures as listed in Table D-1. Figure D-1 compares the model results for Runs 1-4, and Figure D-2 compares the model results for Run 2 and 5 (ie. the effect of allowing for wind dependence in emission rate).

The following observations are noted from the model results:

1. Applying the NPI EFs for handling low moisture content ore from metalliferous mines (Sensitivity test (iii)) results in high PM_{10} concentrations at the Cadia monitoring sites that are not reflected in the monitoring data, therefore is it likely that these emission factors are too high for the Cadia ore.

2. The calculation of emissions from loading and handling requires several assumptions about activity rates, hours of operation, and emission factors. Looking at the remaining three options in Figures D-1 (a) to (c), the model results outside the mining lease boundary are highly sensitive to the EF assumptions.

3. Finally, comparison of Figure D-2 (a) and (b) clearly shows the reduction in model results when wind-speed dependence is taken into account, and this may be an improvement over using a constant emission rate.

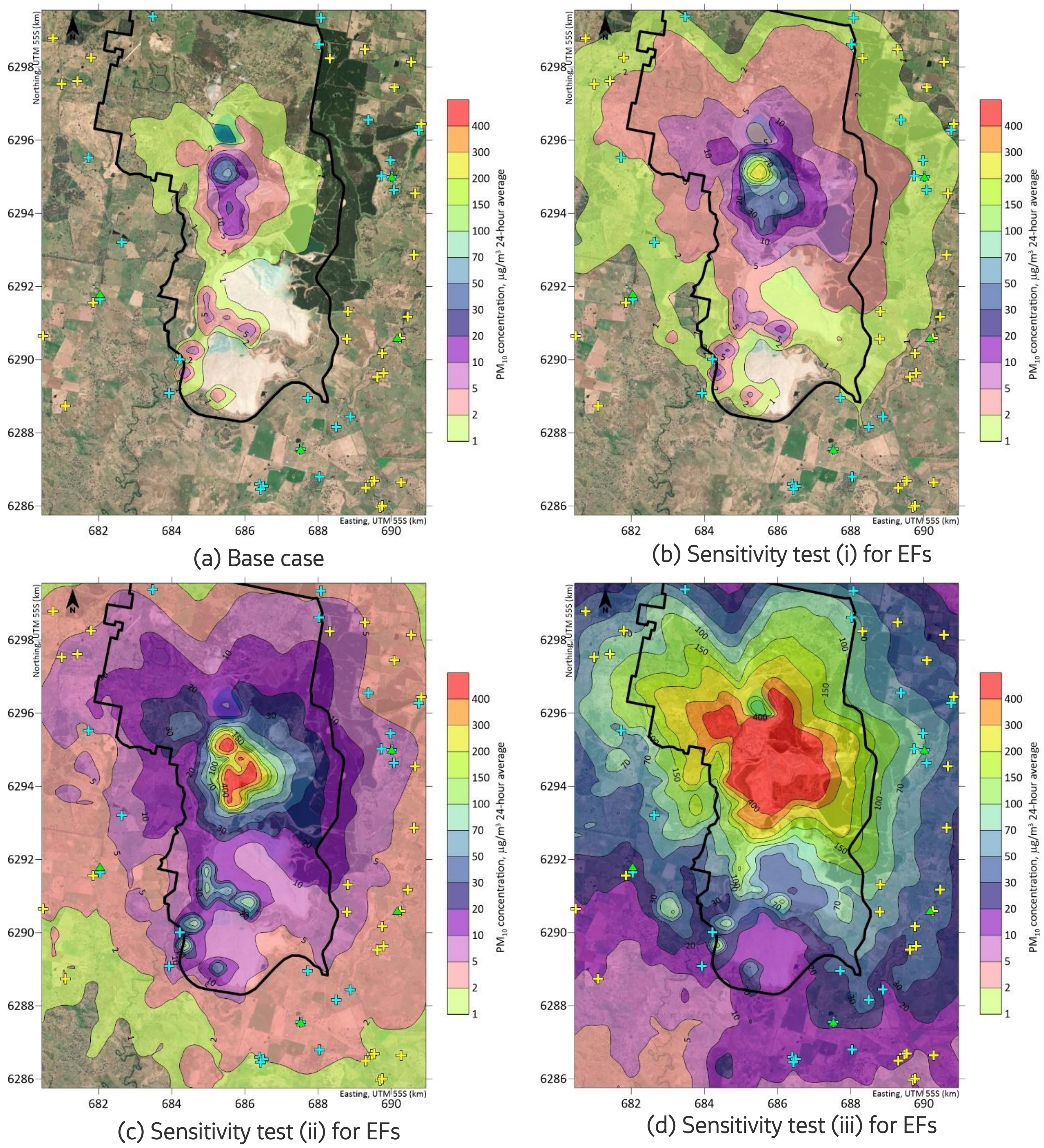

Figure D-1: 24-hour average concentrations of PM$_{10}$ due to loading and handling emissions.

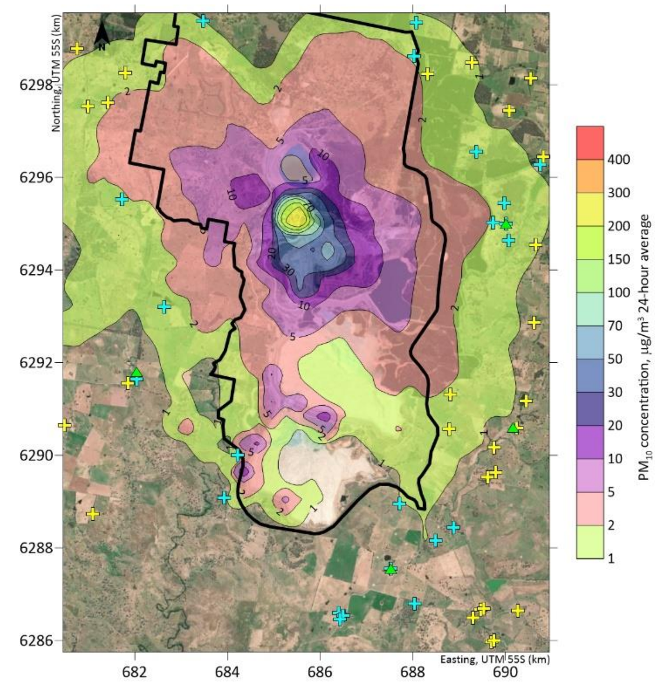

(a) Sensitivity test (i) for EFs (as Figure D-2(b))

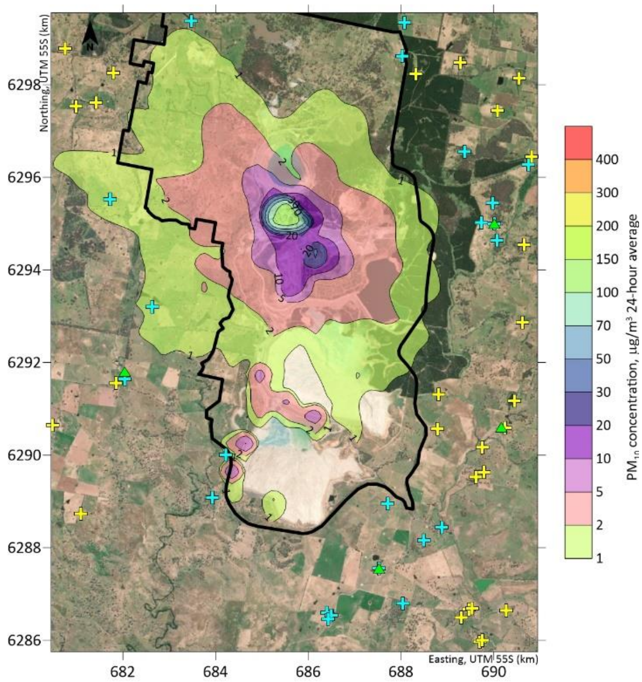

(b) Sensitivity test for EF wind dependence

Figure D-2: 24-hour average concentrations of PM_{10} due to loading and handling emissions.

Appendix E. Emission Sensitivity Testing – Ore processing in mill

Appendix E. Emission Sensitivity Testing – Ore processing in mill

E.1 Model Options Tested

The various sensitivity test runs for emissions from the "ore processing in mine" activity are shown in Table E-1. The activity was assumed to operation 24/7.

Table E-1. Model runs for "ore processing in mill" activity

Run name	Results figure	Description	Total PM_{10} emission rate (kg/h)
1. Base case	Figure E-1(a)	As TAS (2023) emission factor basis and activity intensity rates	7.91
2. Sensitivity test (i) for EFs	Figure E-1(b)	Sensitivity test for EFs from Equation 1	12.1
3. Sensitivity test (ii) for EFs	Figure E-1(c)	NPI emission factors for handling low moisture content ore from metalliferous mines	514

E.2 Model Results

The 24-hour PM_{10} concentrations for these test runs are displayed in the following figures as listed in Table E-1.

As found with the loading and handling sources, applying the NPI emission factors for handling low moisture content ore from metalliferous mines (Sensitivity test (ii)) results in high PM_{10} concentrations at the Cadia monitoring sites that are not reflected in the monitoring data, therefore is it likely that these emission factors are too high for the Cadia ore.

Looking at the remaining two options in Figures E-1 (a) to (b), the model results outside the mining lease boundary in the vicinity of sensitive receptors are not particularly sensitive to the EF assumptions.

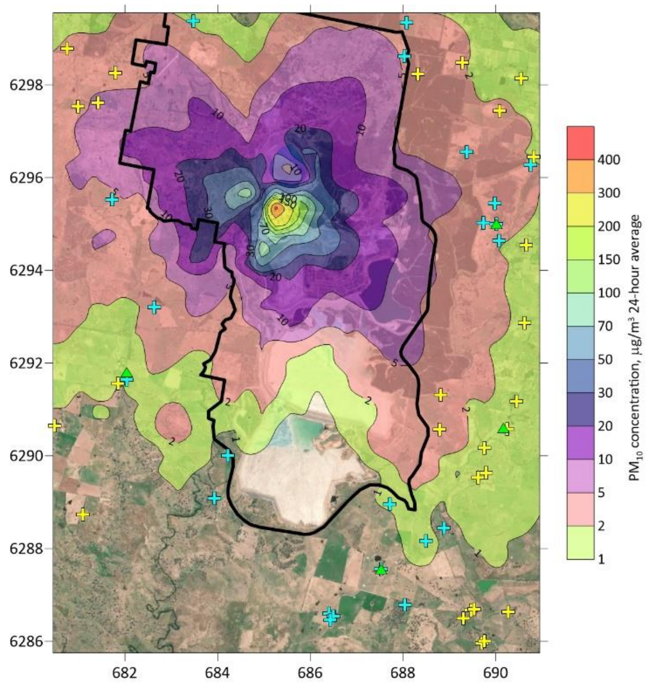

(a) Base case

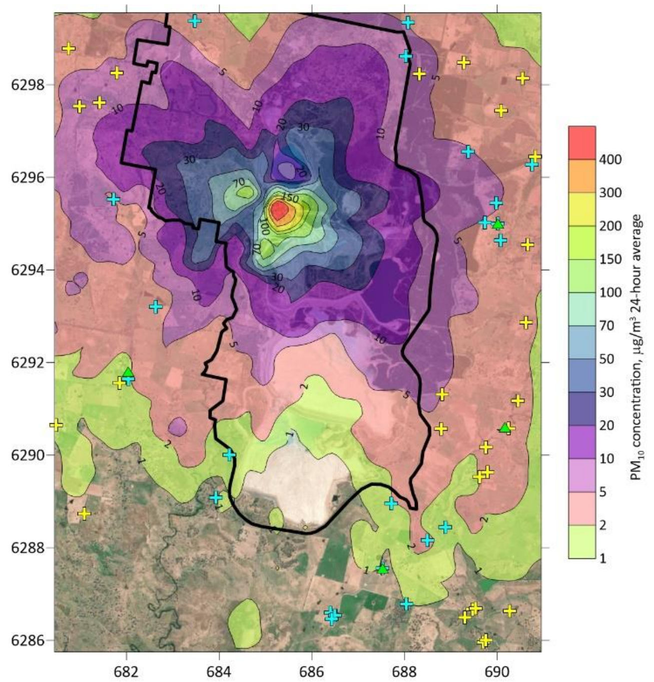

(b) Sensitivity test (i) for EFs

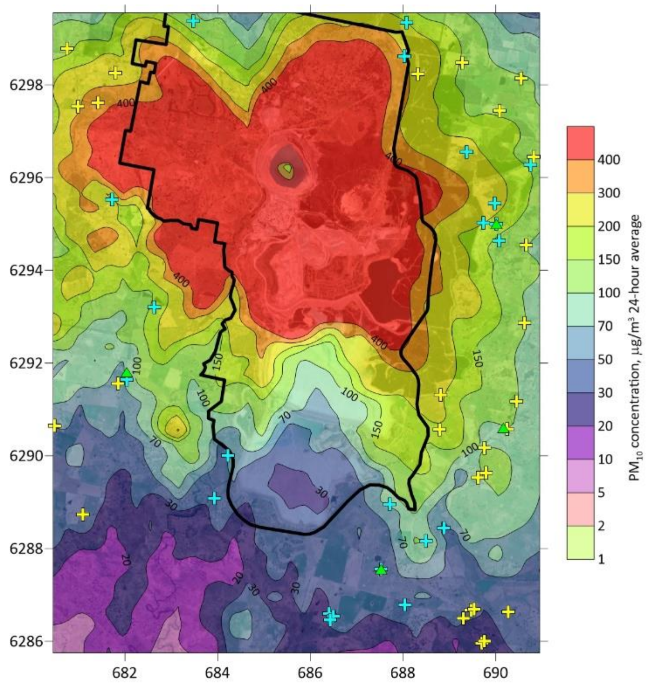

(c) Sensitivity test (ii) for EFs

Figure E-1: 24-hour average concentrations of PM_{10} due to “ore processing in mill” emissions.

Appendix F. Emission Sensitivity Testing - Bulldozers

Appendix F. Emission Sensitivity Testing - Bulldozers

F.1 Model Options Tested

Figure F-1(a) compares the dispersion results for the bulldozer emissions base case with the characterization of sources as either area sources or volume sources for haul roads. The dispersion results are very similar, with the haul road volume sources option generating slightly higher concentrations. The haul road volume sources option was also easier to set up and change emission rates, although it does require longer running times. Jacobs used the volume sources option for all "general and construction" bulldozer emission modelling in this report.

Two additional emission options were tested for the bulldozing activity, as shown in Table F-1. Bulldozers were assumed to operate only during day hours of 7am to 6pm.

The 24-hour PM_{10} concentrations for emissions from the bulldozing activity at the mine are displayed in Appendix F for the two run options shown in Table F-1.

Table F-1. Model runs for bulldozer sensitivity tests

Run name	Results figure	Source group	PM_{10} emission rate (kg/h) (day hours only)
Option 1 – Base case	Figure F-1(b)	Waste dump area General and construction	0.85 63.9
Option 2 – EF Sensitivity Test	Figure F-1(C)	Waste dump area General and construction	1.59 119.1

F.2 Model Results

The 24-hour PM_{10} concentrations for these test runs are displayed in the following figures as listed in Table F-1.

The model results show that ambient air quality concentrations of PM_{10} are moderately sensitive to the emission factor for bulldozing.

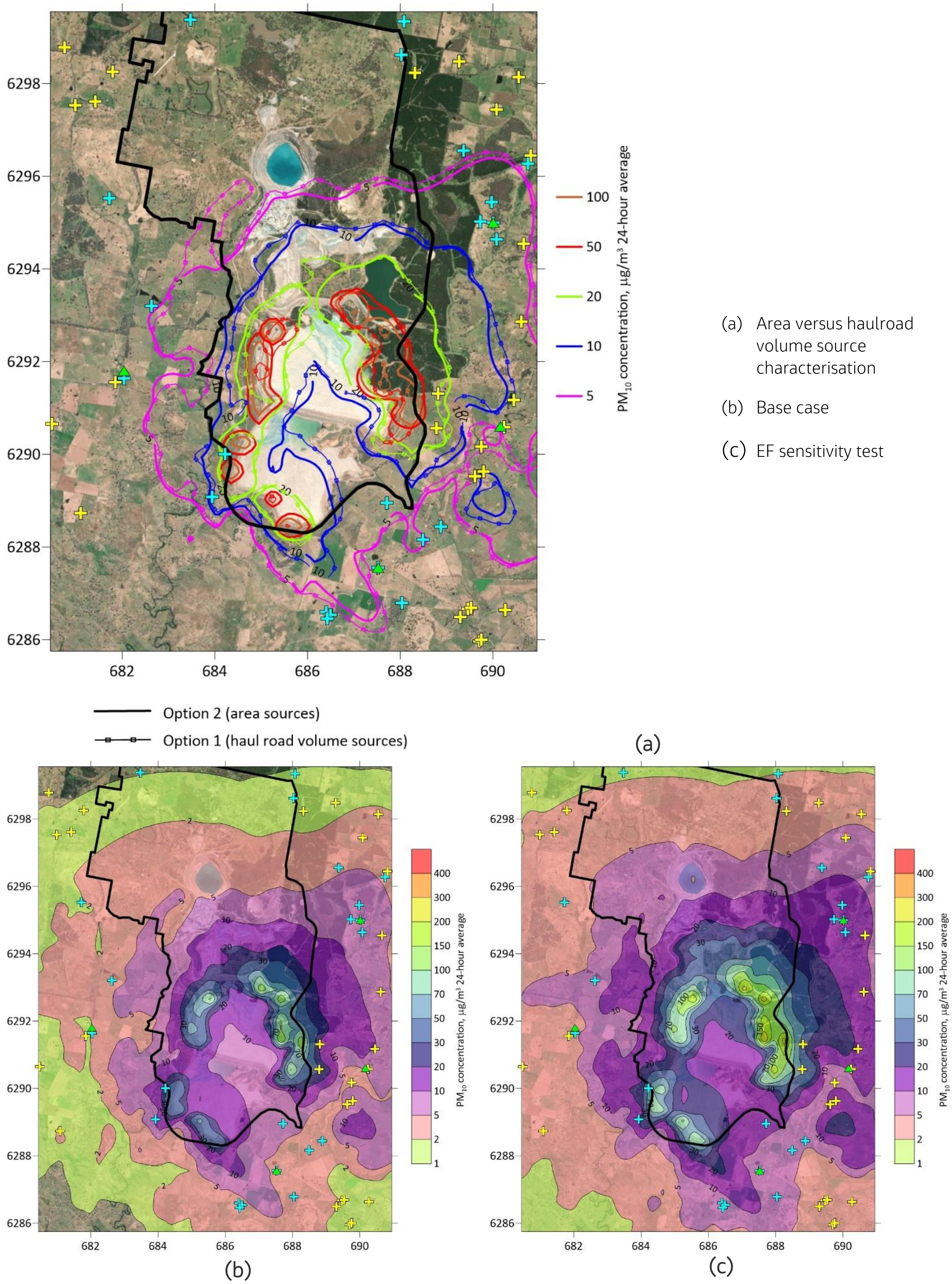

Figure F-1: 24-hour average concentrations of PM_{10} due only to bulldozer emissions.

Appendix G. Emission Sensitivity Testing - Graders

Appendix G. Emission Sensitivity Testing - Graders

G.1 Model Options Tested

The various sensitivity test runs for emissions from the grader activity are shown in Table G-1. The activity was assumed to operate only during day hours of 7am to 6pm.

Table G-1. Model runs for grader sensitivity tests

Run name	Results figure	PM_{10} emission rate (kg/h) (day hours only)
Option 1 – Base case	Figure G-1(a)	0.8
Option 2 – EF Sensitivity Test	Figure G-1(b)	4.3

G.2 Model Results

The 24-hour PM_{10} concentrations for these test runs are displayed in the following figures as listed in Table G-1.

The model results for the grader emissions indicate low concentrations beyond the mining lease boundary, to the extent that the results are insensitive to the selection of emission factors.

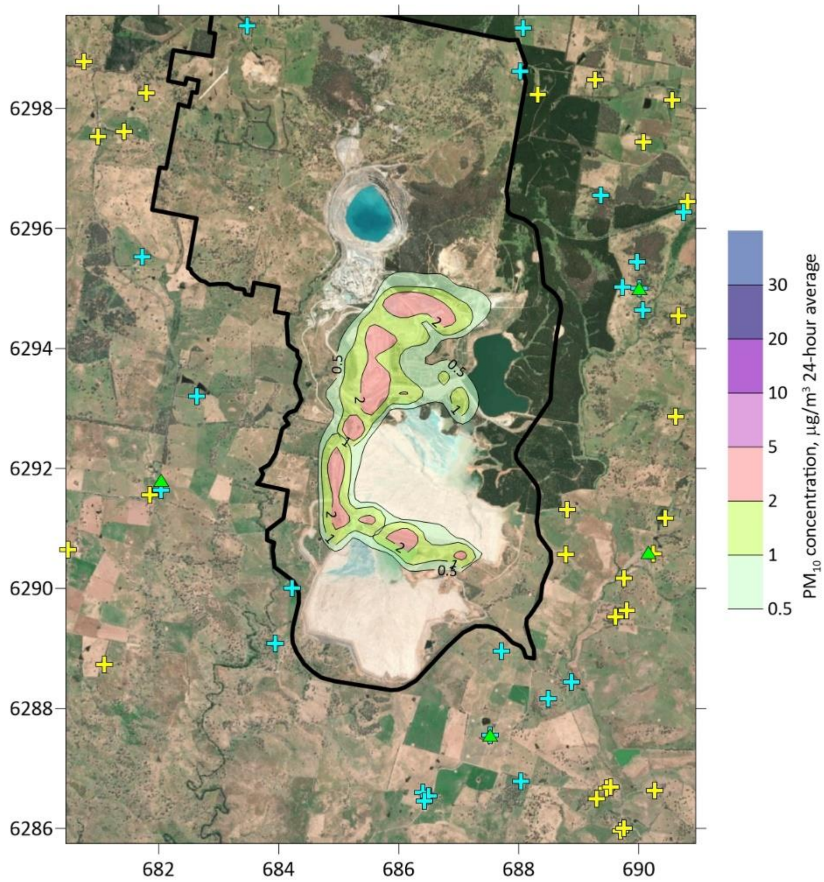

(a) Base case

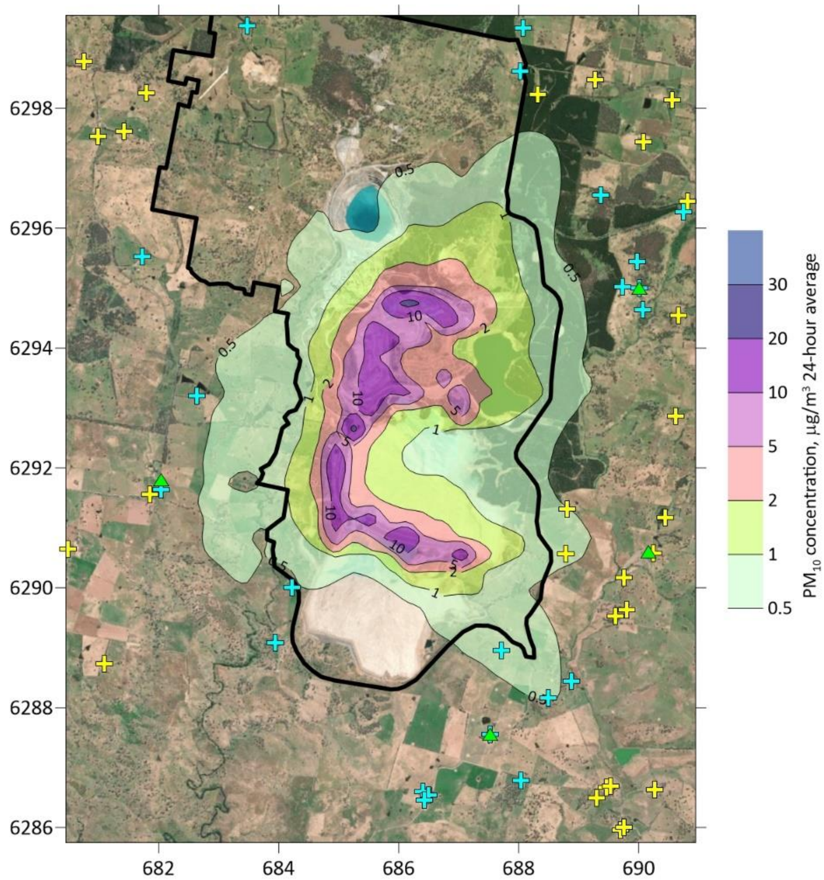

(b) EF sensitivity test

Figure G-1: 24-hour average concentrations of PM_{10} due only to grader emissions.

Appendix H. Emission Sensitivity Testing – Vehicle-Tracked Dust

Appendix H. Emission Sensitivity Testing – Vehicle-Tracked Dust

H.1 Model Options Tested

The various sensitivity test runs for emissions from vehicles driving on the short haul and long haul routes moving waste, aggregate and ore at the mine are shown in Table H-1. This activity group includes:

- Long-haul route for tailings construction (operating 11/7)
- Short-haul route to waste emplacement (operating 24/7)
- Short-haul route for transferring ore to and from COS stockpiles (operating 24/7)

Table H-1. Model runs for loading and handling sensitivity tests

Run ID and description	Results figure	Total PM_{10} emission rate (kg/h)	
		Day time	Night time
1. Base Case	Figure H-1(a)	16.0	16.0
2. Daytime weighting	Figure H-1(b)	34.5	0.41
3. Lower silt content	Figure H-1(c)	15.1	0.18
4. Higher silt content	Figure H-1(d)	40.6	0.48
5. Short haul ore included	Figure H-1(e)	38.7	4.6
6. Lower average control efficiency	Figure H-1(f)	128.9	15.3
7. Effect of excluding emissions on "rain days"	Figure H-1(g)	128.9 (or 0 on "rain days")	15.3 (or 0 on "rain days")

H.2 Model Results

The 24-hour PM_{10} concentrations for these test runs are displayed in the following figures as listed in Table H-1.

The model results are moderately sensitive to daytime weighting, lower silt content, assumed average control efficiency, and whether short haul ore routes are included. Overall, combinations of variations to these factors can make a large difference to the model results.

Figure H-2 compares Options 6 and 7 directly for both 24-hour and annual average PM_{10}, showing the effect of excluding emissions on "rain days". There are very minor differences between the model results for the 24-hour average, but slightly reduced concentrations in the annual averages when "rain days" are accounted for. The impact of accounting for "rain days" is also explored for wind erosion sources in the next section, and is found to be a potentially significant influence on dispersion.

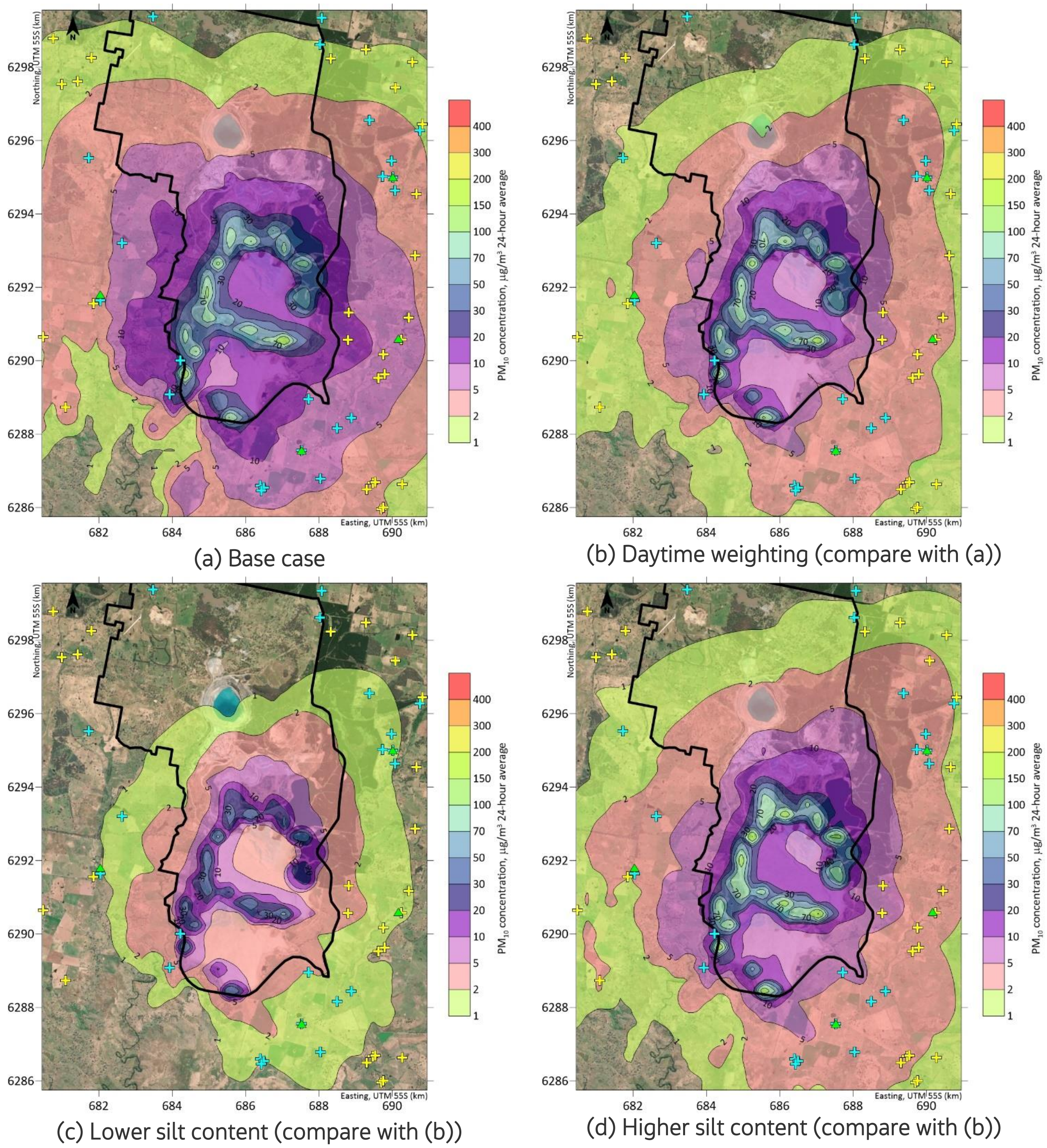

Figure H-1: 24-hour average concentrations of PM_{10} due to vehicle tracked emissions.

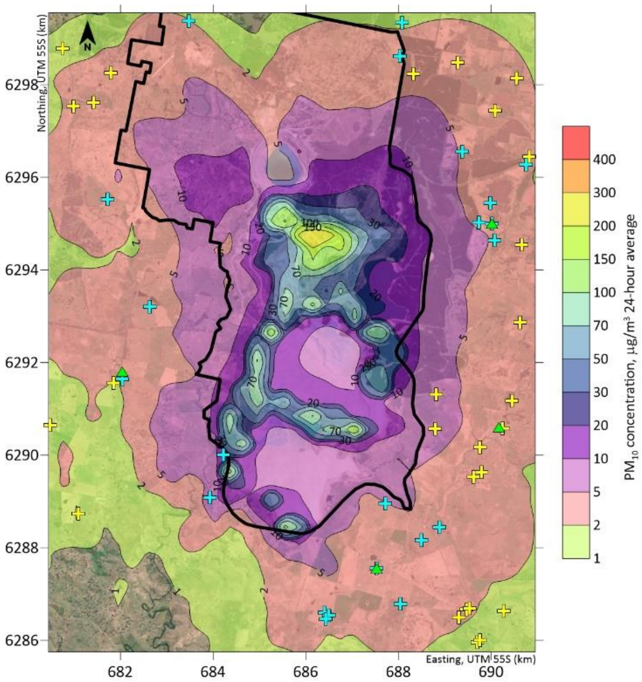

(e) Short haul ore included (compare with (b))

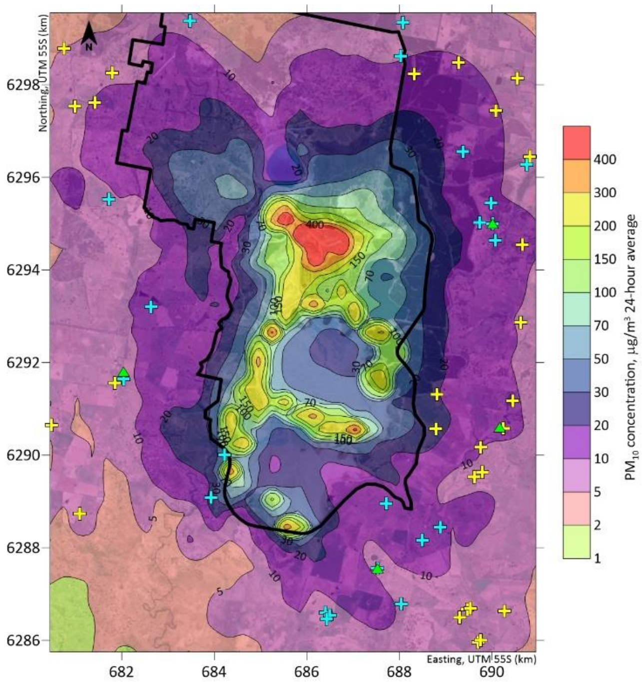

(f) Lower average control efficiency (compare with (e))

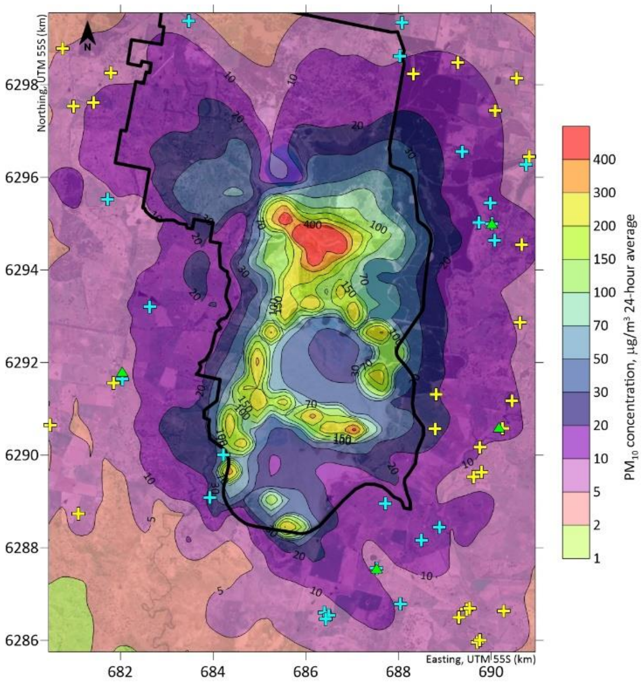

(g) Effect of excluding emissions on "rain days" (compare with (f))

Figure H-1 (cont'd): 24-hour average concentrations of PM_{10} due to vehicle tracked emissions.

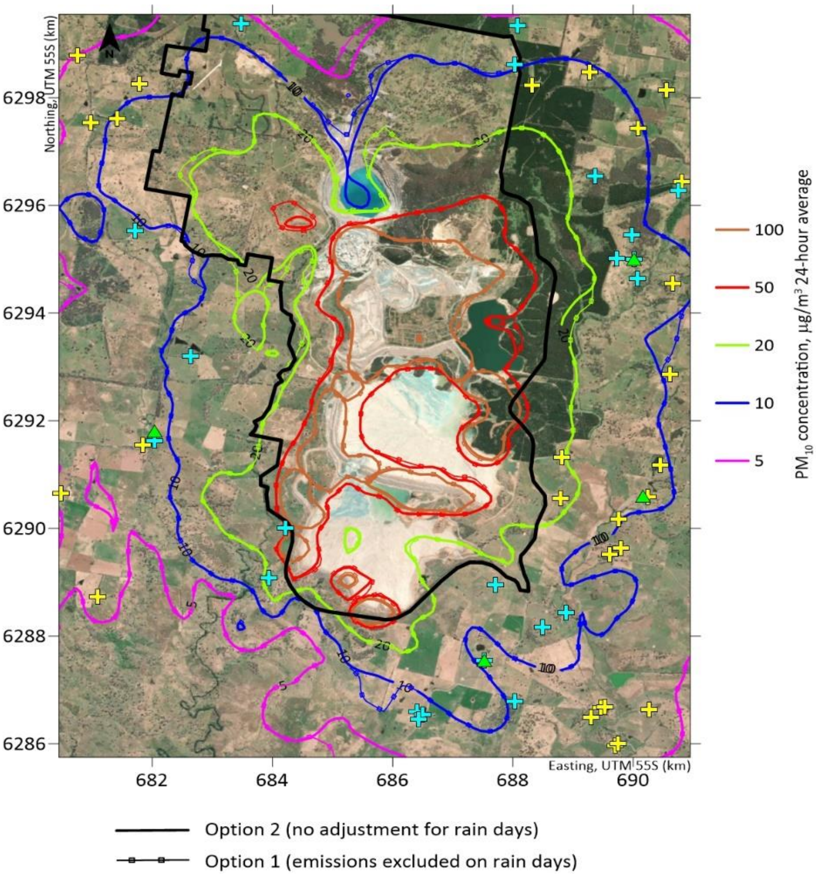

(a) 24-hour average

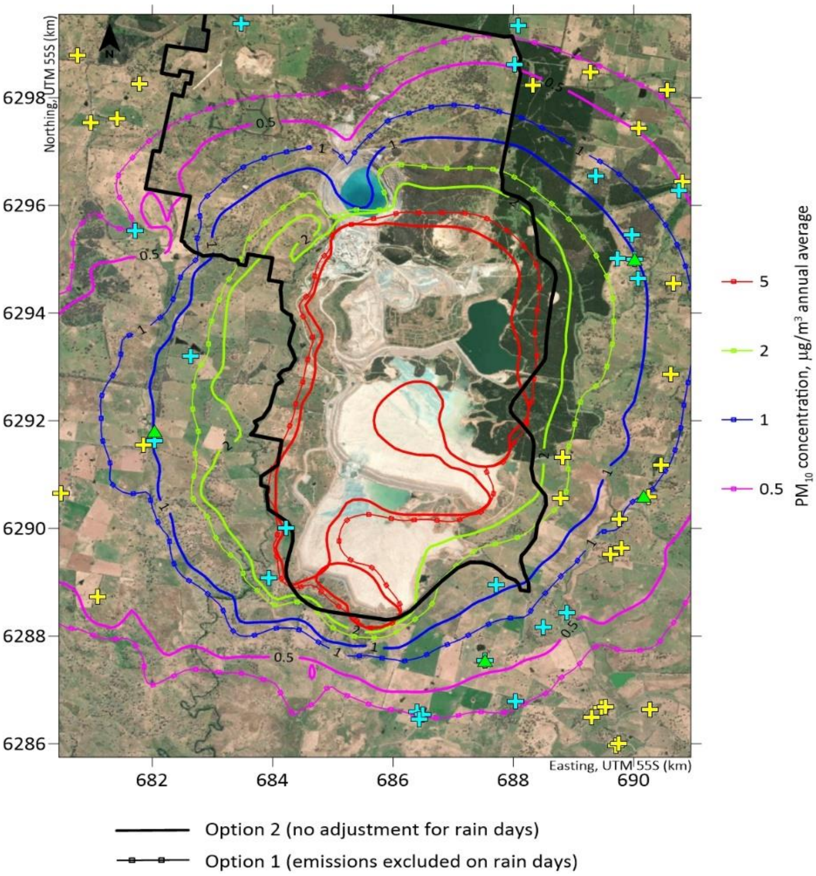

(b) Annual average

Figure H-2: Comparison of dispersion from vehicle-tracked emissions – treatment of "rain days".

Appendix I. Emission Sensitivity Testing – Wind Erosion 24-hour average PM_{10}

Appendix I. Emission Sensitivity Testing – Wind Erosion 24-hour average PM_{10}

I.1 Model Options Tested

The various sensitivity test runs for wind erosion from different open area sources at the mine are shown in Table I-1.

Table I-1. Model runs for wind erosion source groups

Run ID and description	Source group	Results figures
1. Based case (uniform 24/7 emission rate of 0.2 kg/ha/h with no controls)	TSFs	Figures I-1(a) and I-2(a)
	Dry areas around TSFs	Figures I-1(b) and I-2(b)
	Processing, active waste rock dumps, and other areas	Figures I-1(c) and I-2(c)
	All groups	Figures I-1(d) and I-2(d)
2. Wind speed weighting	TSFs	Figures I-3(a) and I-4(a)
	Dry areas around TSFs	Figures I-3(b) and I-4(b)
	Processing, active waste rock dumps, and other areas	Figures I-3(c) and I-4(c)
	All groups	Figures I-3(d) and I-4(d)
3. Controls	TSFs	Figures I-5(a) and I-6(a)
	Dry areas around TSFs	Figures I-5(b) and I-6(b)
	Processing, active waste rock dumps, and other areas	Figures I-5(c) and I-6(c)
	All groups	Figures I-5(d) and I-6(d)
4. Rain days approach	TSFs	Figures I-7(a) and I-8(a)
	Dry areas around TSFs	Figures I-7(b) and I-8(b)
	Processing, active waste rock dumps, and other areas	Figures I-7(c) and I-8(c)
	All groups	Figures I-7(d) and I-8(d)
5. Site-specific values for s, p and f in wind erosion equation	TSFs	Figures I-9(a) and I-10(a)
	Dry areas around TSFs	Figures I-9(b) and I-10(b)
	Processing, active waste rock dumps, and other areas	Figures I-9(c) and I-10(c)
	All groups	Figures I-9(d) and I-10(d)
6. Assume p=0 and apply controls and rain days	TSFs	Figures I-11(a) and I-12(a)
	Dry areas around TSFs	Figures I-11(b) and I-12(b)
	Processing, active waste rock dumps, and other areas	Figures I-11(c) and I-12(c)
	All groups	Figures I-11(d) and I-12(d)

I.2 Model Results

The 24-hour PM_{10} concentrations for these test runs are displayed in the figures as listed in Table I-1.

The following observations are noted:

1. Distributing the emissions as a function of the cube of the wind speed (Base case versus Option 2) has a very significant impact on model results both at the 24-hour and annual average.

2. Allowing for control efficiency has a very significant impact on model results (Option 2 versus Option 3) and would be sensitive to the amount of control that is assumed; noting that this may vary for different open area types.

3. Eliminating wind erosion emissions on rain days (essentially assuming 100% control effectiveness after a rain event) (Option 3 versus Option 4) has a moderate impact on model results in some parts of the domain, and a minor impact in other areas.

4. Applying site-specific values for s, p and f in the wind erosion equation (Option 3 versus Option 5) causes the concentrations from the TSFs to approximately double for both the 24-hour and annual average, but the concentrations resulting from the other open area sources are only slightly higher.

5. Comparing Option 4 versus Option 6, the model is sensitive to the approach of assuming p=0 in the wind erosion equation and eliminating wind erosion emissions on “rain days”, particularly for the TSFs. The model results for Option 6 are about three times higher than for Option 4 for the TSFs, and about twice as high as Option 4 for the other open area sources.

Overall, whilst there is variation between the options 2 to 6, the comparison is constrained by the uncertainty in the input assumptions for silt content of the various surfaces, and the efficiency of controls. The lower the silt content and the better the control efficiency, the less significant the variations in model results between the options. Therefore, site-specific validation of the silt content and control efficiency off the various open area types would refine the comparison of emission estimation methods.

Regardless, it is clear that the TSFs represent a potentially dominant source of wind erosion emissions.

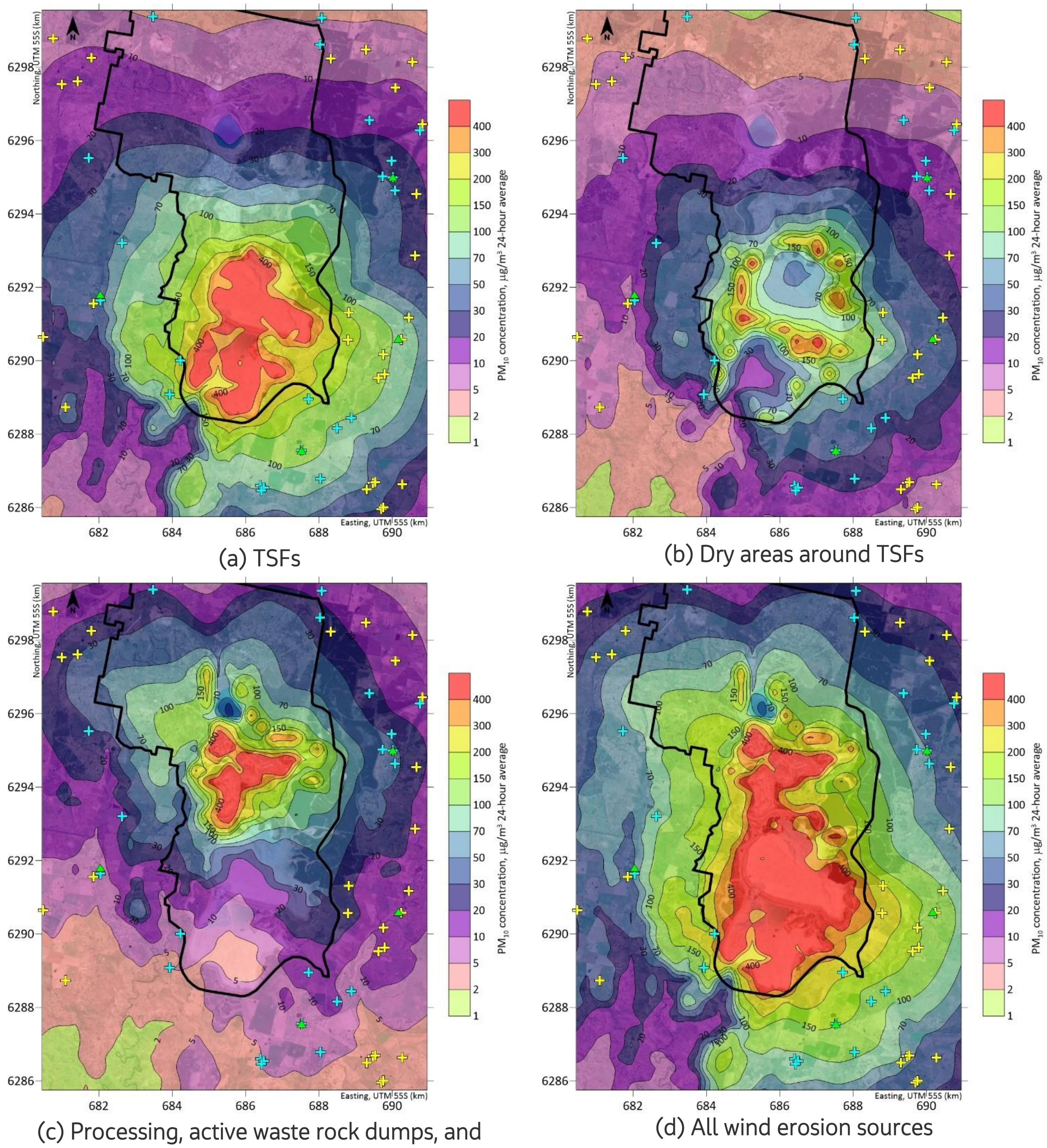

(a) TSFs

(b) Dry areas around TSFs

(c) Processing, active waste rock dumps, and other areas

(d) All wind erosion sources

Figure I-1: 24-hour average concentrations of PM_{10} due to wind erosion – Option 1 Base case, no controls.

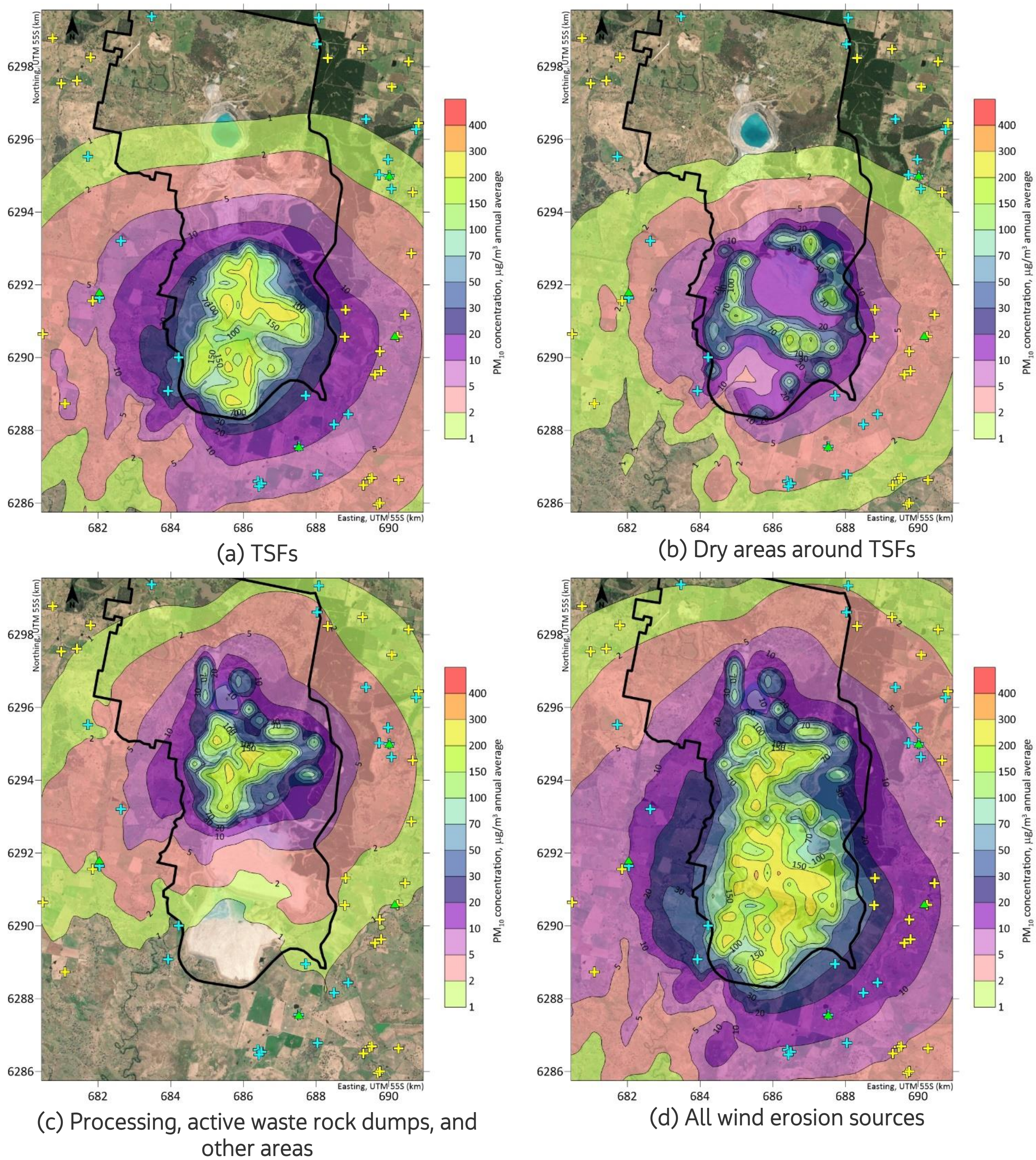

Figure I-2: Annual average concentrations of PM_{10} due to wind erosion – Option 1 Base case.

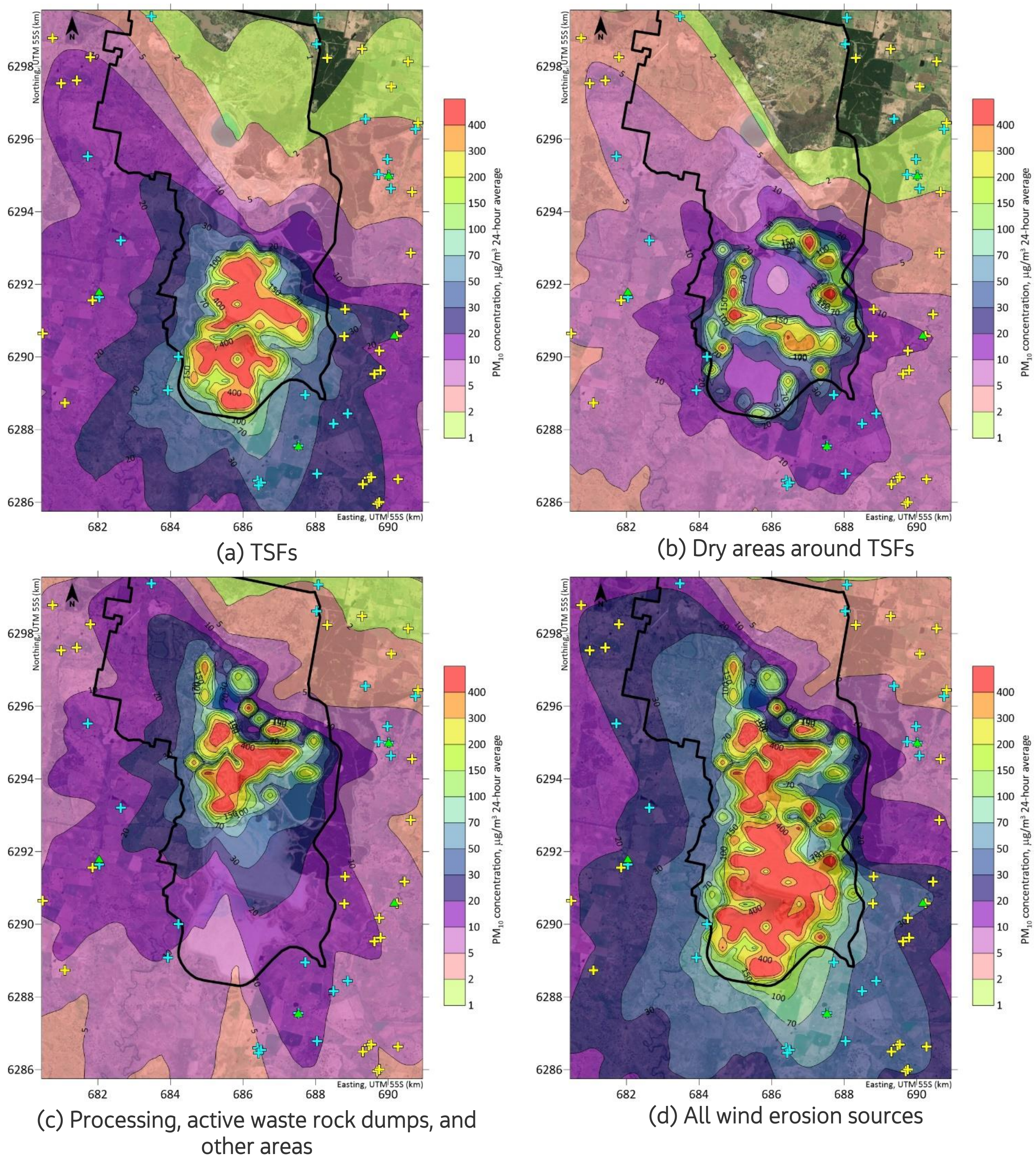

Figure I-3: 24-hour average concentrations of PM_{10} due to wind erosion – Option 2 effect of wind speed weighting, no controls.

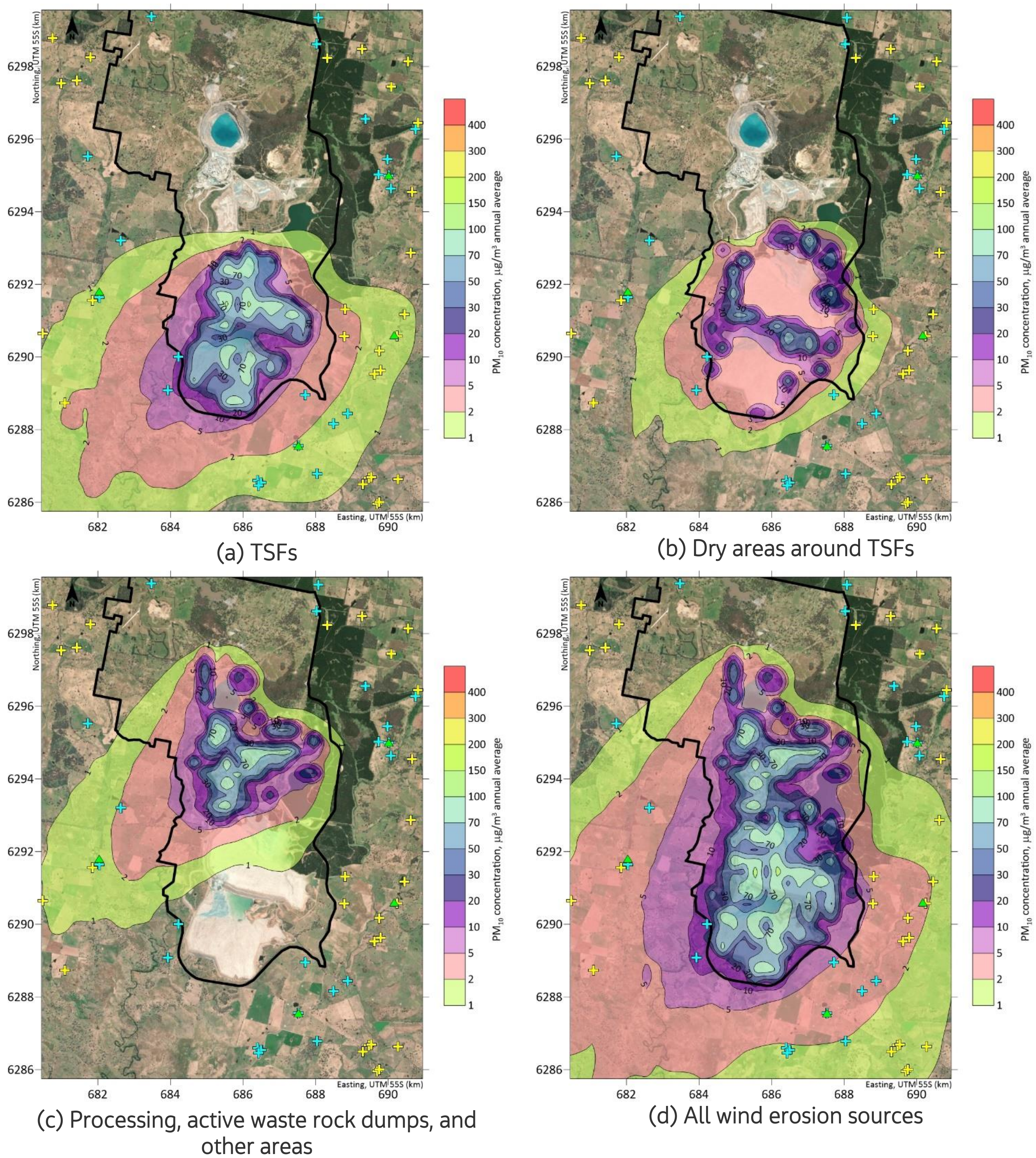

Figure I-4: Annual average concentrations of PM_{10} due to wind erosion – Option 2 effect of wind speed weighting.

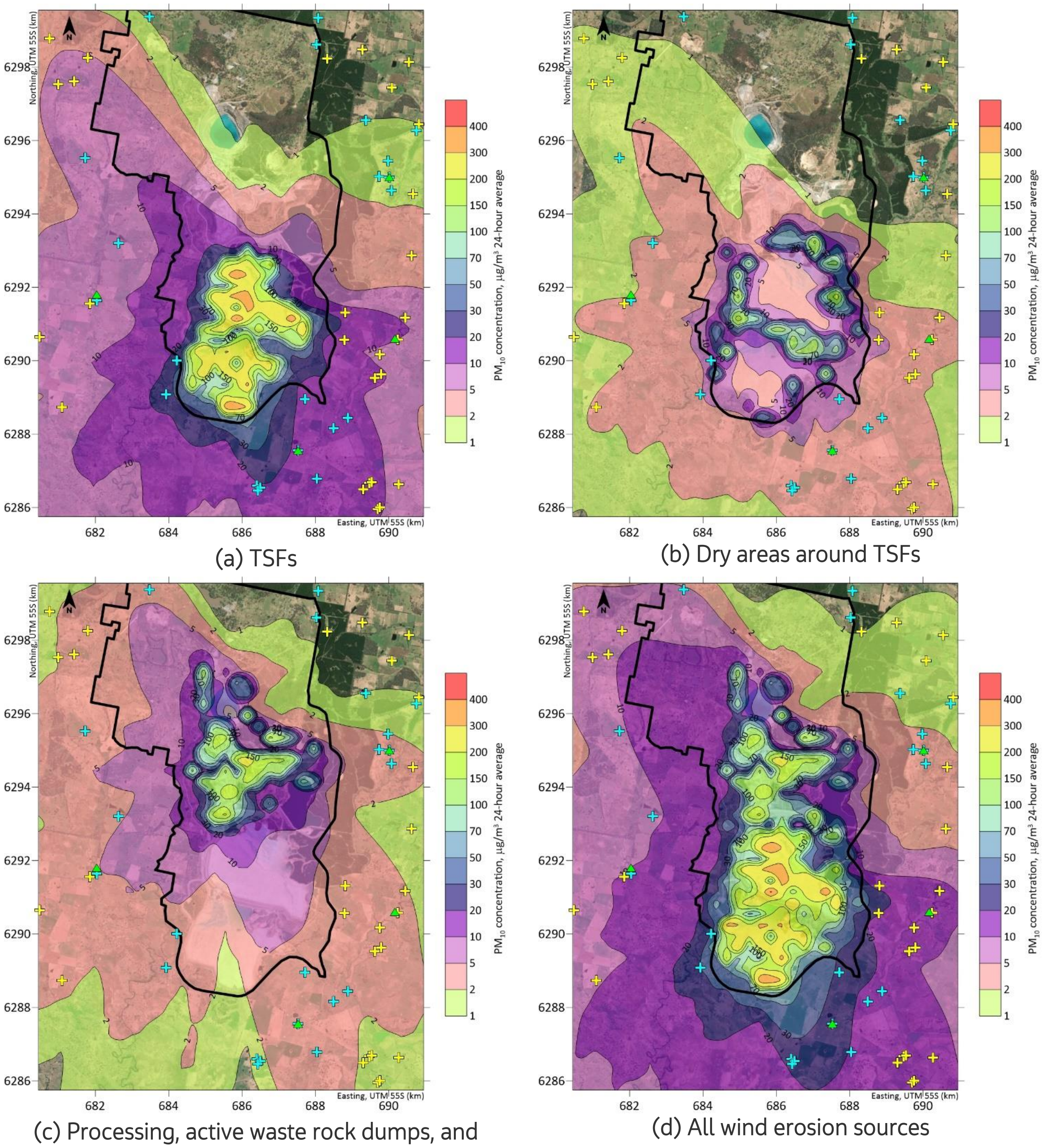

(a) TSFs

(b) Dry areas around TSFs

(c) Processing, active waste rock dumps, and other areas

(d) All wind erosion sources

Figure I-5: 24-hour average concentrations of PM$_{10}$ due to wind erosion – Option 3 effect of adding controls.

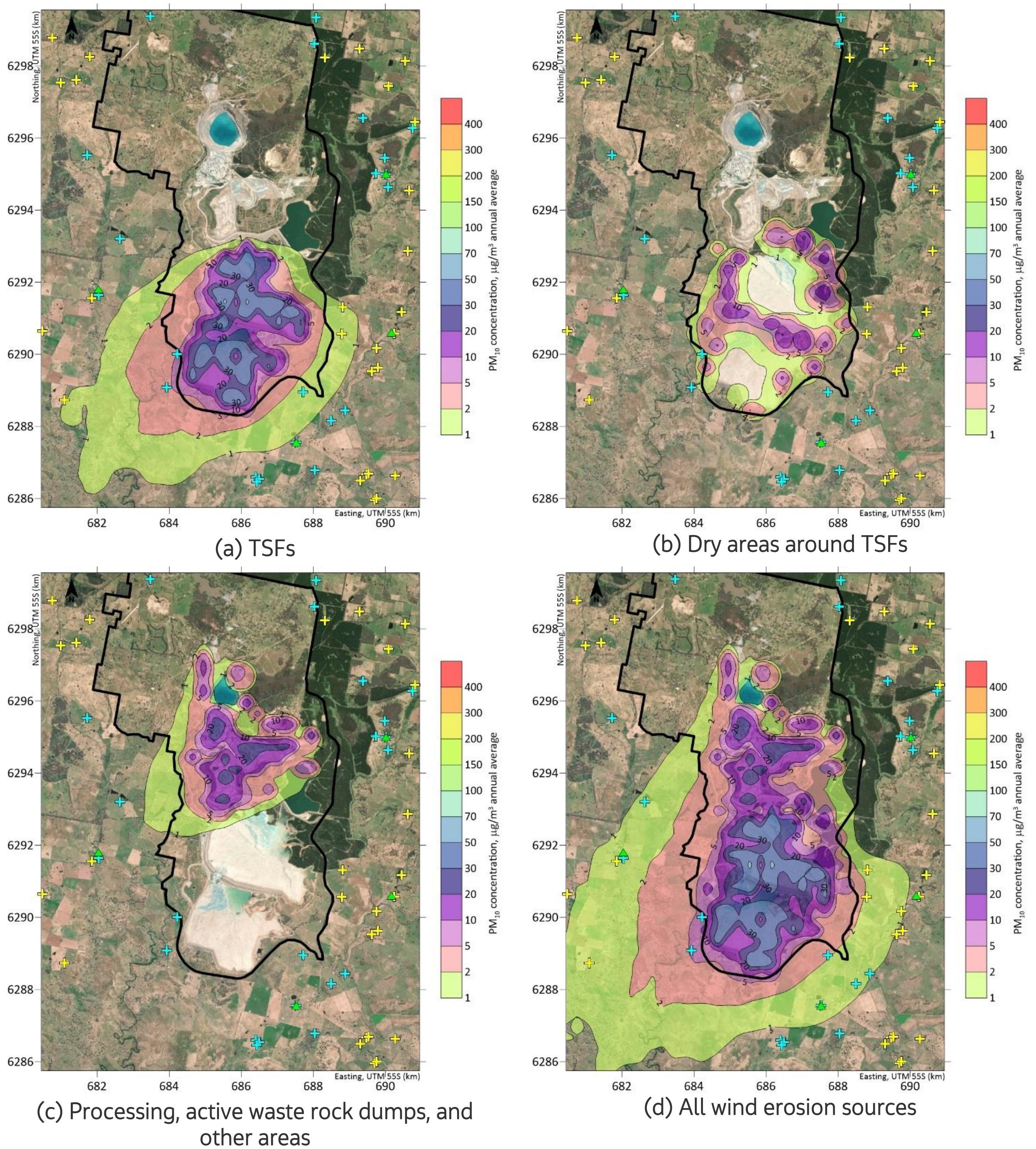

Figure I-6: Annual average concentrations of PM_{10} due to wind erosion – Option 3 effect of adding controls.

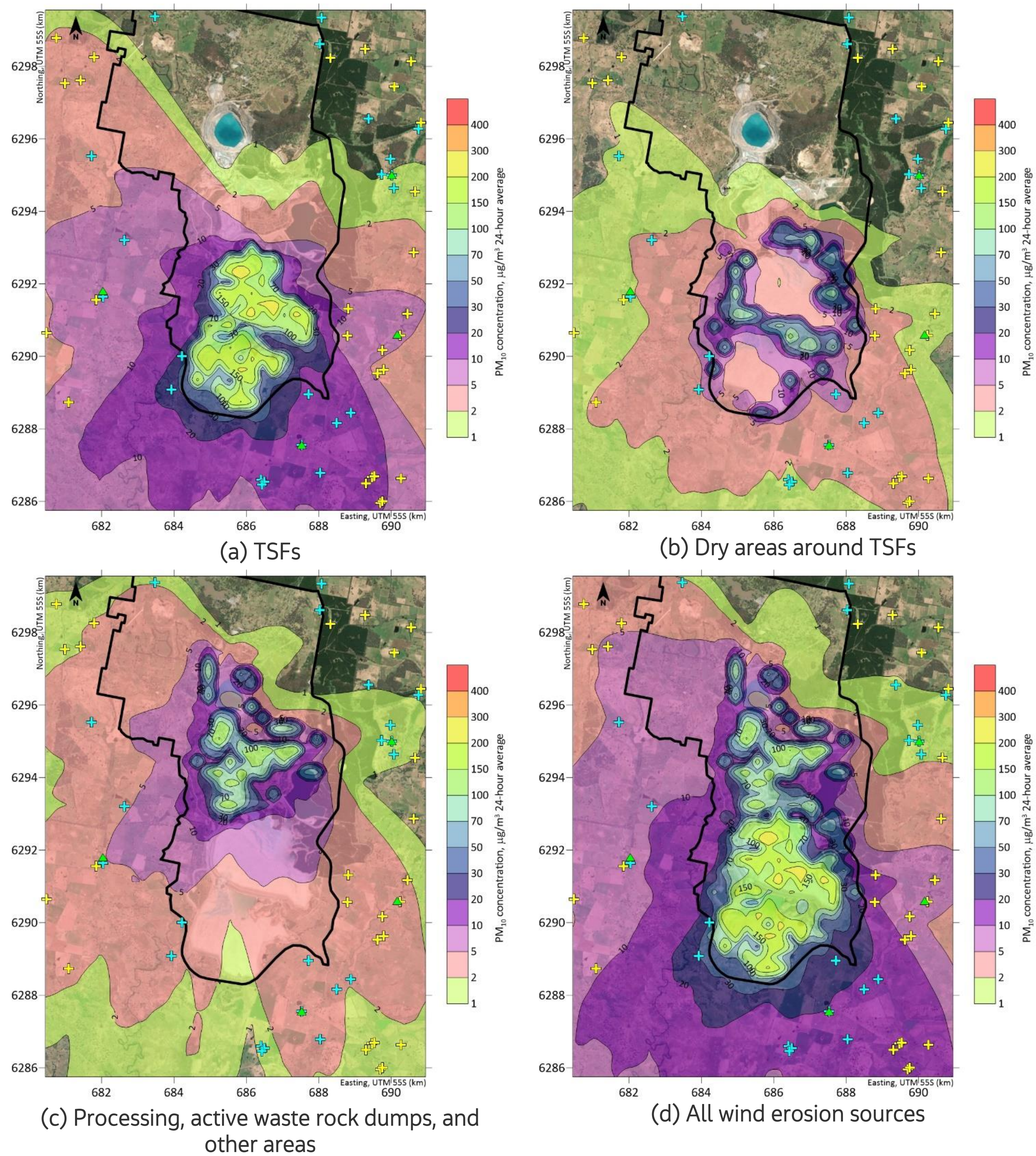

(a) TSFs

(b) Dry areas around TSFs

(c) Processing, active waste rock dumps, and other areas

(d) All wind erosion sources

Figure I-7: 24-hour average concentrations of PM$_{10}$ due to wind erosion – Option 4 effect of applying "rain days" approach.

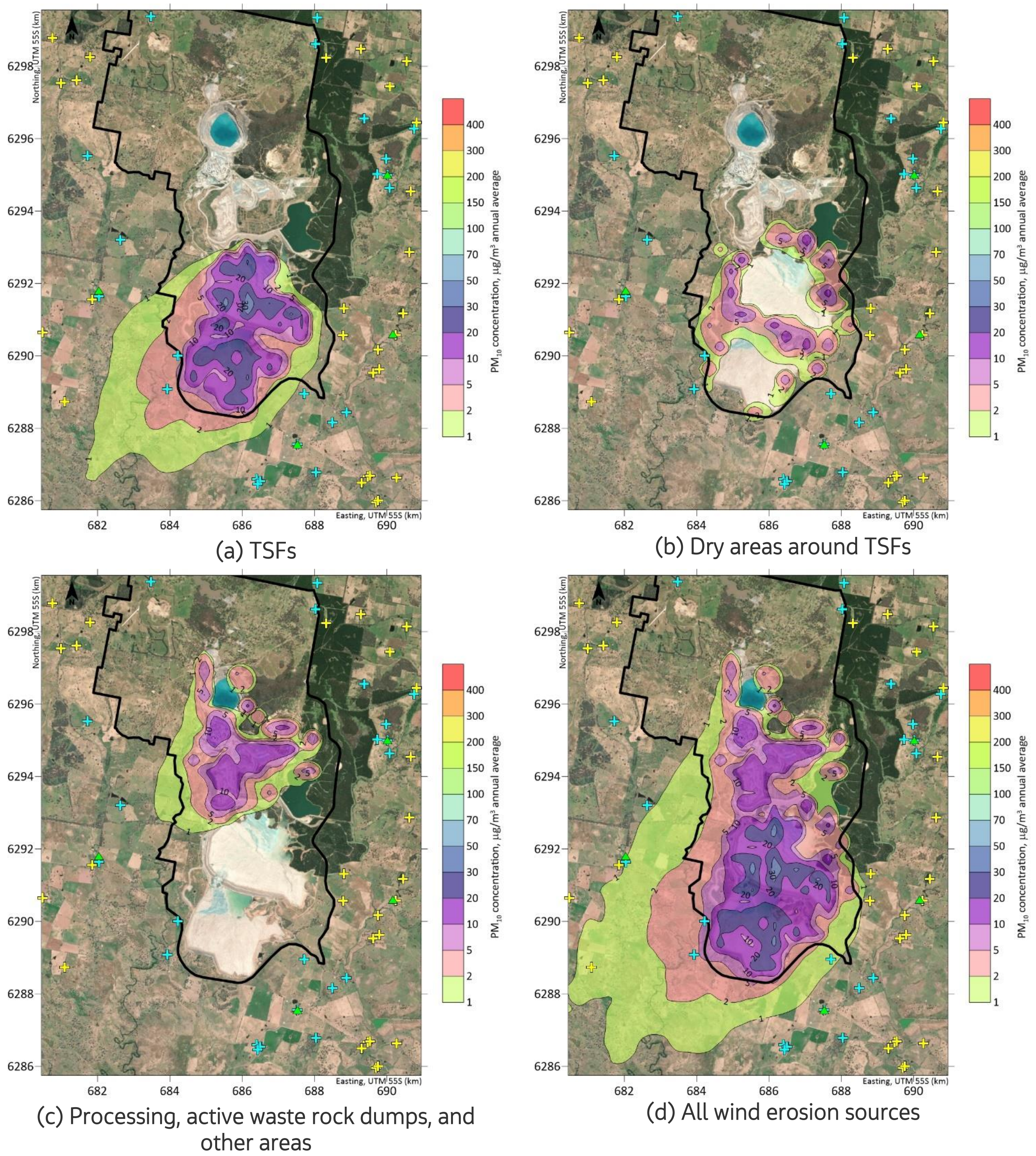

Figure I-8: Annual average concentrations of PM_{10} due to wind erosion – Option 4 effect of applying "rain days" approach.

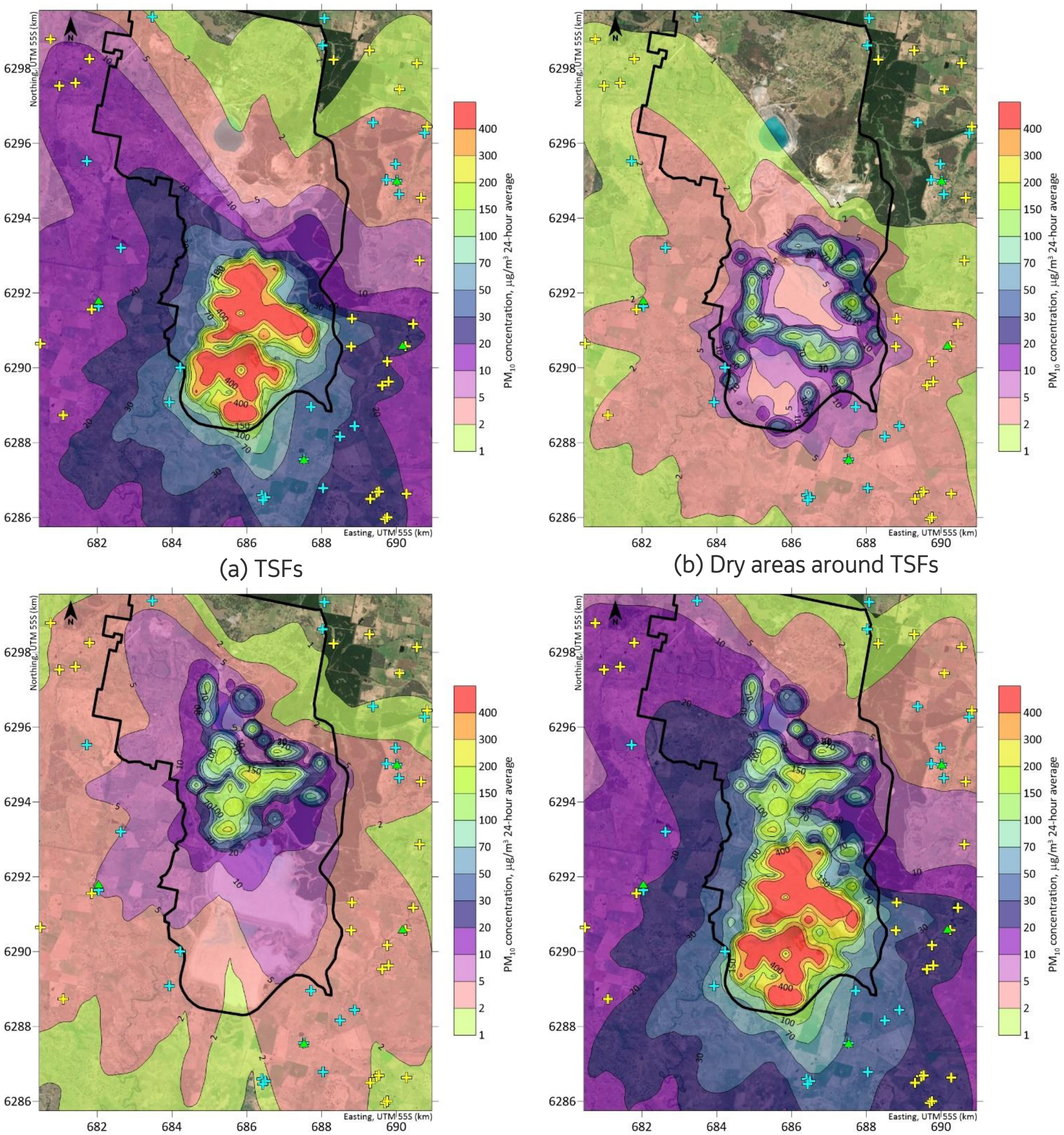

(a) TSFs

(b) Dry areas around TSFs

(c) Processing, active waste rock dumps, and other areas

(d) All wind erosion sources

Figure I-9: 24-hour average concentrations of PM$_{10}$ due to wind erosion – Option 5 effect of site-specific values for s, p and f in wind erosion equation.

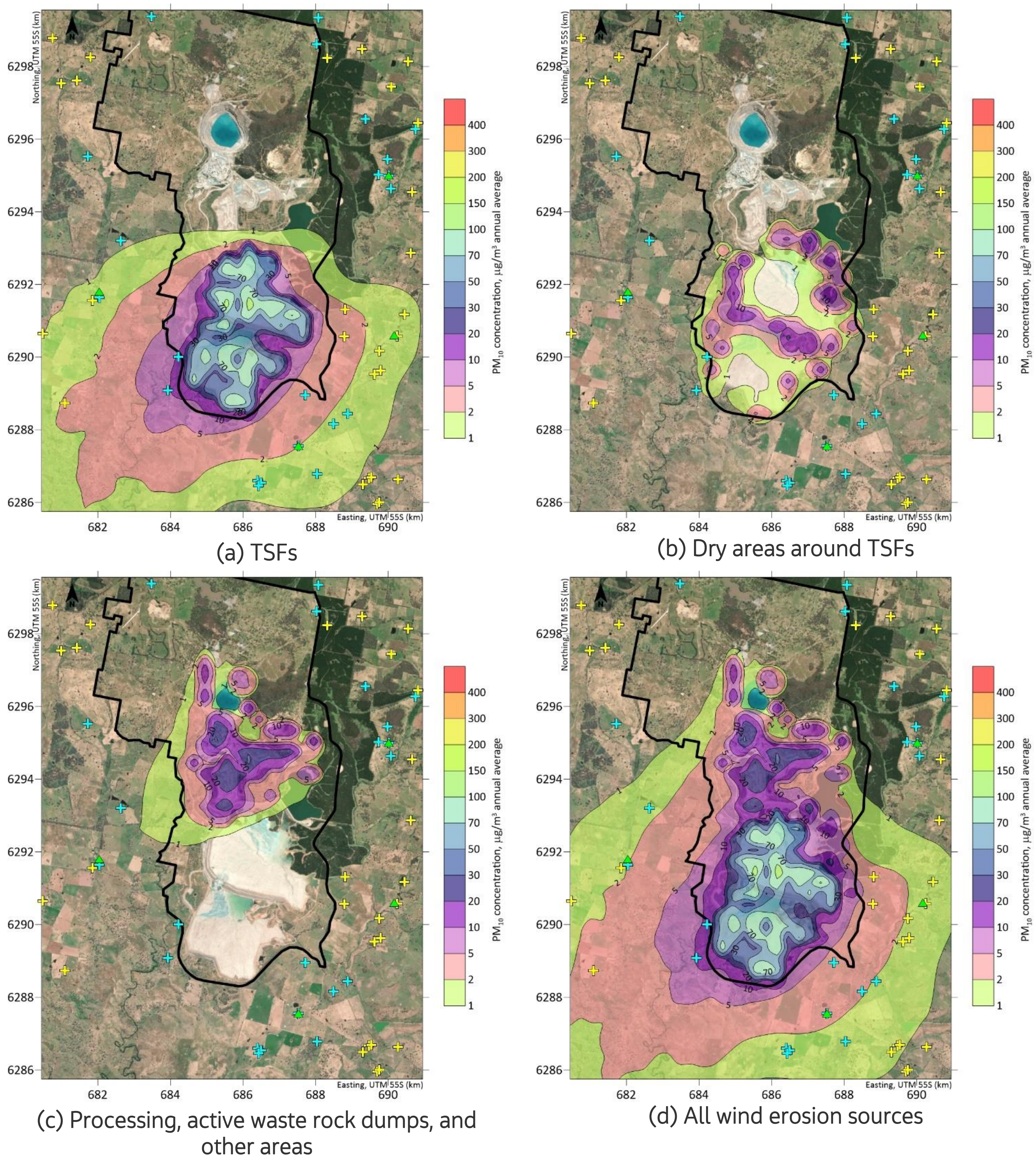

Figure I-10: Annual average concentrations of PM_{10} due to wind erosion – Option 5 effect of site-specific values for s, p and f in wind erosion equation.

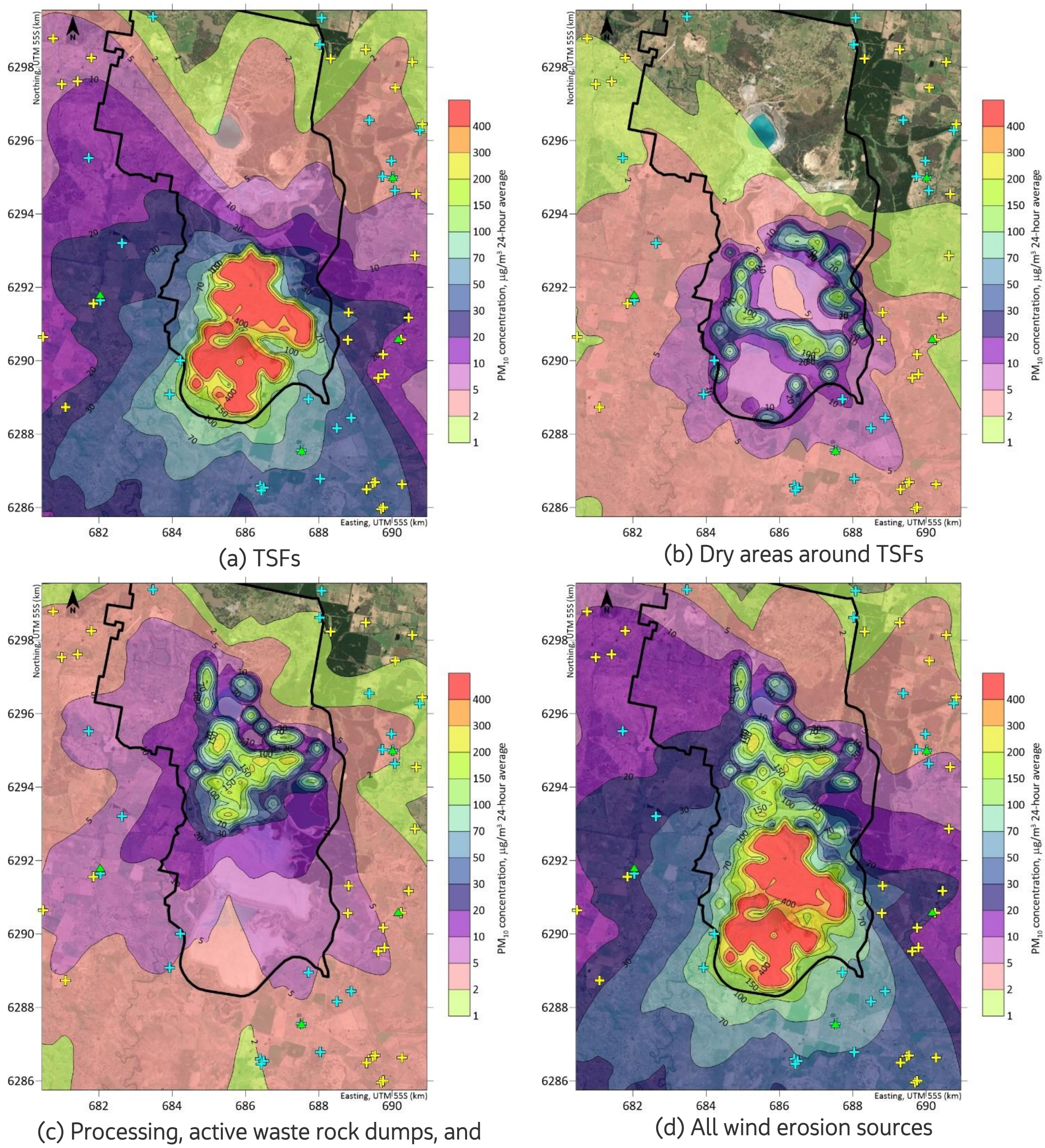

(a) TSFs

(b) Dry areas around TSFs

(c) Processing, active waste rock dumps, and other areas

(d) All wind erosion sources

Figure I-11: 24-hour average concentrations of PM_{10} due to wind erosion – Option 6 effect of assuming p=0 in wind erosion equation and applying controls and “rain days”.

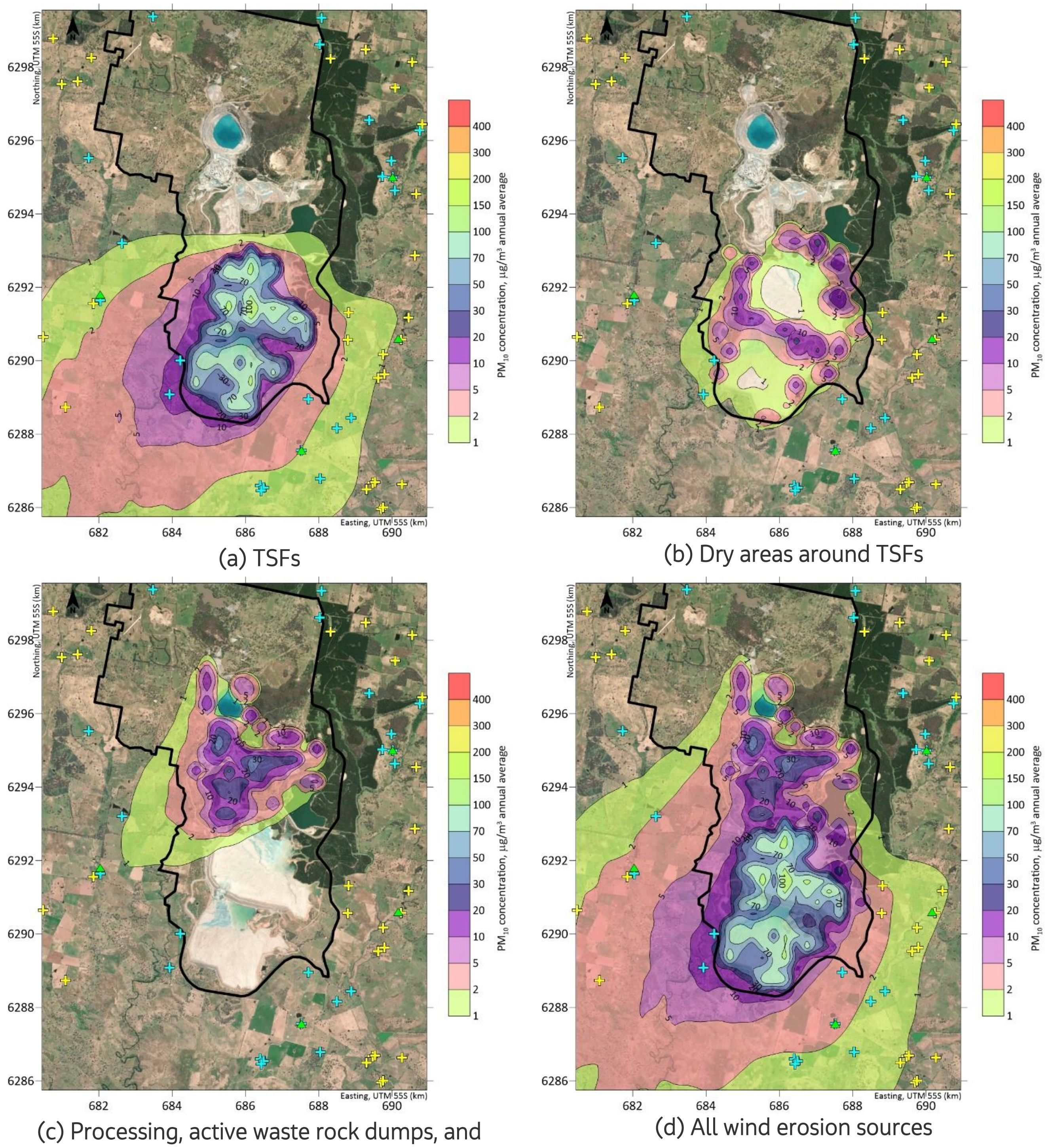

Figure I-12: Annual average concentrations of PM_{10} due to wind erosion – Option 6 effect of assuming p=0 in wind erosion equation and applying controls and "rain days".

Appendix J. TSF Wind Erosion Potential Timeseries for Selected Dates in 2022

Appendix J. TSF Wind Erosion Potential Timeseries for Selected Dates in 2022

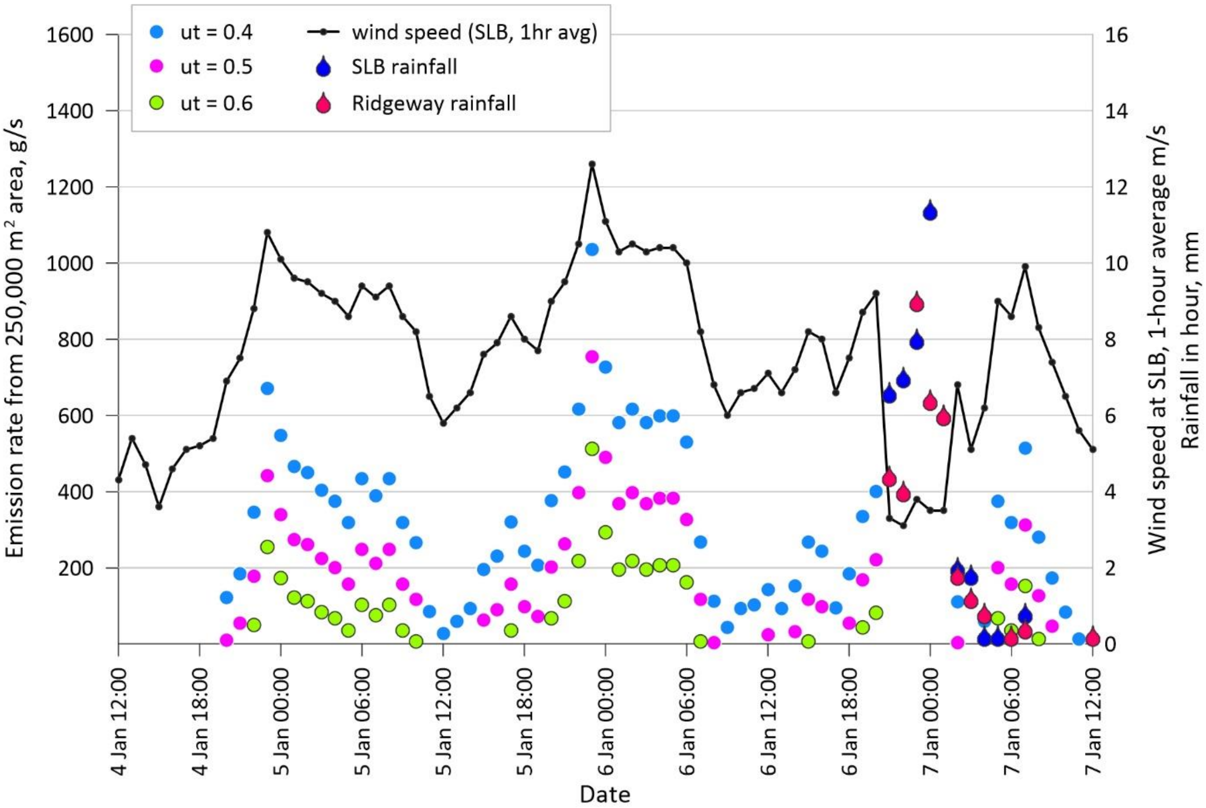

Figure J-1: Wind erosion rates for a 250,000 m^2 area source (representing a 500m x 500m square patch of TSF surface) based on the threshold friction velocity calculation method – 4-6 January 2022.

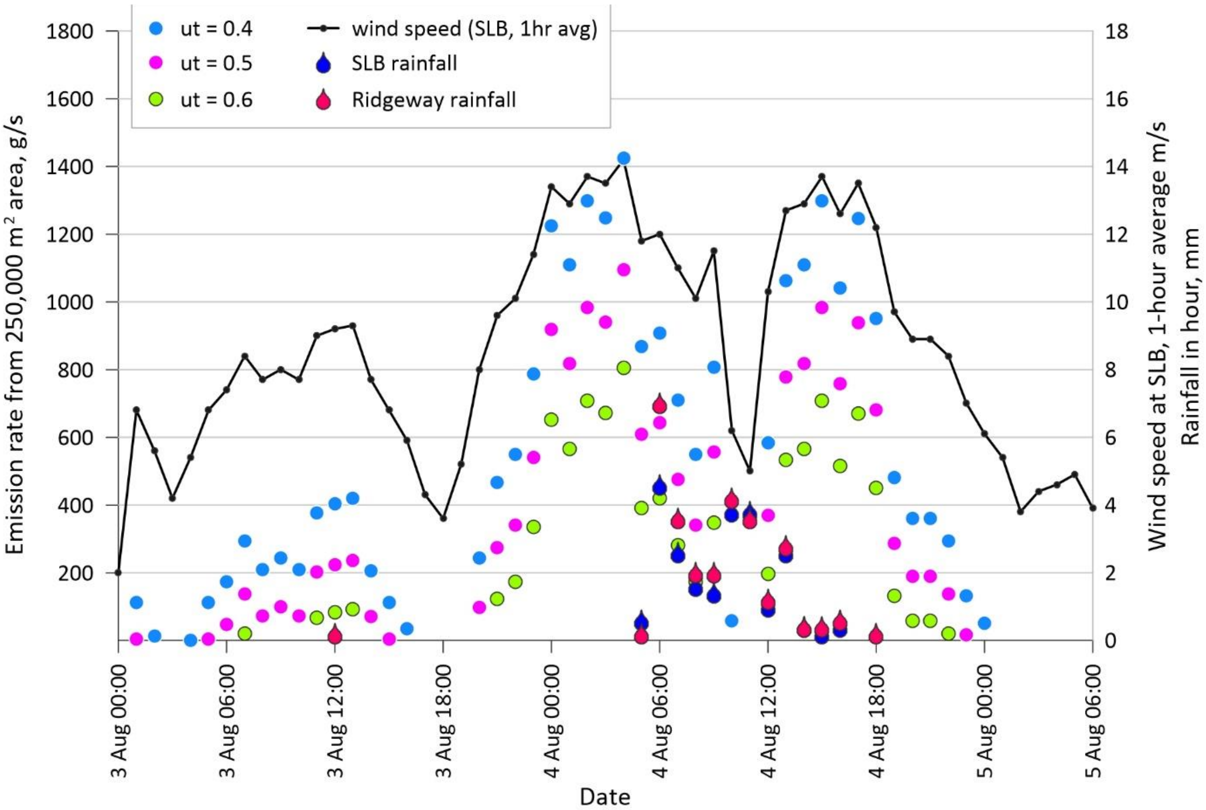

Figure J-2: Wind erosion rates for a 250,000 m^2 area source (representing a 500m x 500m square patch of TSF surface) based on the threshold friction velocity calculation method – 3-4 August 2022.

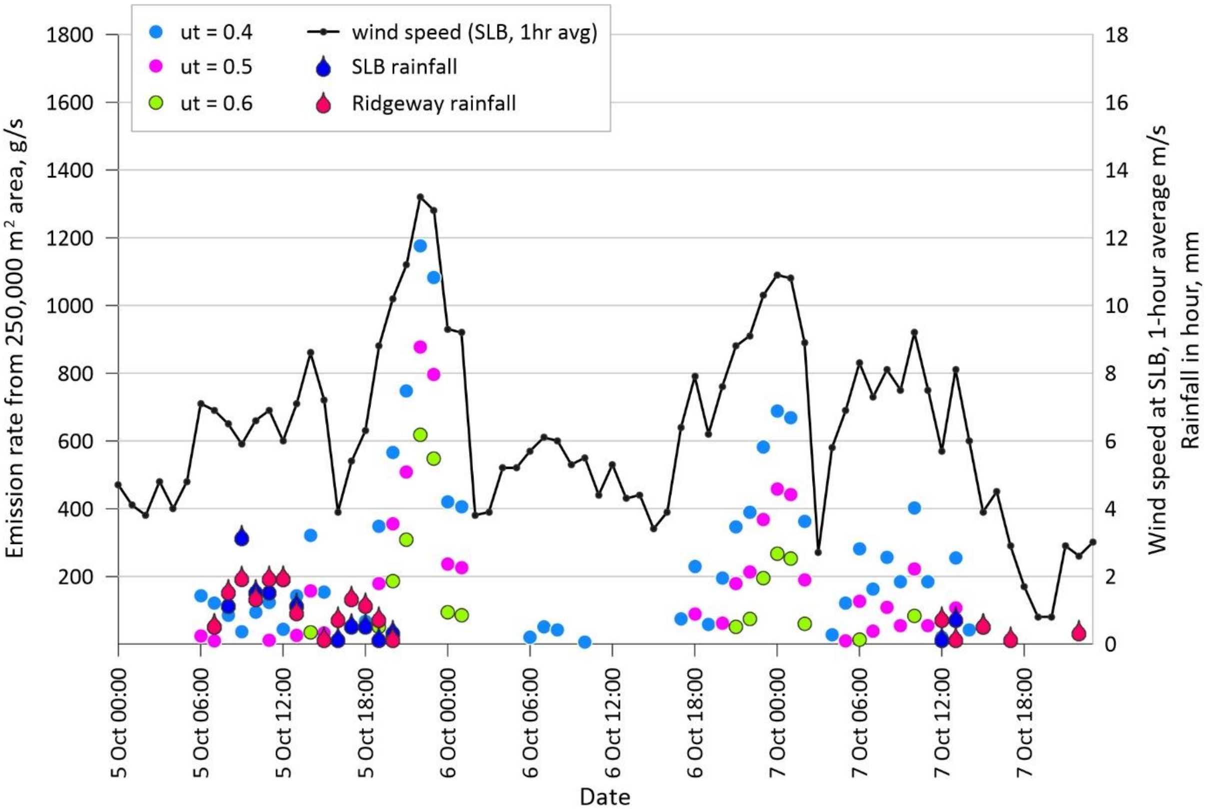

Figure J-3: Wind erosion rates for a 250,000 m^2 area source (representing a 500m x 500m square patch of TSF surface) based on the threshold friction velocity calculation method – 5-6 October 2022.

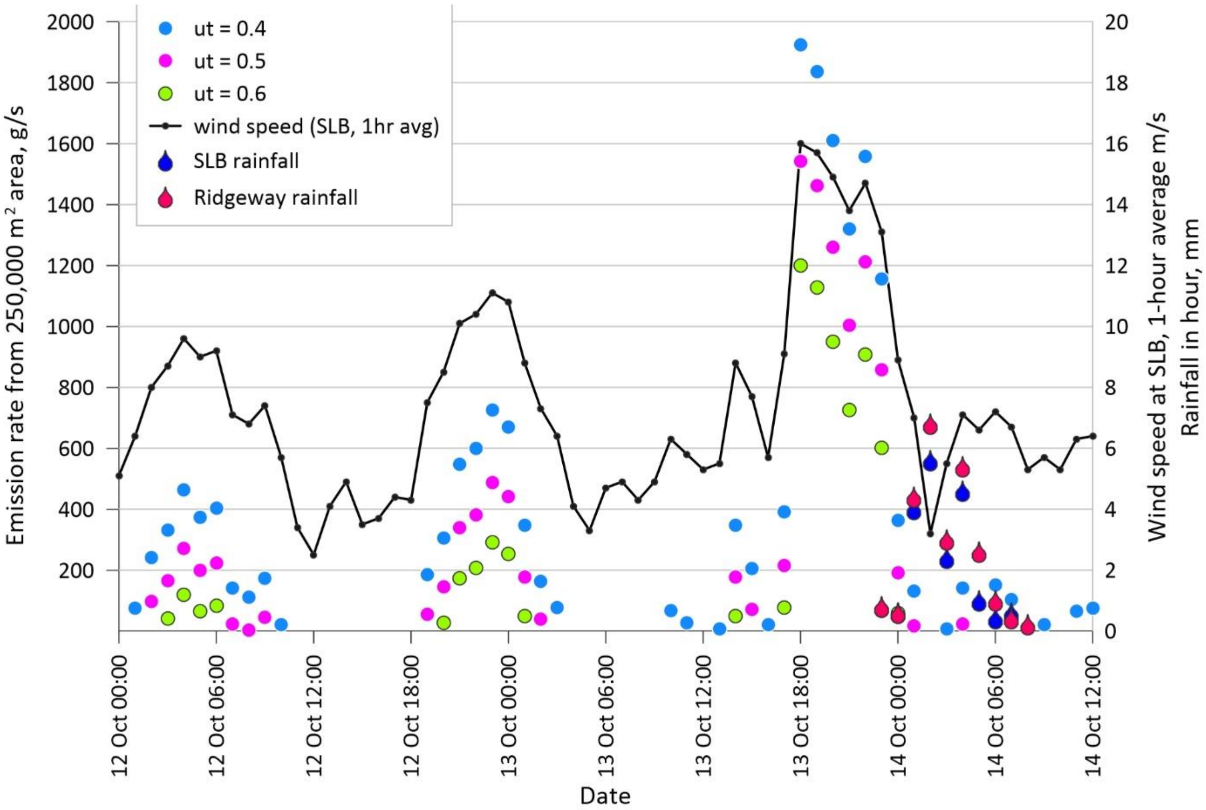

Figure J-4: Wind erosion rates for a 250,000 m^2 area source (representing a 500m x 500m square patch of TSF surface) based on the threshold friction velocity calculation method – 13 October 2022.

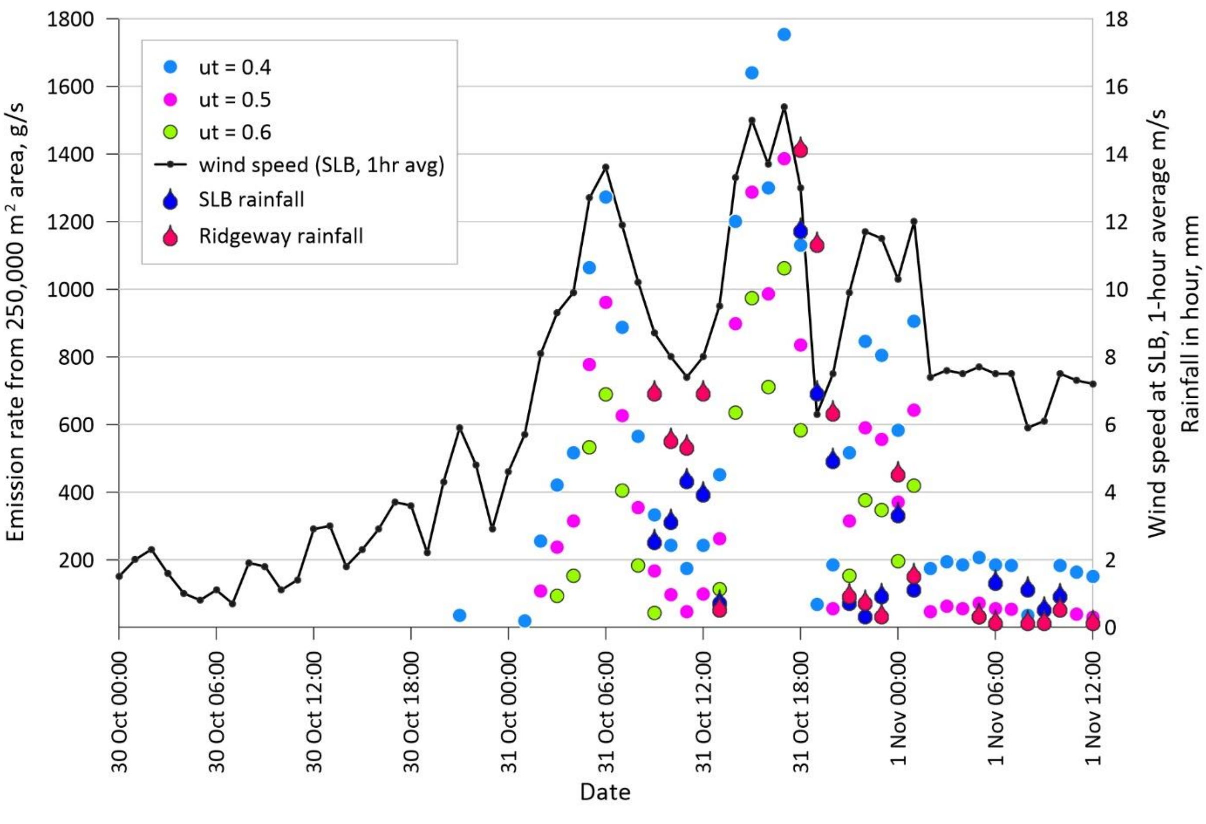

Figure J-5: Wind erosion rates for a 250,000 m^2 area source (representing a 500m x 500m square patch of TSF surface) based on the threshold friction velocity calculation method – 31 October 2022.

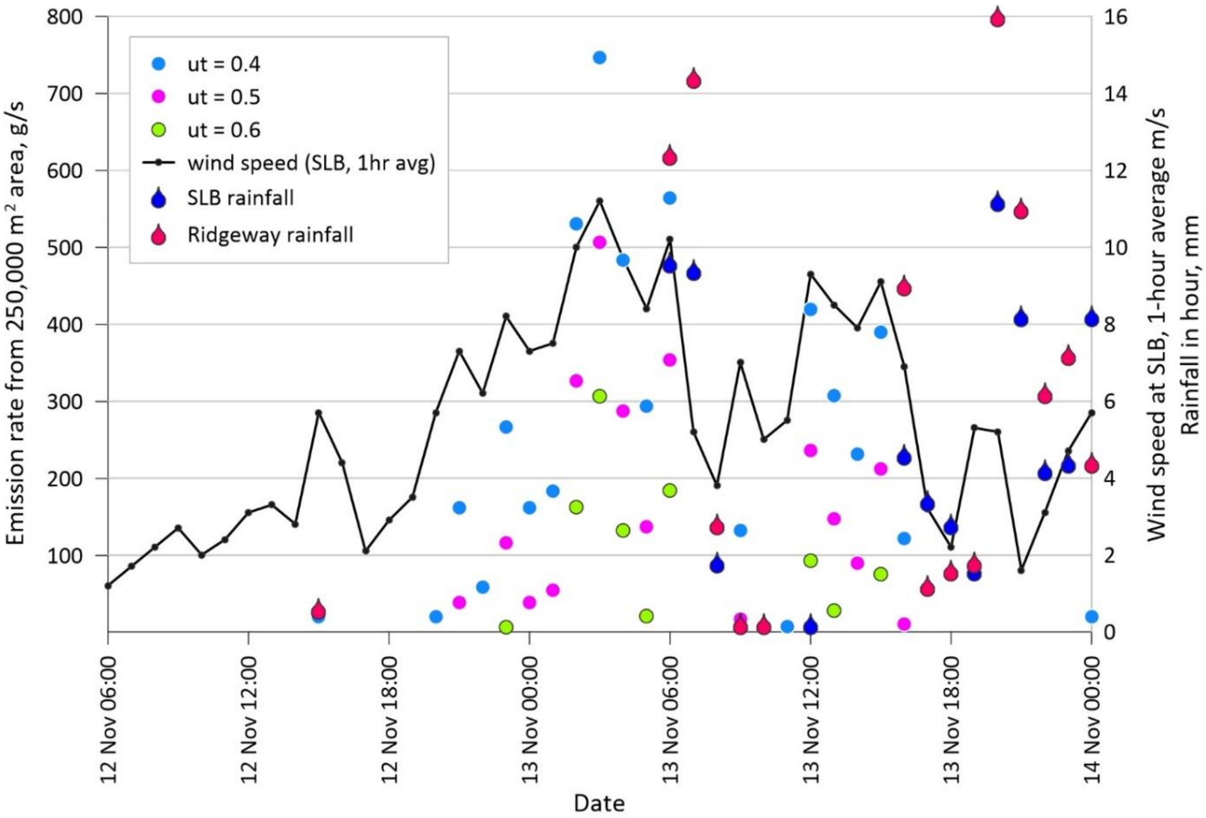

Figure J-6: Wind erosion rates for a 250,000 m² area source (representing a 500m x 500m square patch of TSF surface) based on the threshold friction velocity calculation method – 13 November 2022.

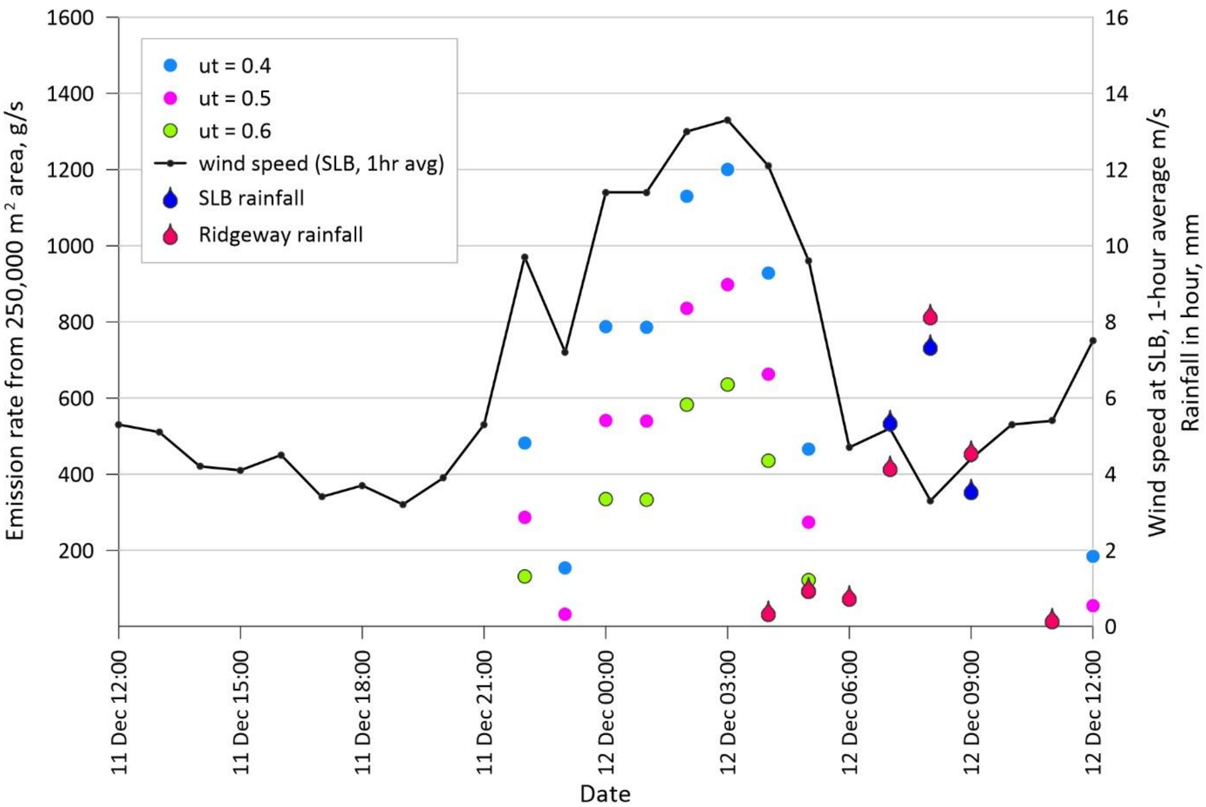

Figure J-7: Wind erosion rates for a 250,000 m² area source (representing a 500m x 500m square patch of TSF surface) based on the threshold friction velocity calculation method – 11-12 December 2022.

Appendix K. TSF Wind Erosion Potential Timeseries for 5-6 January 2022

Appendix K. TSF Wind Erosion Potential Timeseries for 5-6 January 2022

Scale for all plume screenshots in this Appendix:

Concentration of PM_{10}, 1-hour average, in g/m^3 (multiply by $1x10^6$ for $\mu g/m^3$)

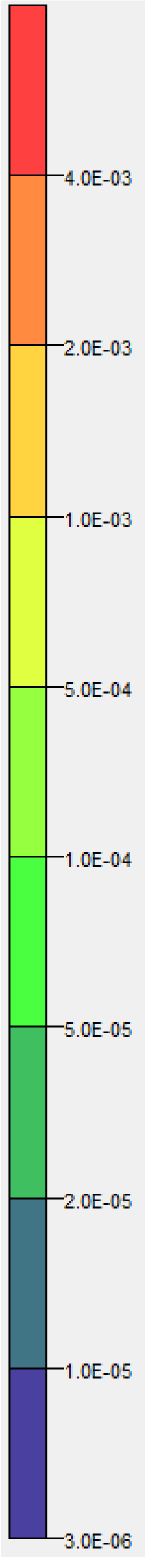

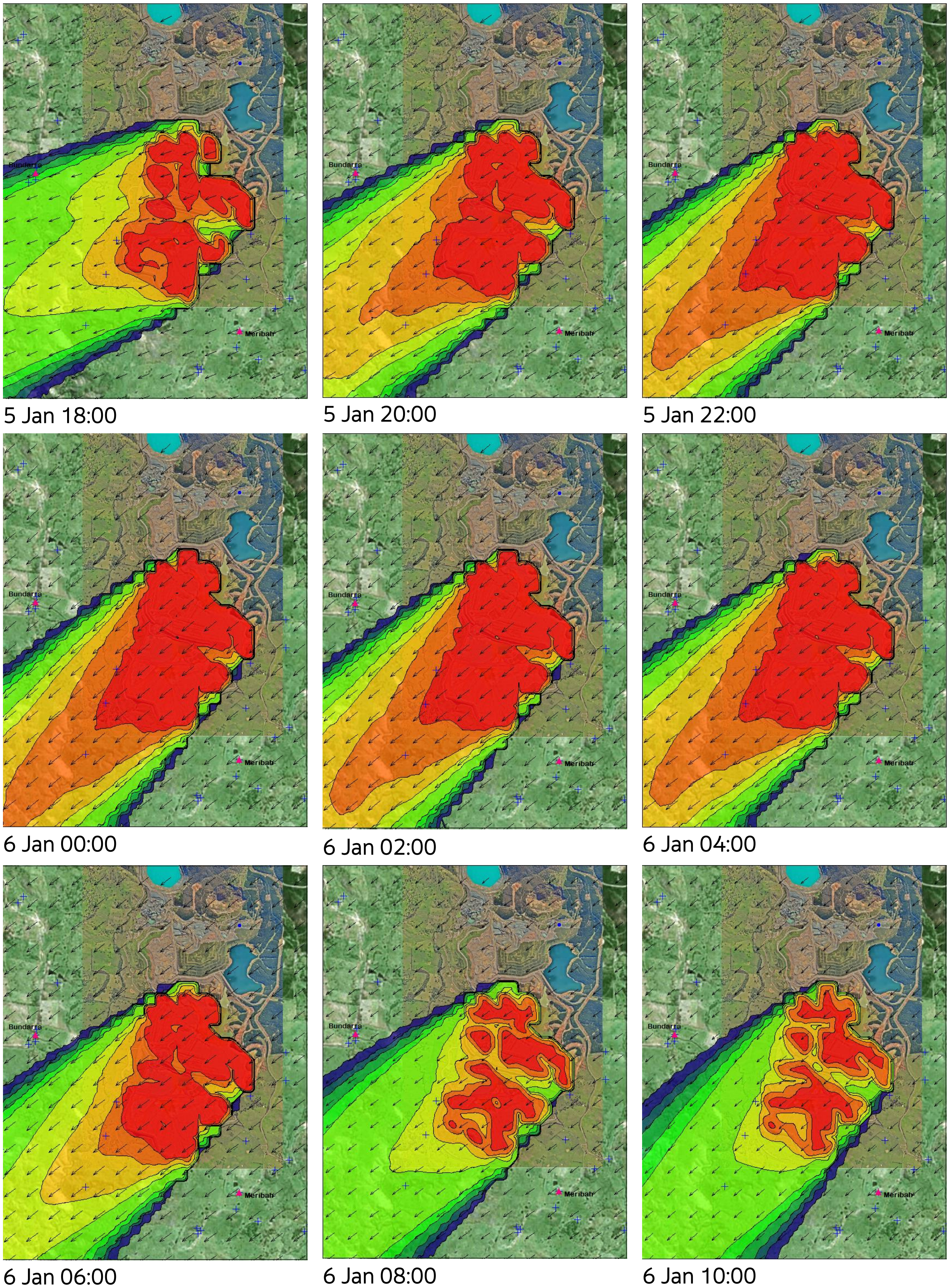

Figure K-1: Simulation of dust lift-off from TSFs on 5-6 January 2022, based on the threshold friction velocity calculation method and assuming u_t = 0.4 m/s and no controls.

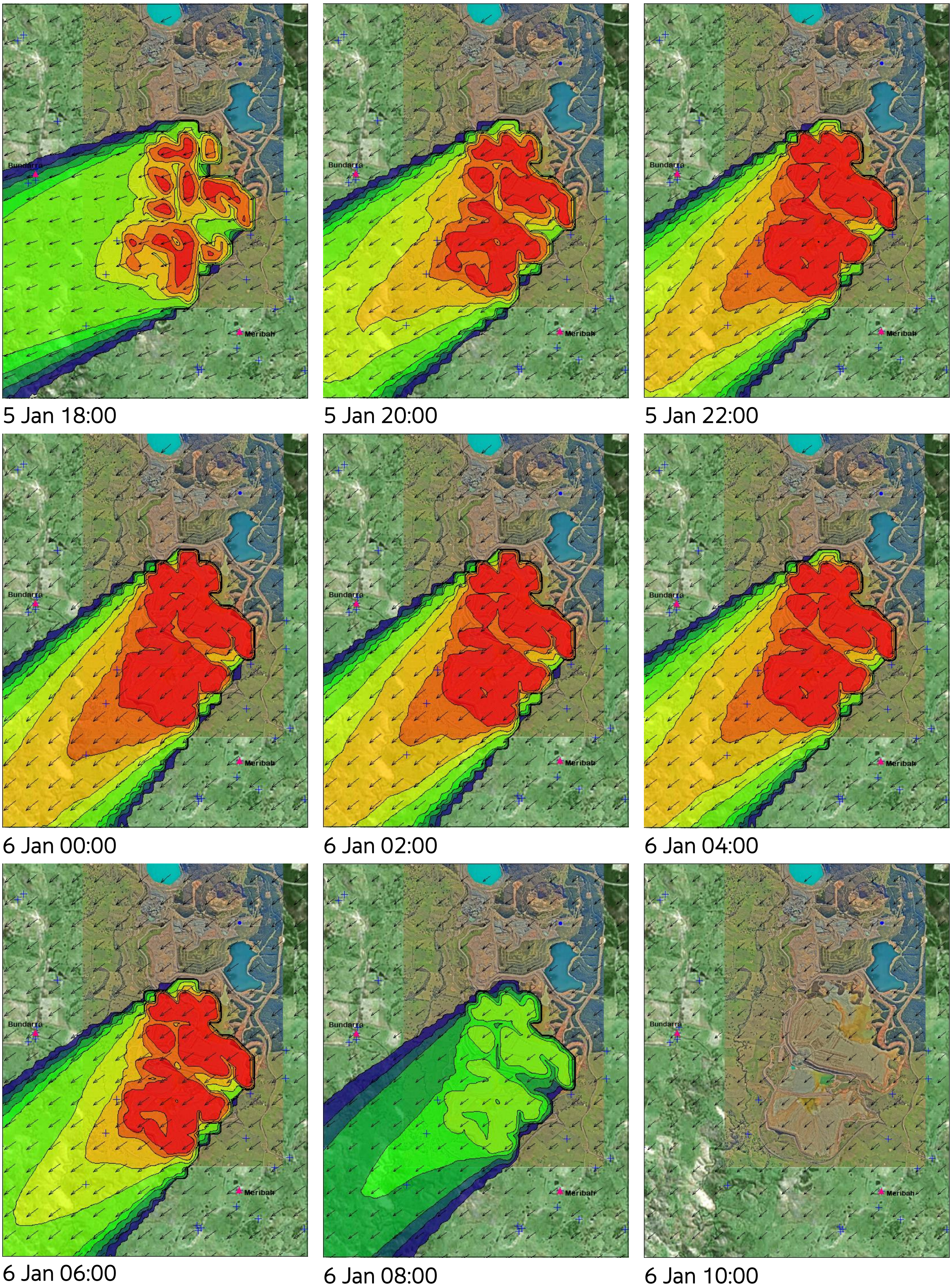

Figure K-2: Simulation of dust lift-off from TSFs on 5-6 January 2022, based on the threshold friction velocity calculation method and assuming u_t = 0.5 m/s and no controls.

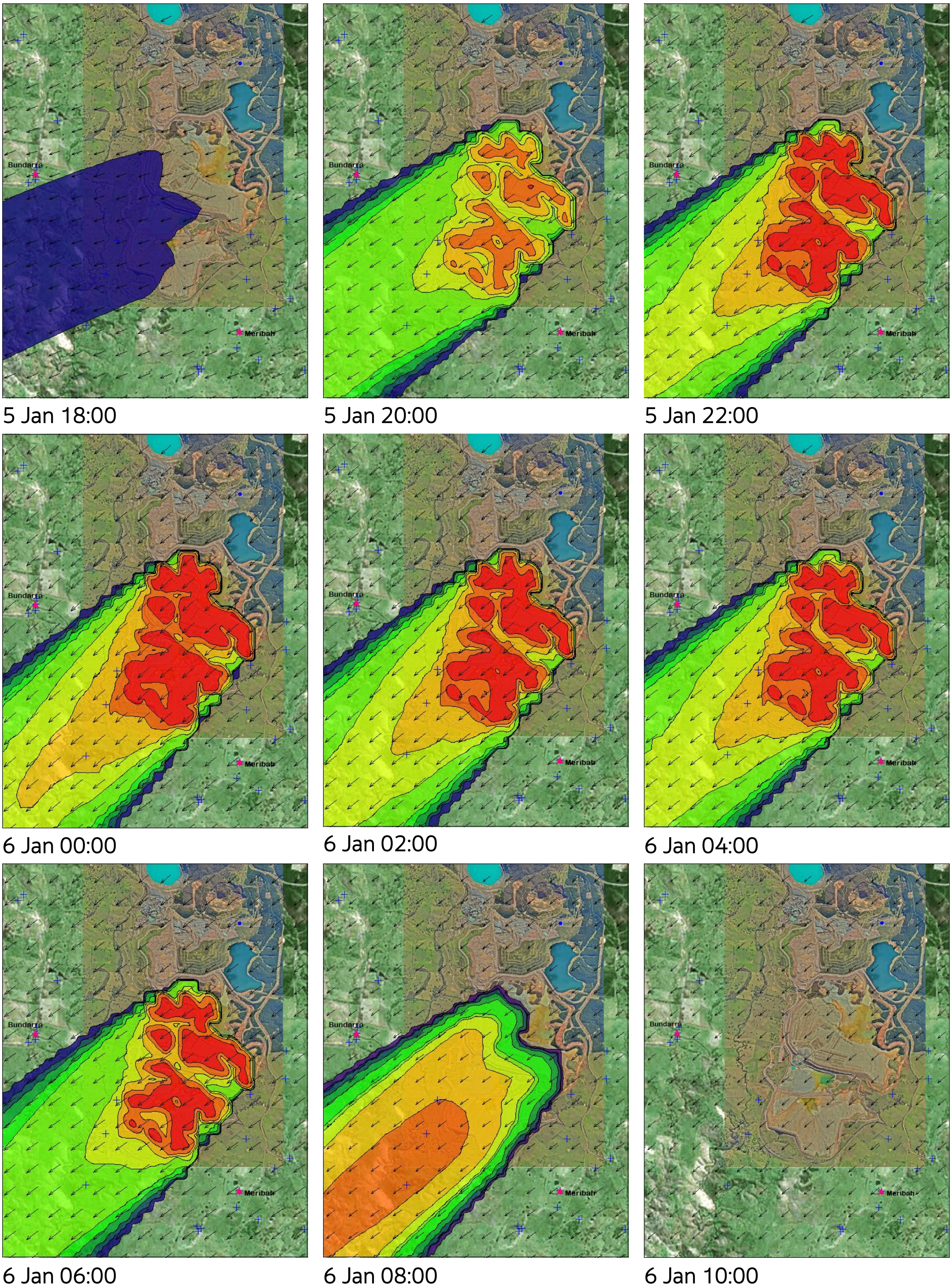

Figure K-3: Simulation of dust lift-off from TSFs on 5-6 January 2022, based on the threshold friction velocity calculation method and assuming u_t = 0.6 m/s and no controls.

Appendix L. TSF Wind Erosion Potential Timeseries for 3-4 August 2022

Appendix L. TSF Wind Erosion Potential Timeseries for 3-4 August 2022

Scale for all plume screenshots in this Appendix:

Concentration of PM_{10}, 1-hour average, in g/m^3 (multiply by 1×10^6 for µg/m^3)

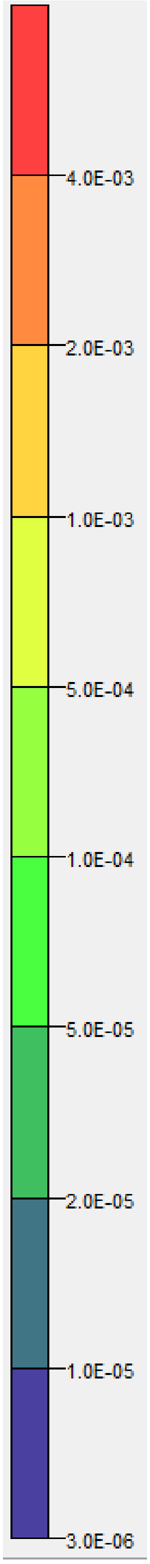

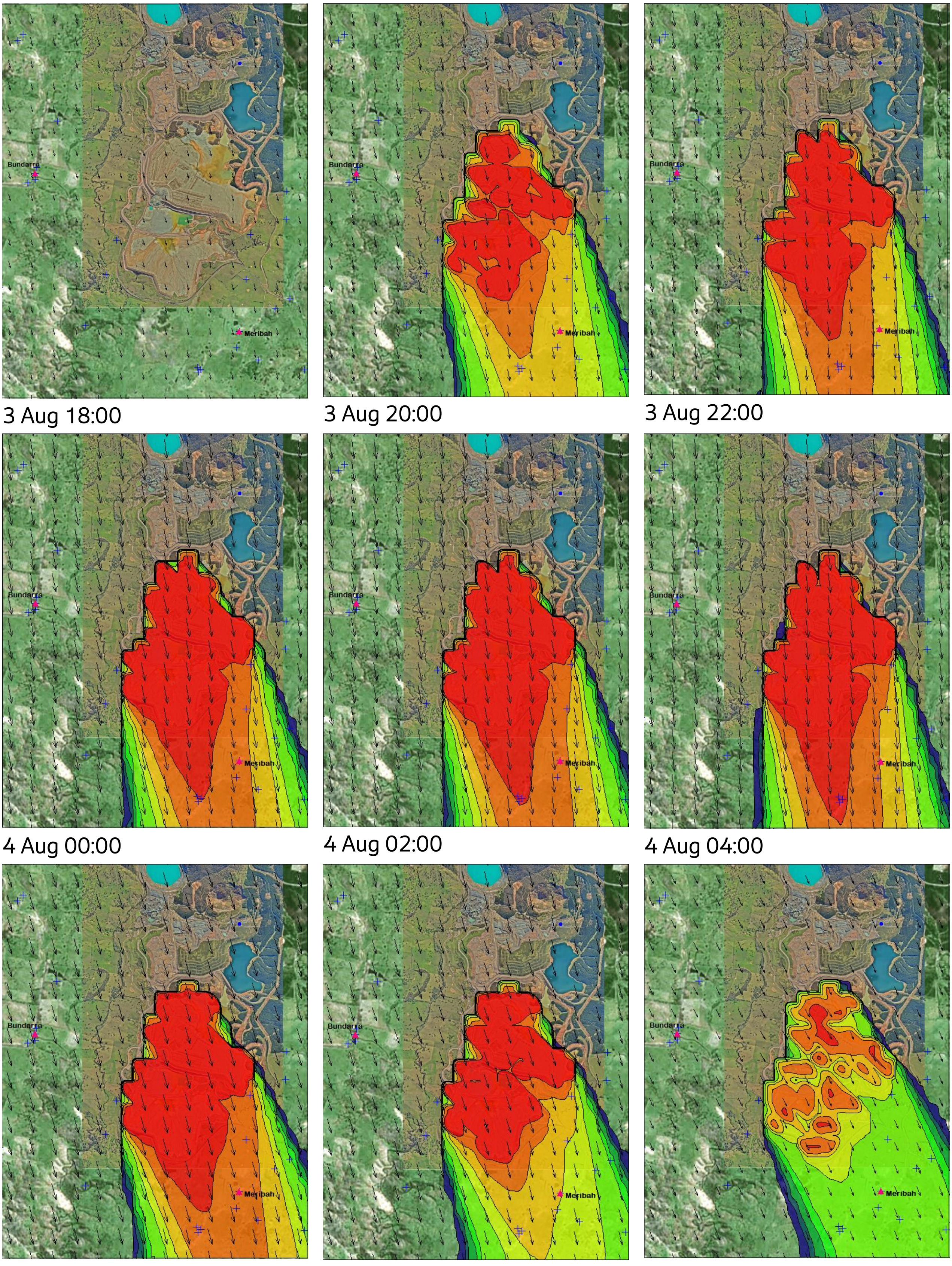

Figure L-1: Simulation of dust lift-off from TSFs on 3-4 August 2022, based on the threshold friction velocity calculation method and assuming u_t = 0.4 m/s and no controls.

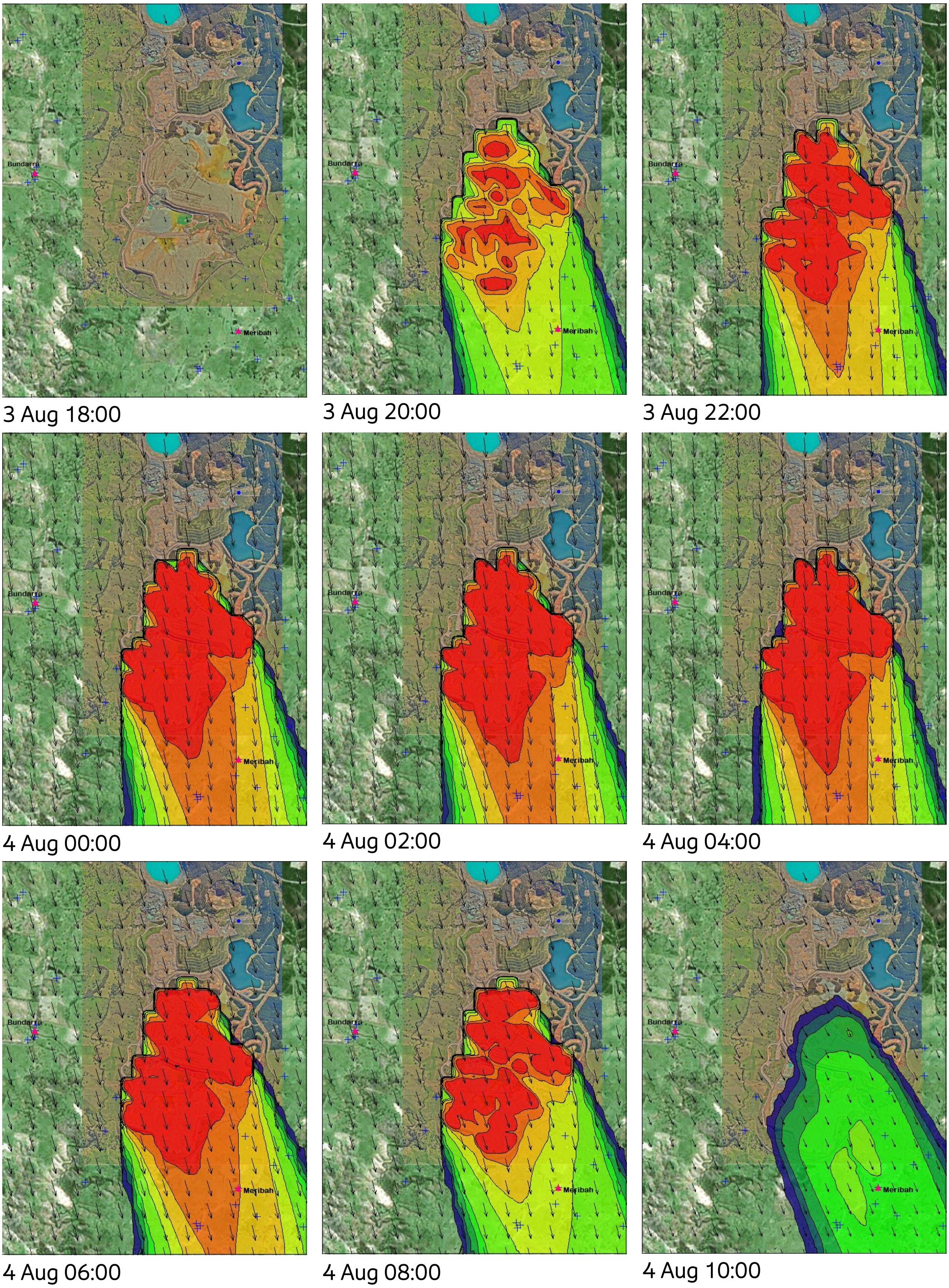

Figure L-2: Simulation of dust lift-off from TSFs on 3-4 August 2022, based on the threshold friction velocity calculation method and assuming u_t = 0.5 m/s and no controls.

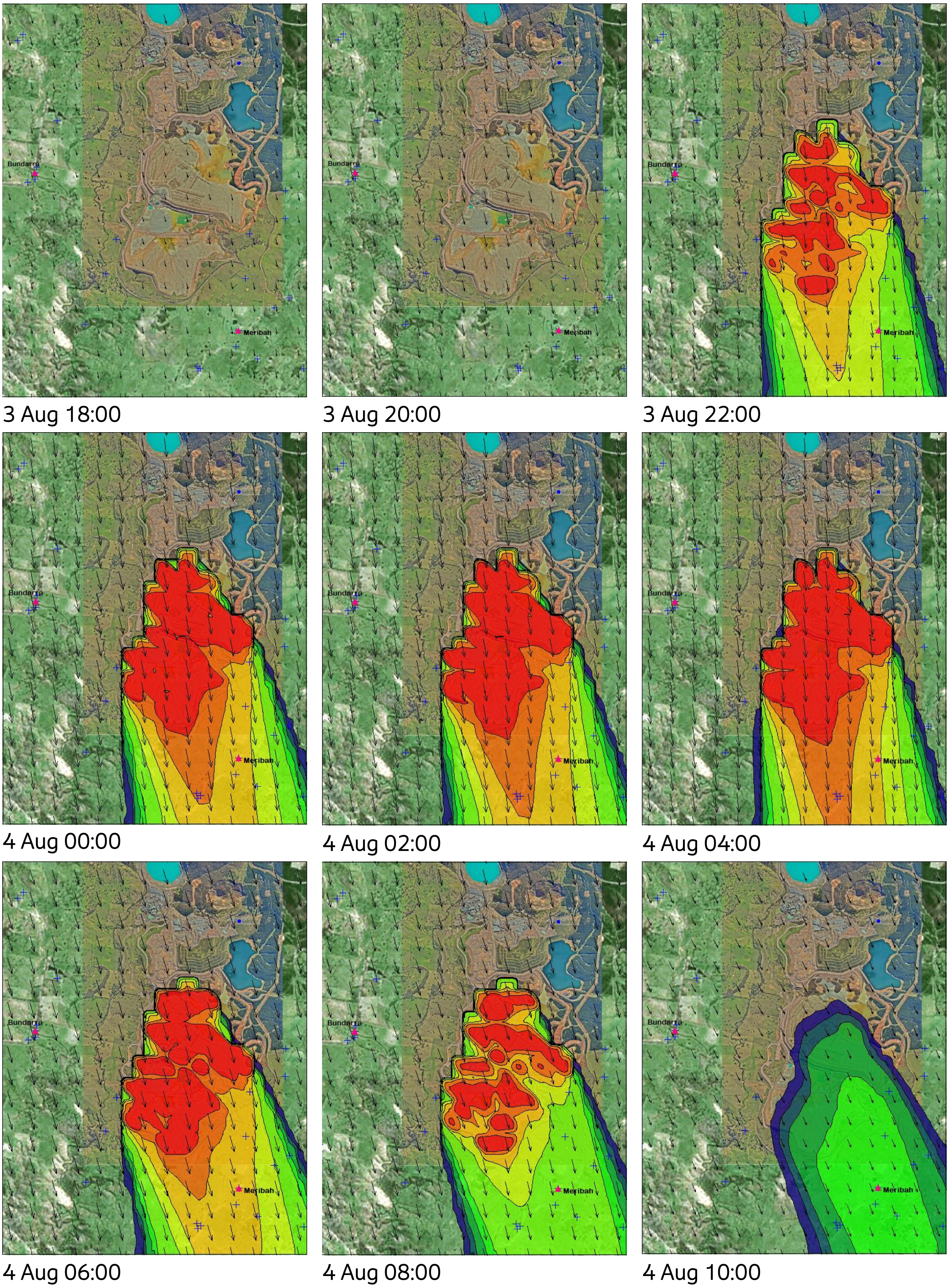

Figure L-3: Simulation of dust lift-off from TSFs on 3-4 August 2022, based on the threshold friction velocity calculation method and assuming u_t = 0.6 m/s and no controls.

Appendix M. TSF Wind Erosion Potential Timeseries for 13 October 2022

Appendix M. TSF Wind Erosion Potential Timeseries for 13 October 2022

Scale for all plume screenshots in this Appendix:

Concentration of PM_{10}, 1-hour average, in g/m^3 (multiply by $1x10^6$ for µg/m^3)

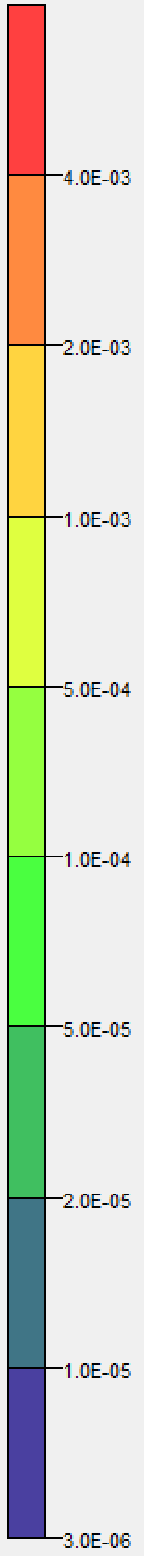

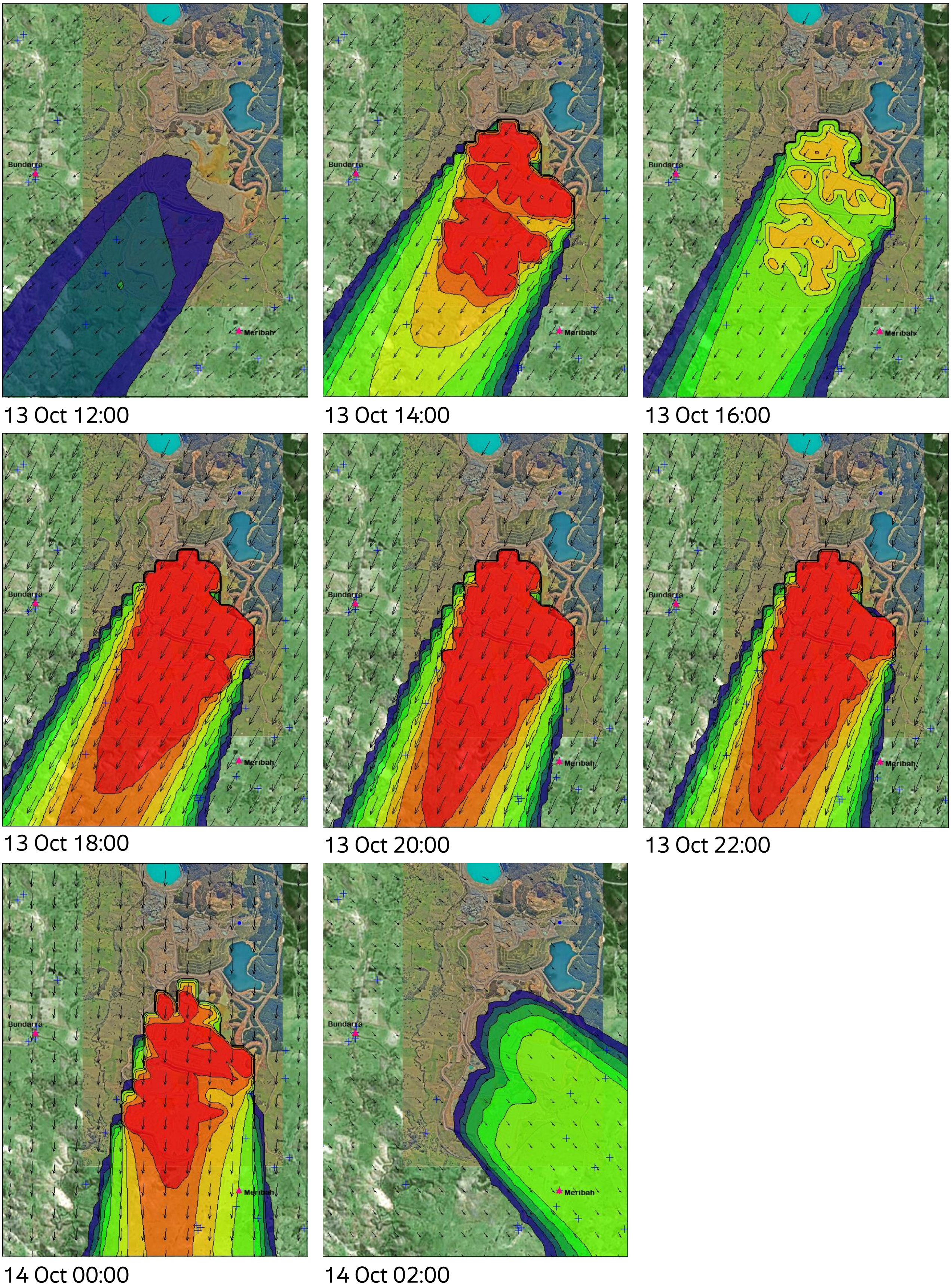

Figure M-1: Simulation of dust lift-off from TSFs on 13 October 2022, based on the threshold friction velocity calculation method and assuming u_t = 0.4 m/s and no controls.

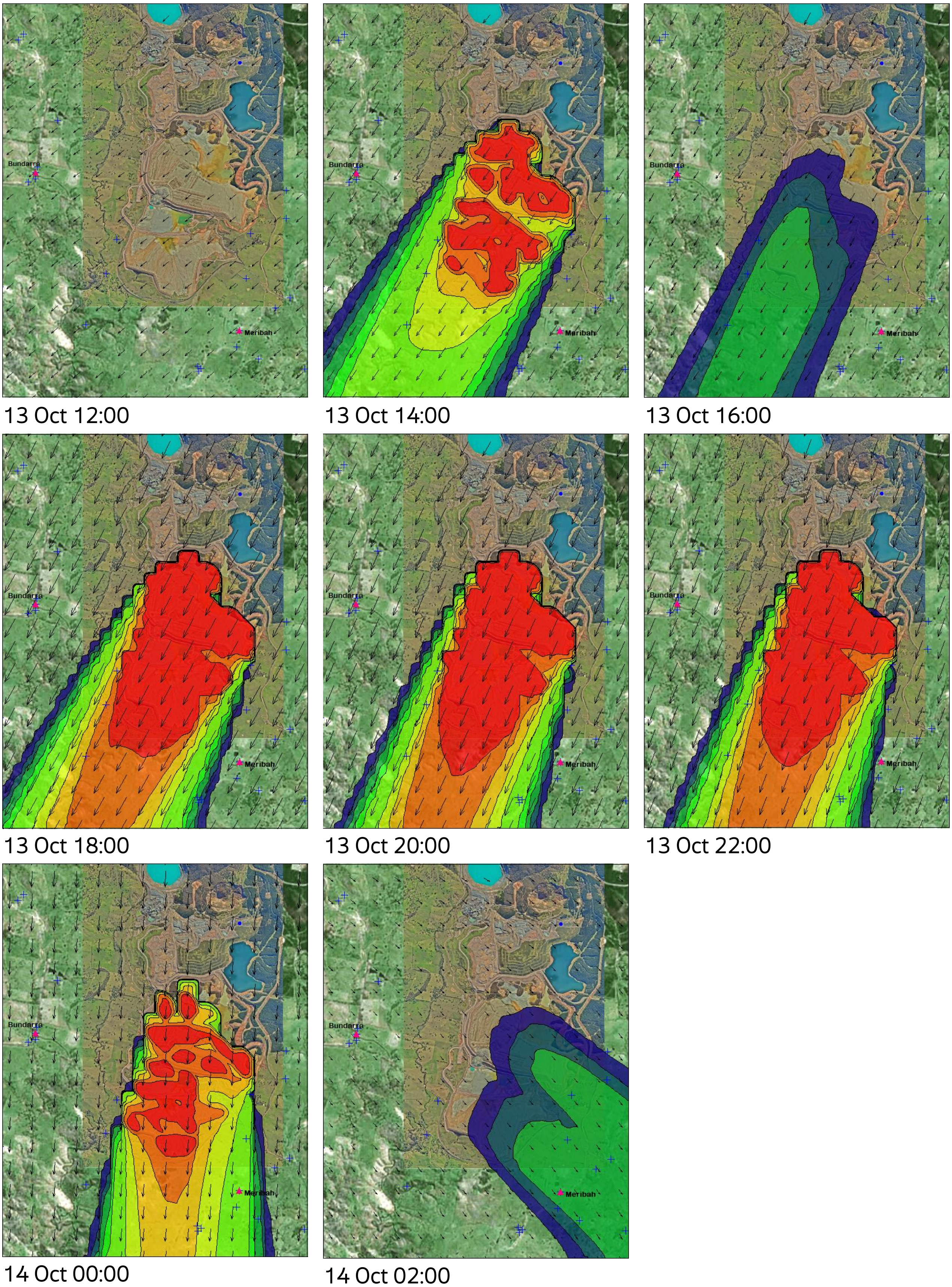

Figure M-2: Simulation of dust lift-off from TSFs on 13 October 2022, based on the threshold friction velocity calculation method and assuming u_t = 0.5 m/s and no controls.

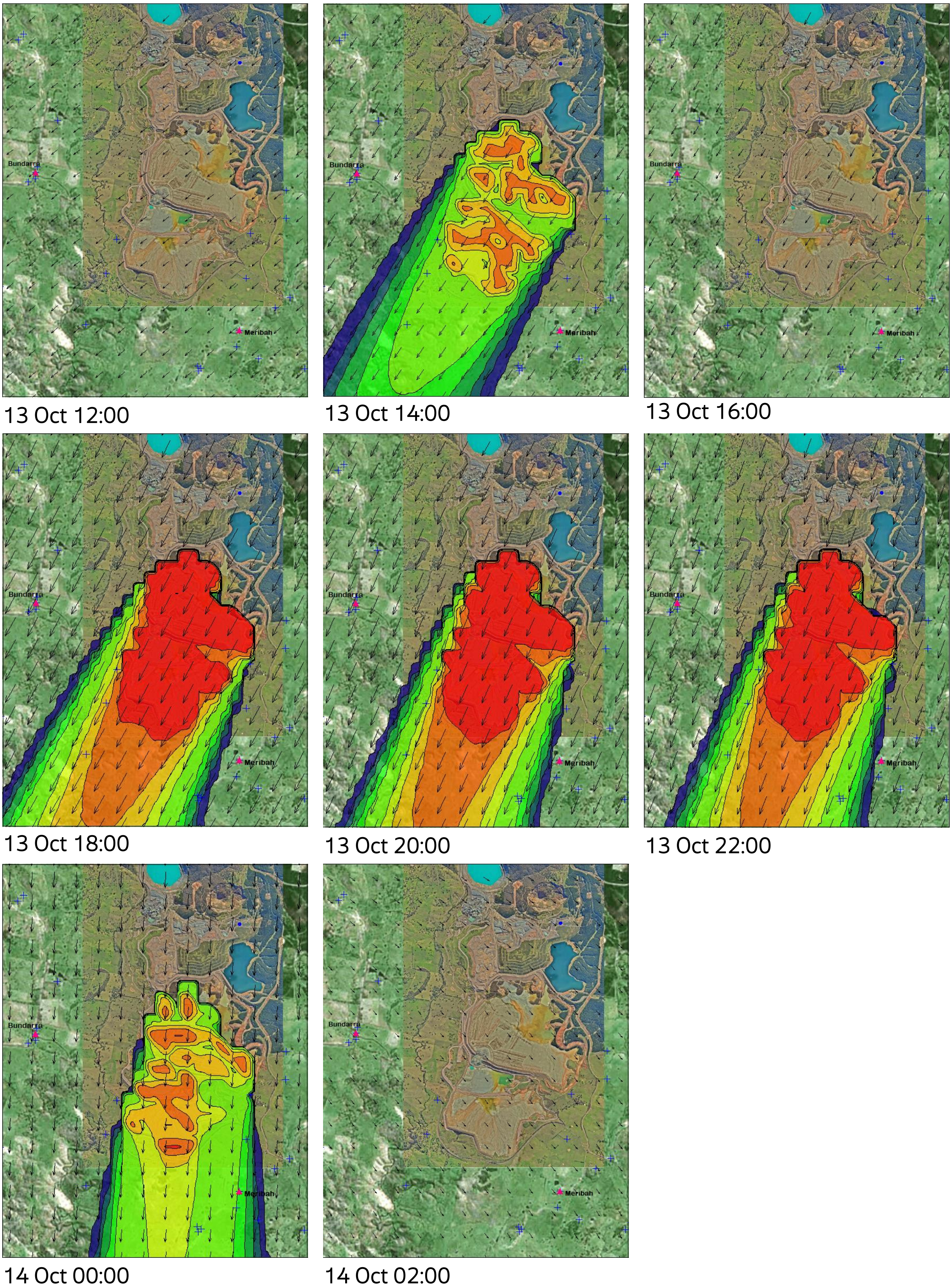

Figure M-3: Simulation of dust lift-off from TSFs on 13 October 2022, based on the threshold friction velocity calculation method and assuming u_t = 0.6 m/s and no controls.

Appendix N. TSF Wind Erosion Potential Timeseries for 31 October 2022

Appendix N. TSF Wind Erosion Potential Timeseries for 31 October 2022

Scale for all plume screenshots in this Appendix:

Concentration of PM_{10}, 1-hour average, in g/m^3 (multiply by 1×10^6 for μg/m^3)

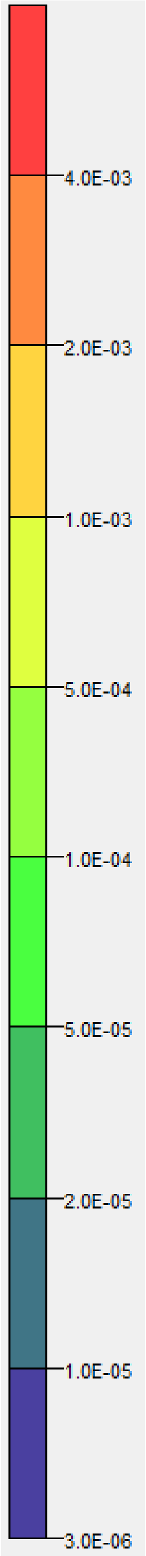

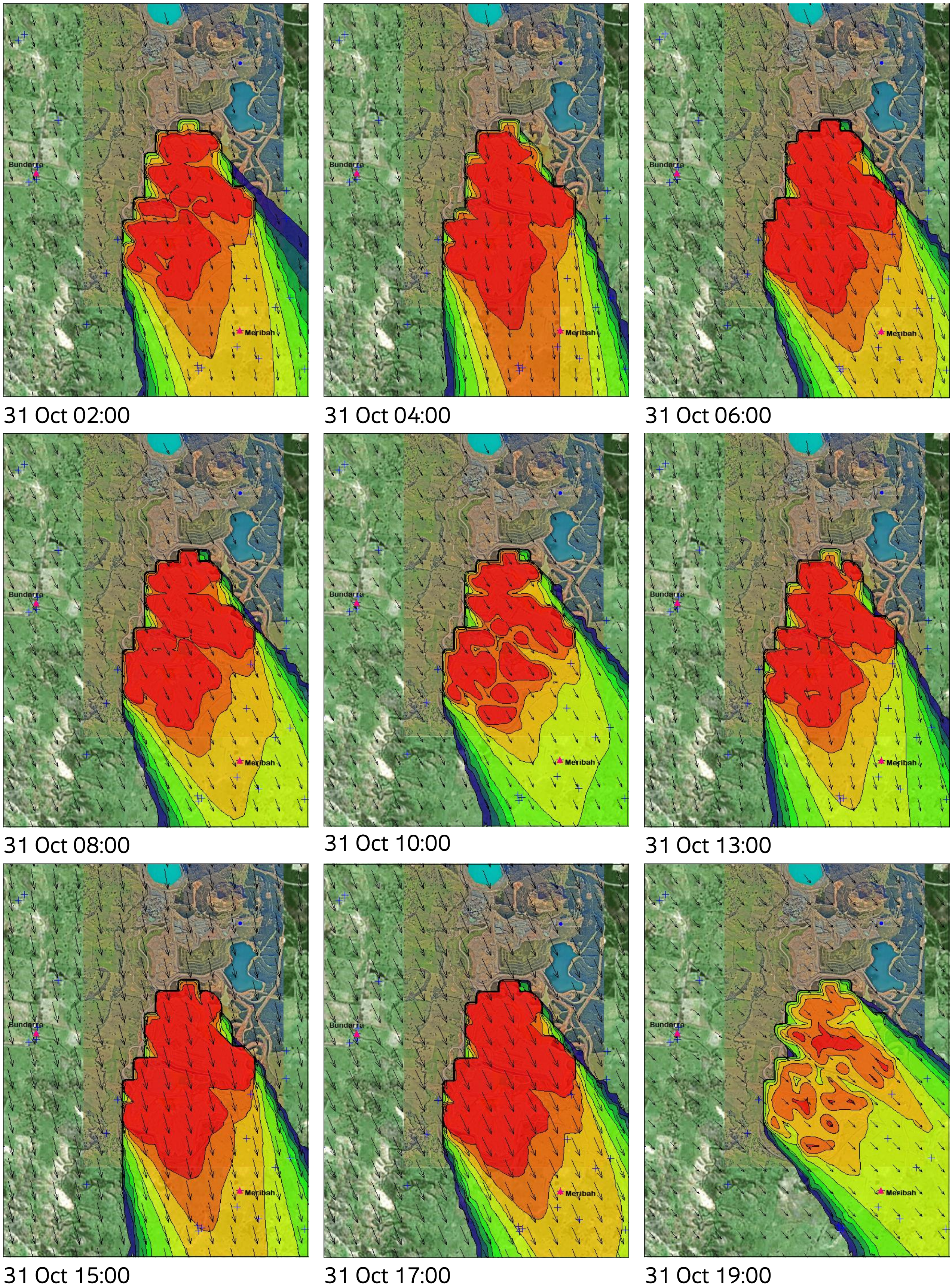

Figure N-1: Simulation of dust lift-off from TSFs on 31 October 2022, based on the threshold friction velocity calculation method and assuming u_t = 0.4 m/s and no controls.

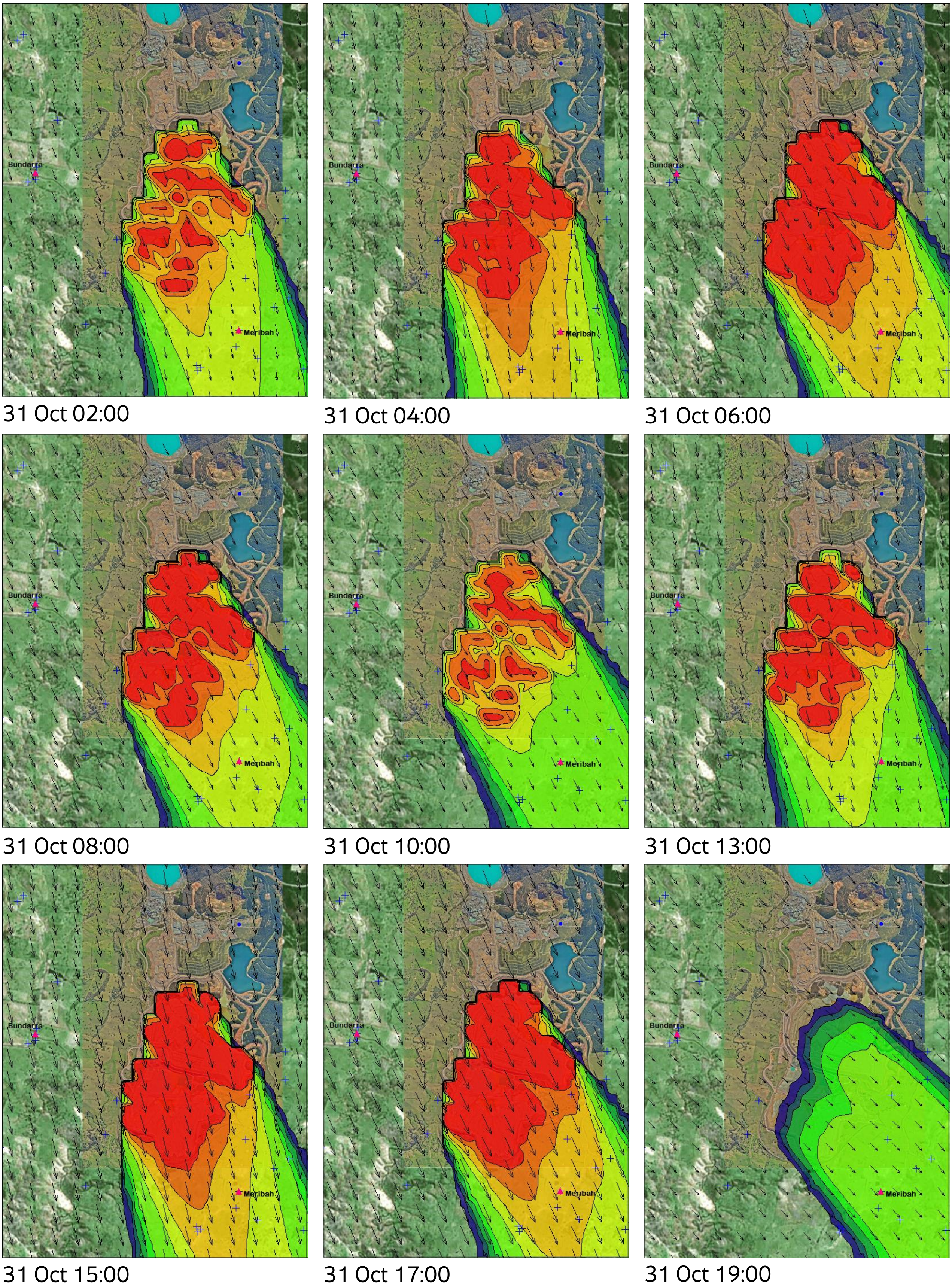

Figure N-2: Simulation of dust lift-off from TSFs on 31 October 2022, based on the threshold friction velocity calculation method and assuming u_t = 0.5 m/s and no controls.

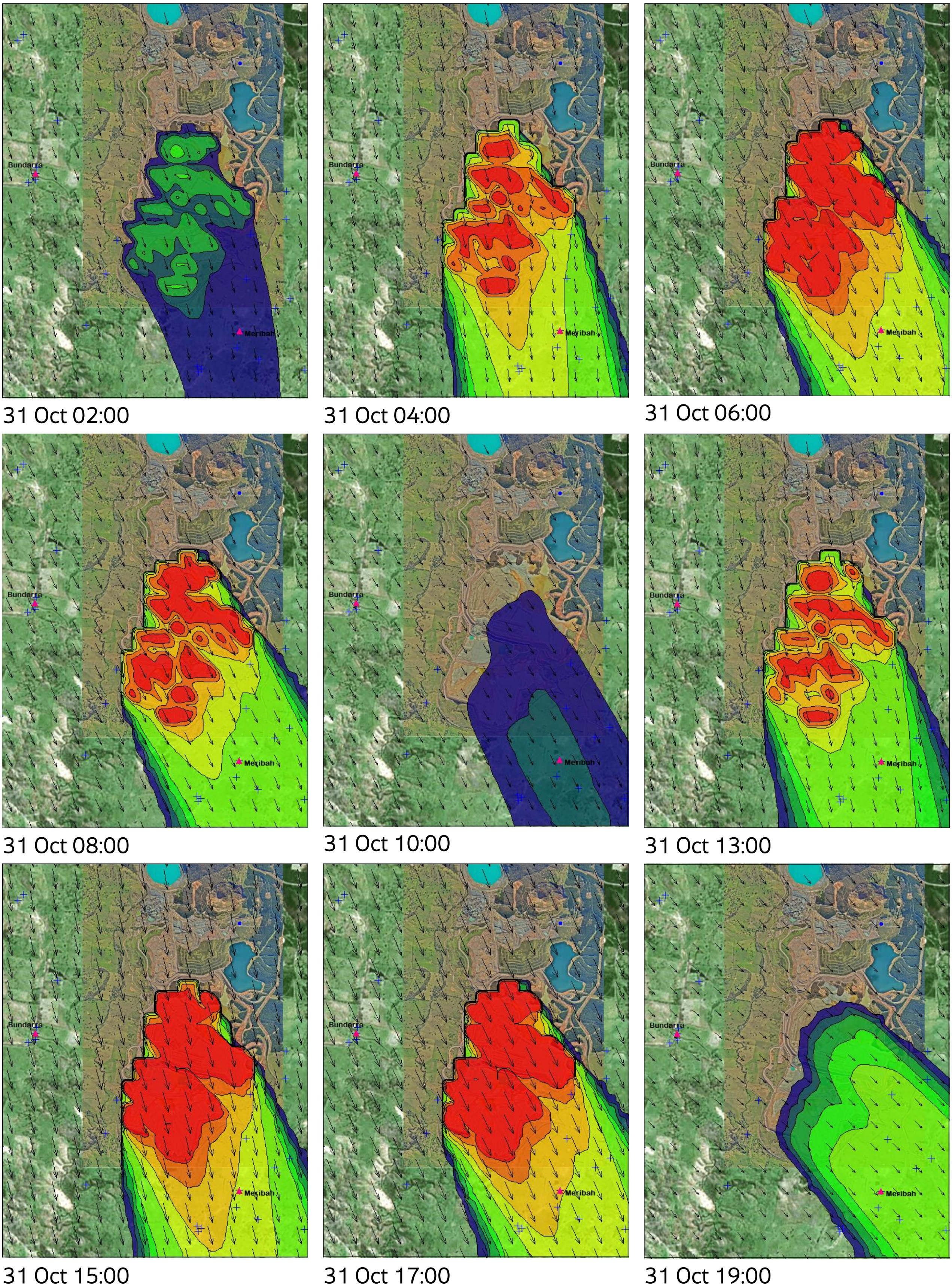

Figure N-3: Simulation of dust lift-off from TSFs on 31 October 2022, based on the threshold friction velocity calculation method and assuming u_t = 0.6 m/s and no controls.

Appendix O. TSF Wind Erosion Potential Timeseries for 12-13 November 2022

Appendix O. TSF Wind Erosion Potential Timeseries for 12-13 November 2022

Scale for all plume screenshots in this Appendix:

Concentration of PM_{10}, 1-hour average, in g/m^3 (multiply by $1x10^6$ for µg/m^3)

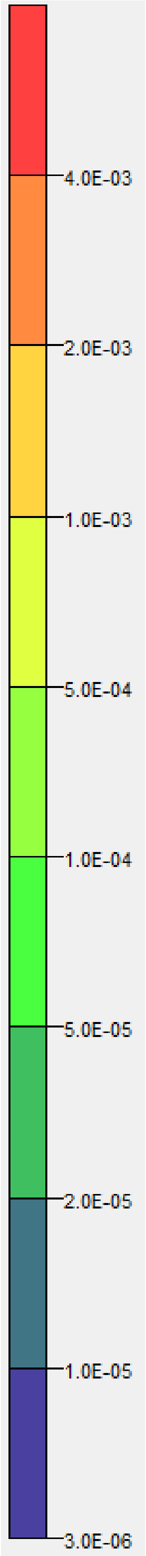

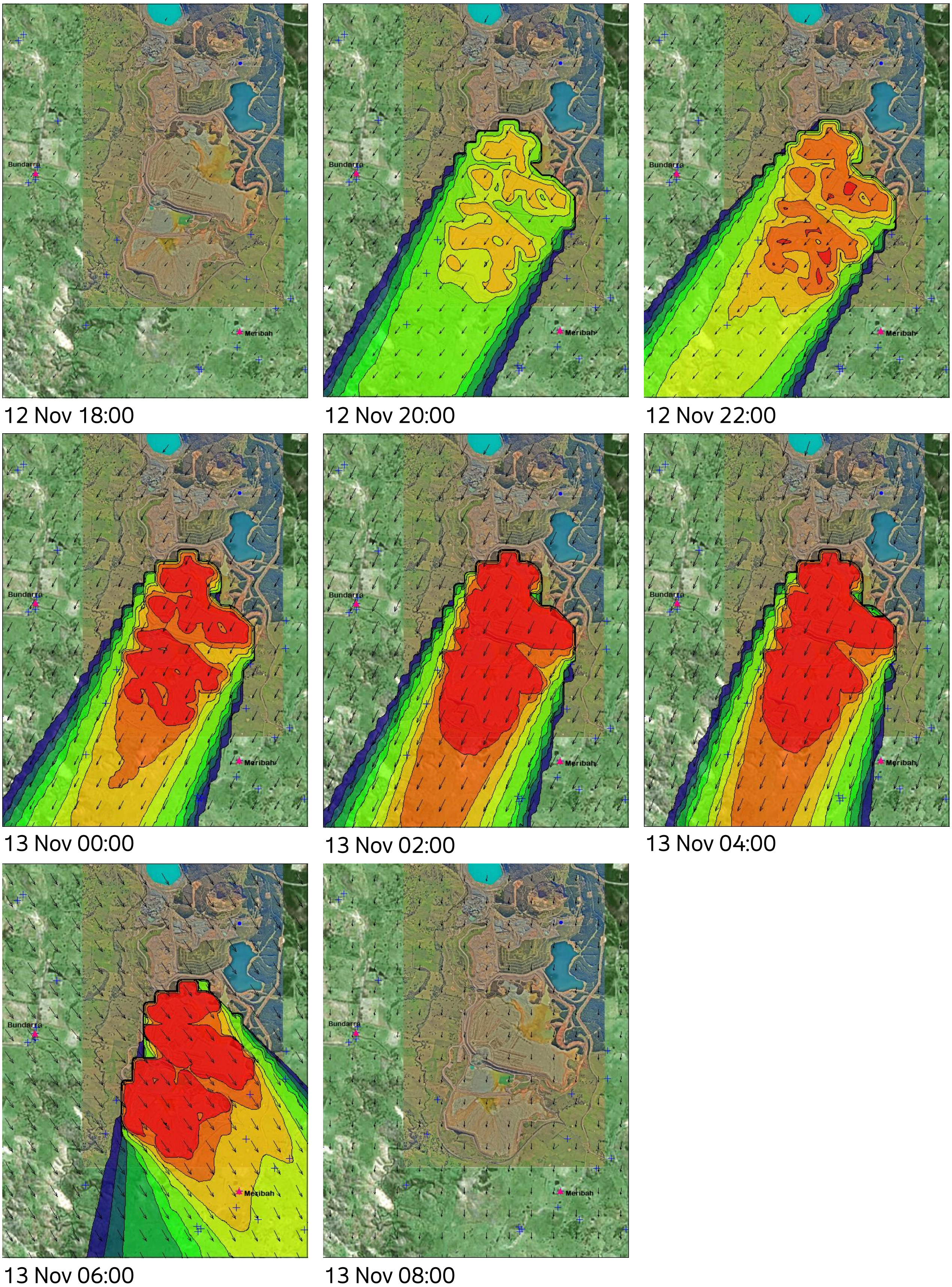

Figure O-1: Simulation of dust lift-off from TSFs on 12-13 November 2022, based on the threshold friction velocity calculation method and assuming u_t = 0.4 m/s and no controls.

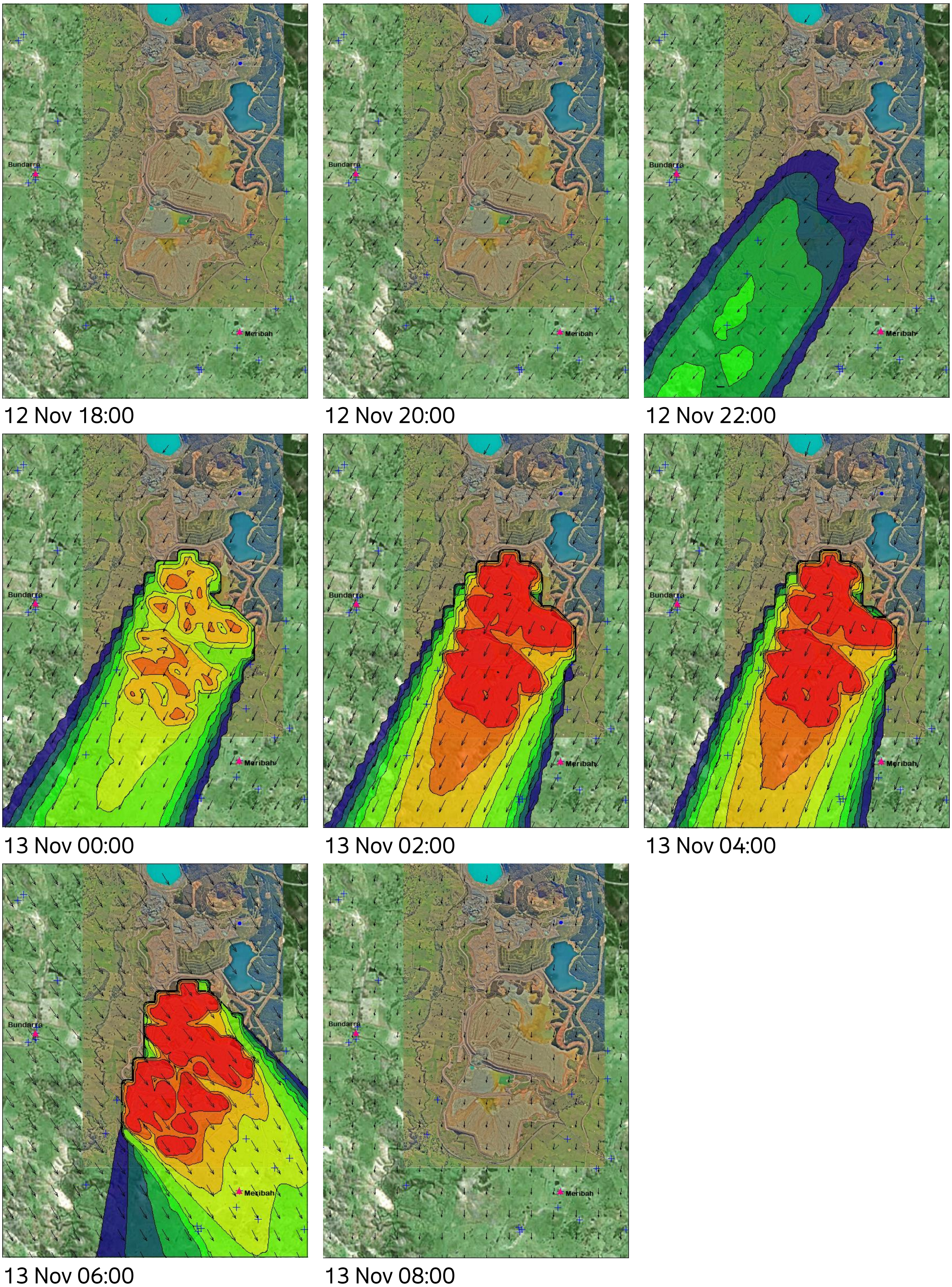

Figure O-2: Simulation of dust lift-off from TSFs on 12-13 November 2022, based on the threshold friction velocity calculation method and assuming u_t = 0.5 m/s and no controls.

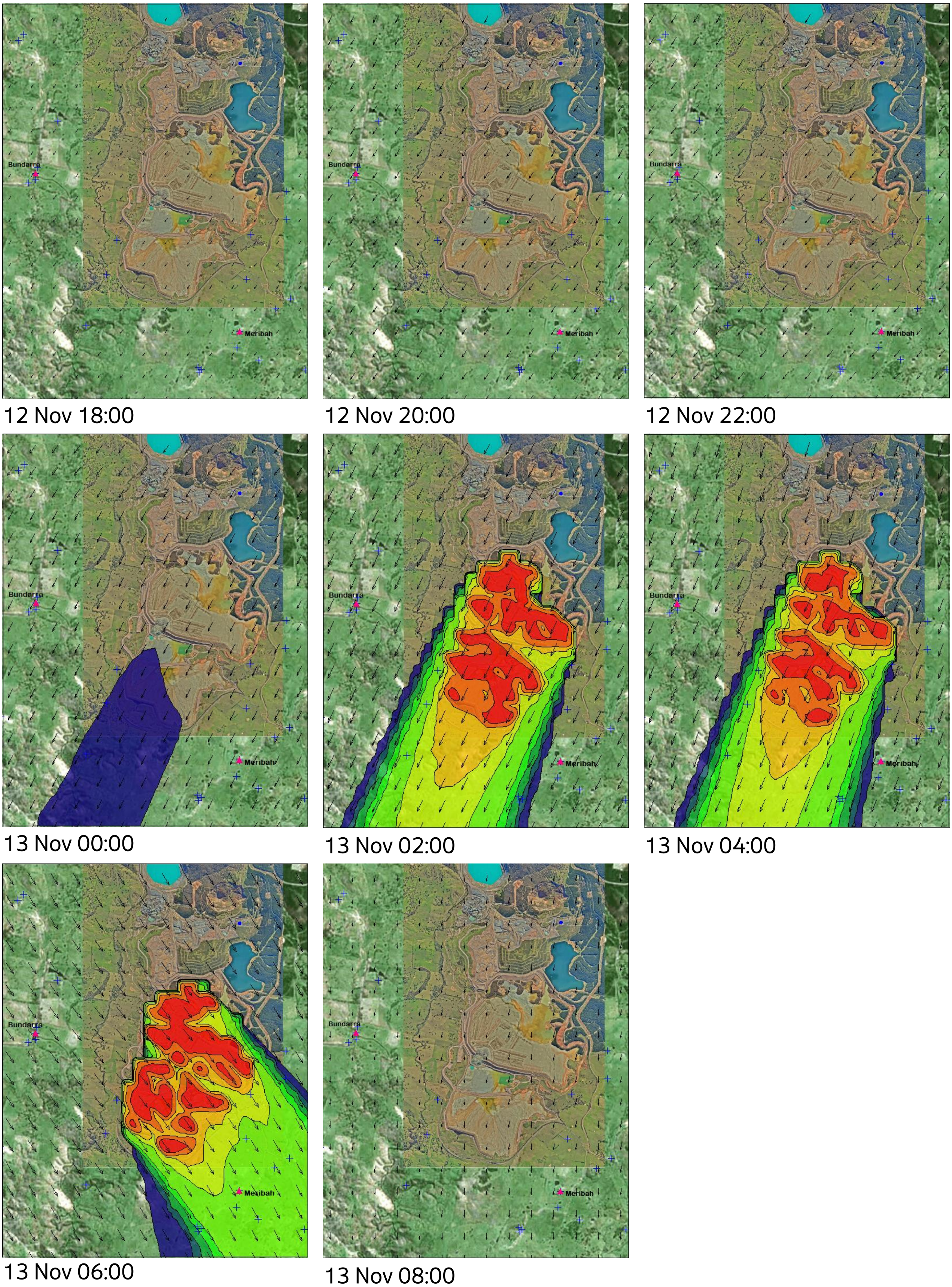

Figure O-3: Simulation of dust lift-off from TSFs on 12-13 November 2022, based on the threshold friction velocity calculation method and assuming u_t = 0.6 m/s and no controls.

Appendix P. TSF Wind Erosion Potential Timeseries for 11-12 December 2022

Appendix P. TSF Wind Erosion Potential Timeseries for 11-12 December 2022

Scale for all plume screenshots in this Appendix:

Concentration of PM_{10}, 1-hour average, in g/m^3 (multiply by 1x10^6 for µg/m^3)

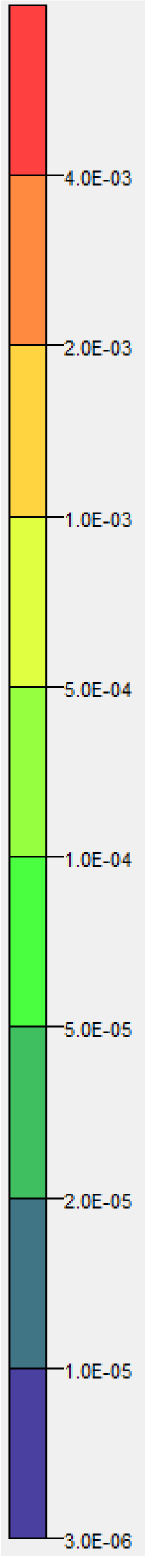

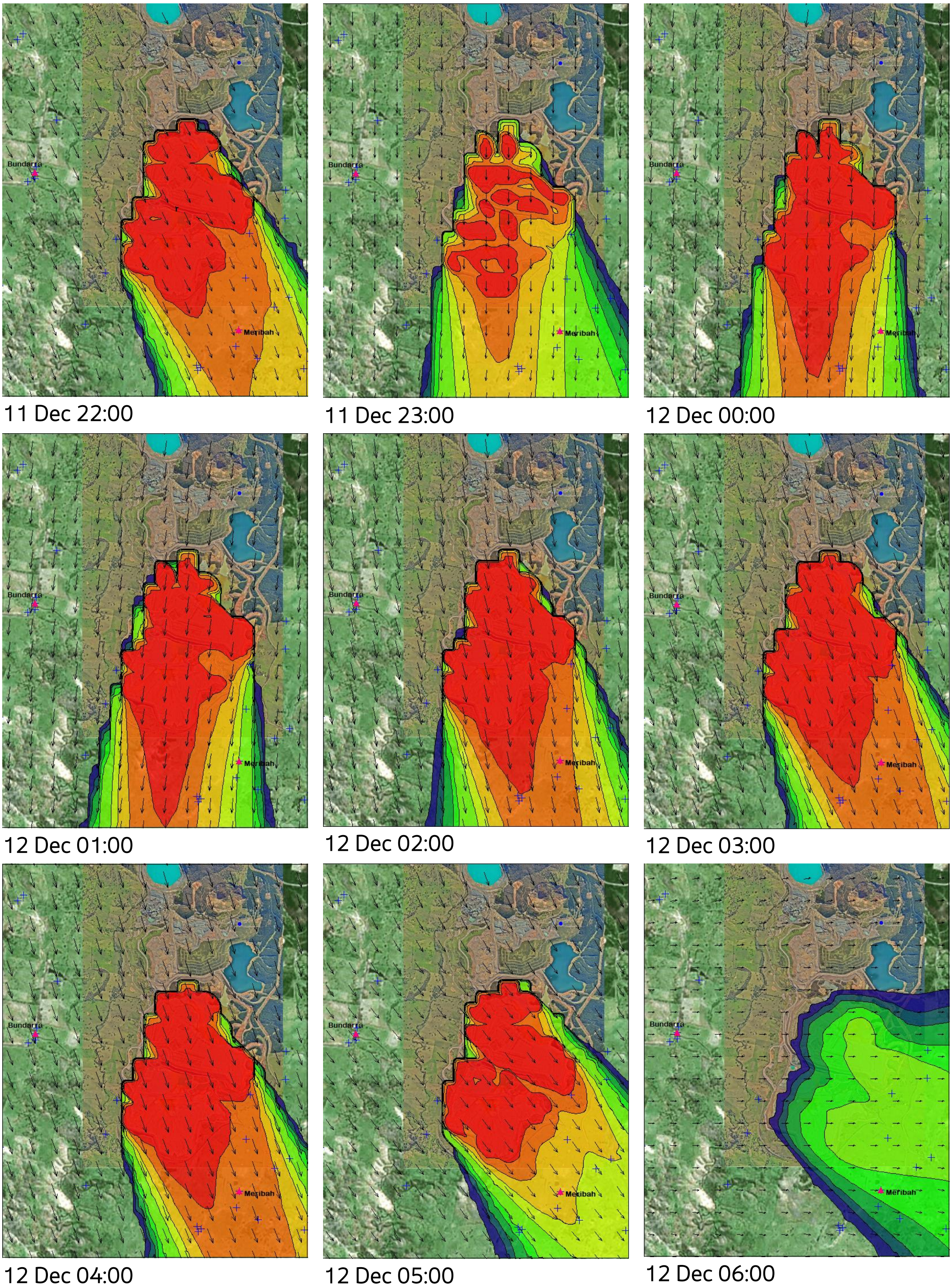

Figure P-1: Simulation of dust lift-off from TSFs on 11-12 December 2022, based on the threshold friction velocity calculation method and assuming u_t = 0.4 m/s and no controls.

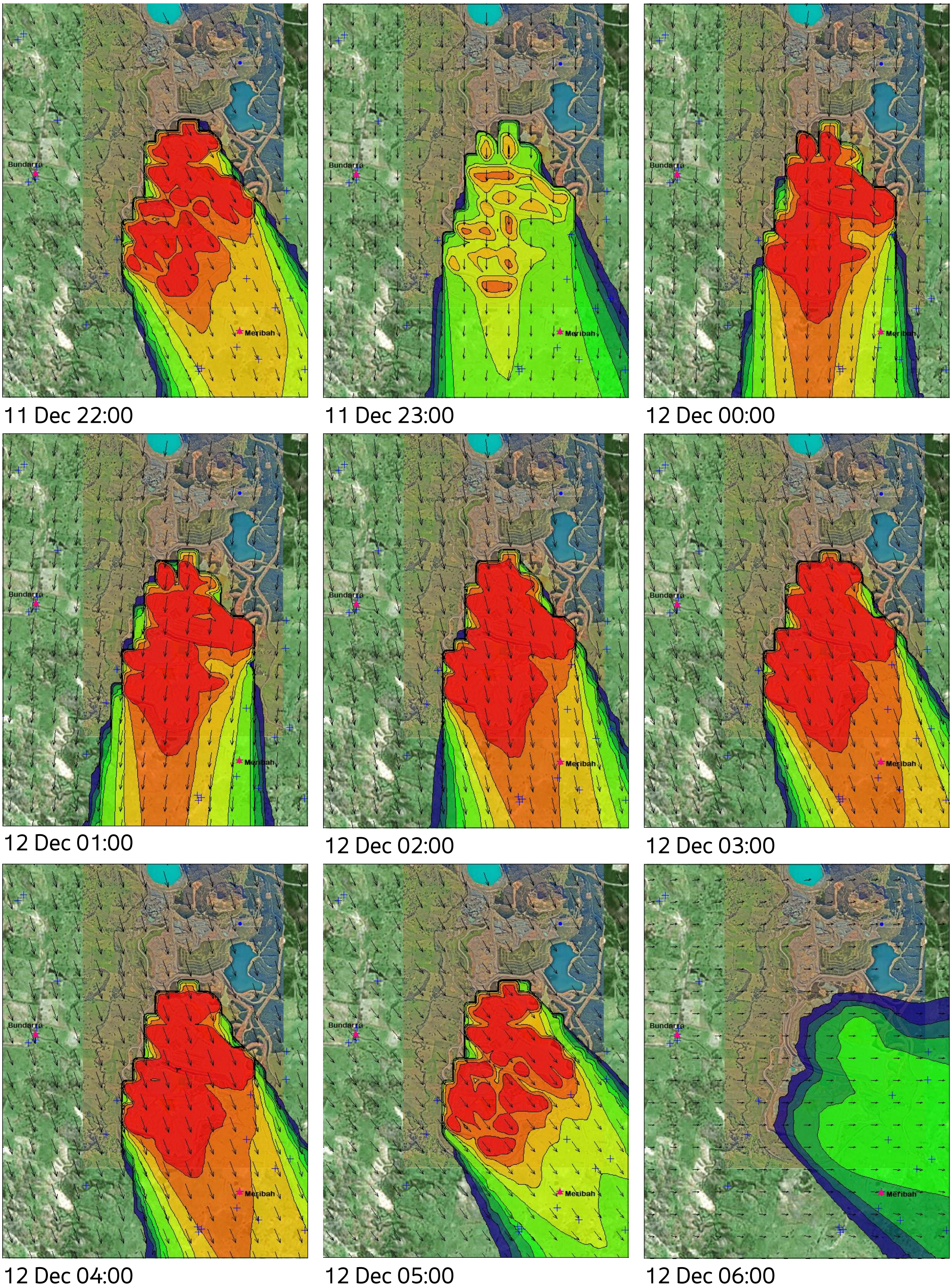

Figure P-2: Simulation of dust lift-off from TSFs on 11-12 December 2022, based on the threshold friction velocity calculation method and assuming u_t = 0.5 m/s and no controls.

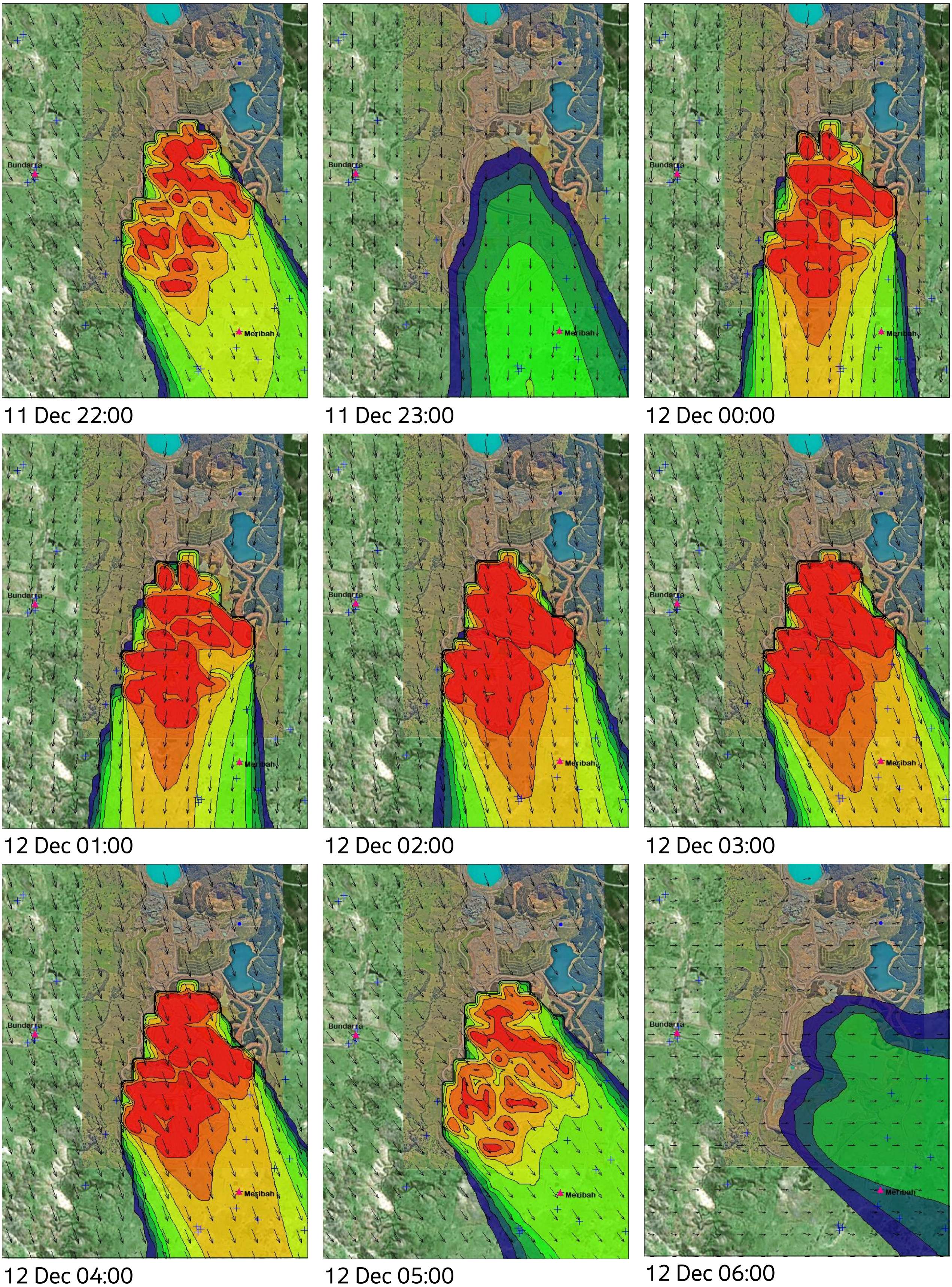

Figure P-3: Simulation of dust lift-off from TSFs on 11-12 December 2022, based on the threshold friction velocity calculation method and assuming u_t = 0.6 m/s and no controls.

Appendix Q. Model Results for Vents

Appendix Q. Model Results for Vents

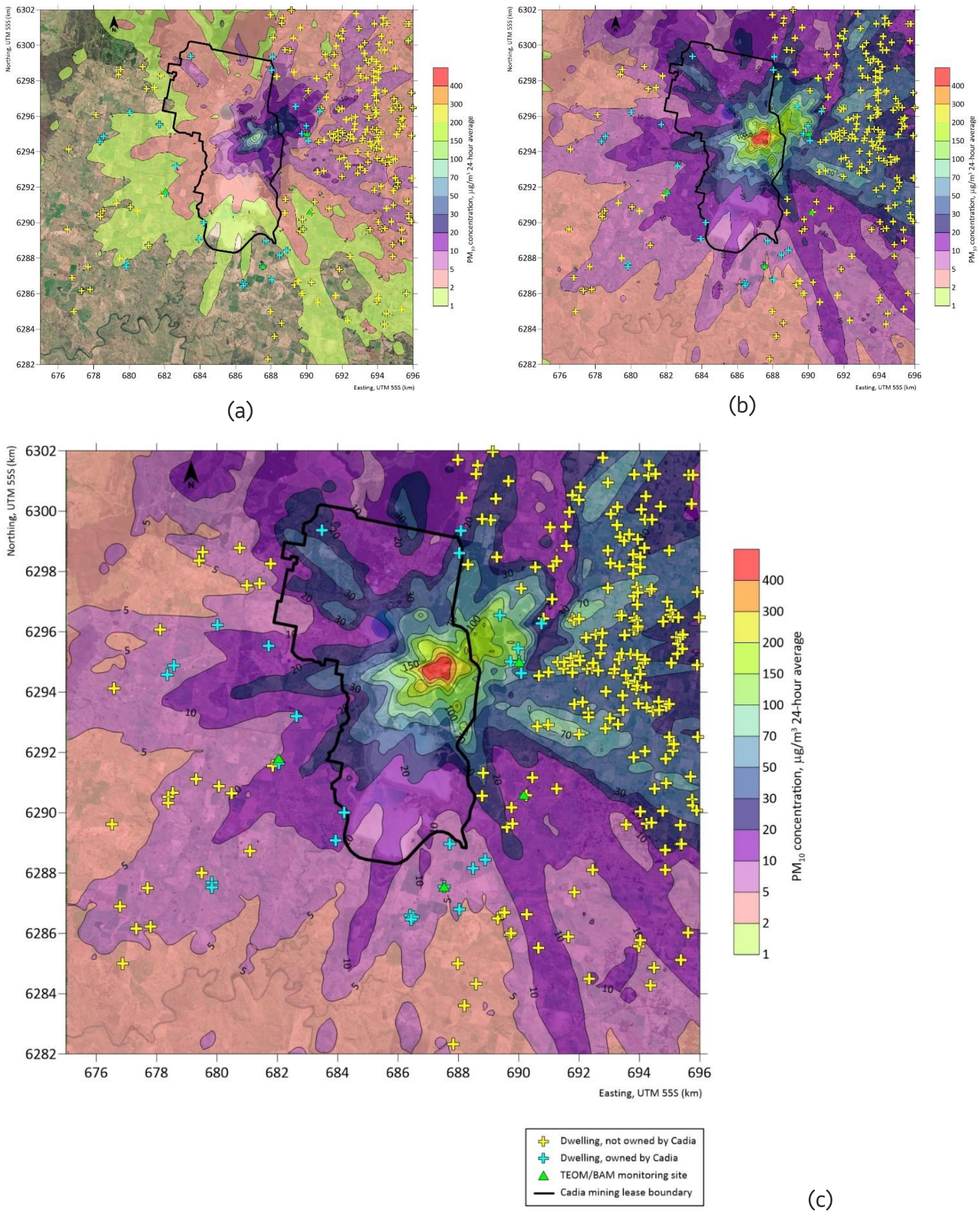

Figure Q-1: 24-hour average concentrations of PM_{10} due only to vent emissions, Option 1.
(a) VR3A, VR5 and VR7 (b) VR8 (c) All vents combined

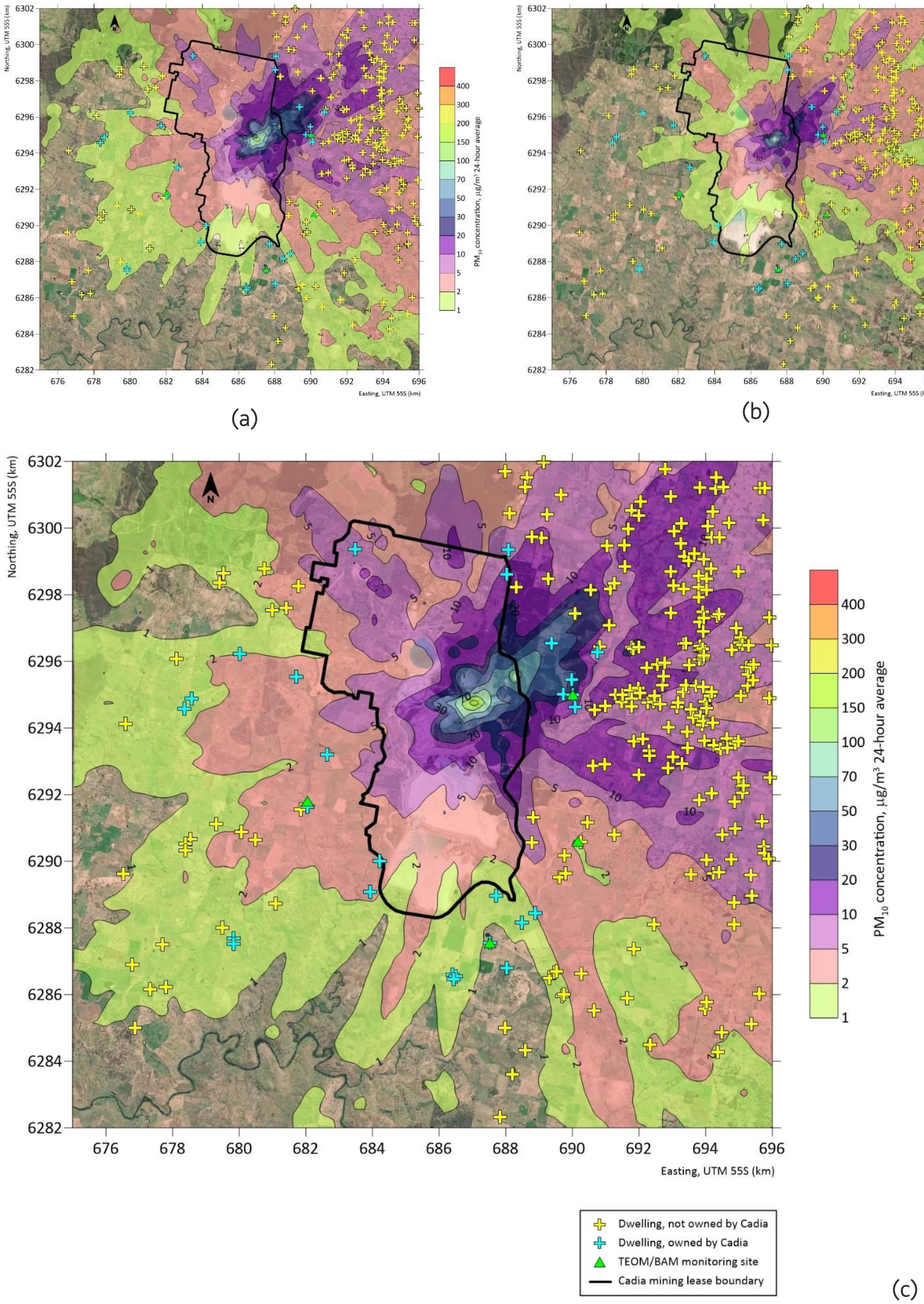

Figure Q-2: 24-hour average concentrations of PM$_{10}$ due only to vent emissions, Option 2.
(a) VR3A, VR5 and VR7 (b) VR8 (c) All vents combined

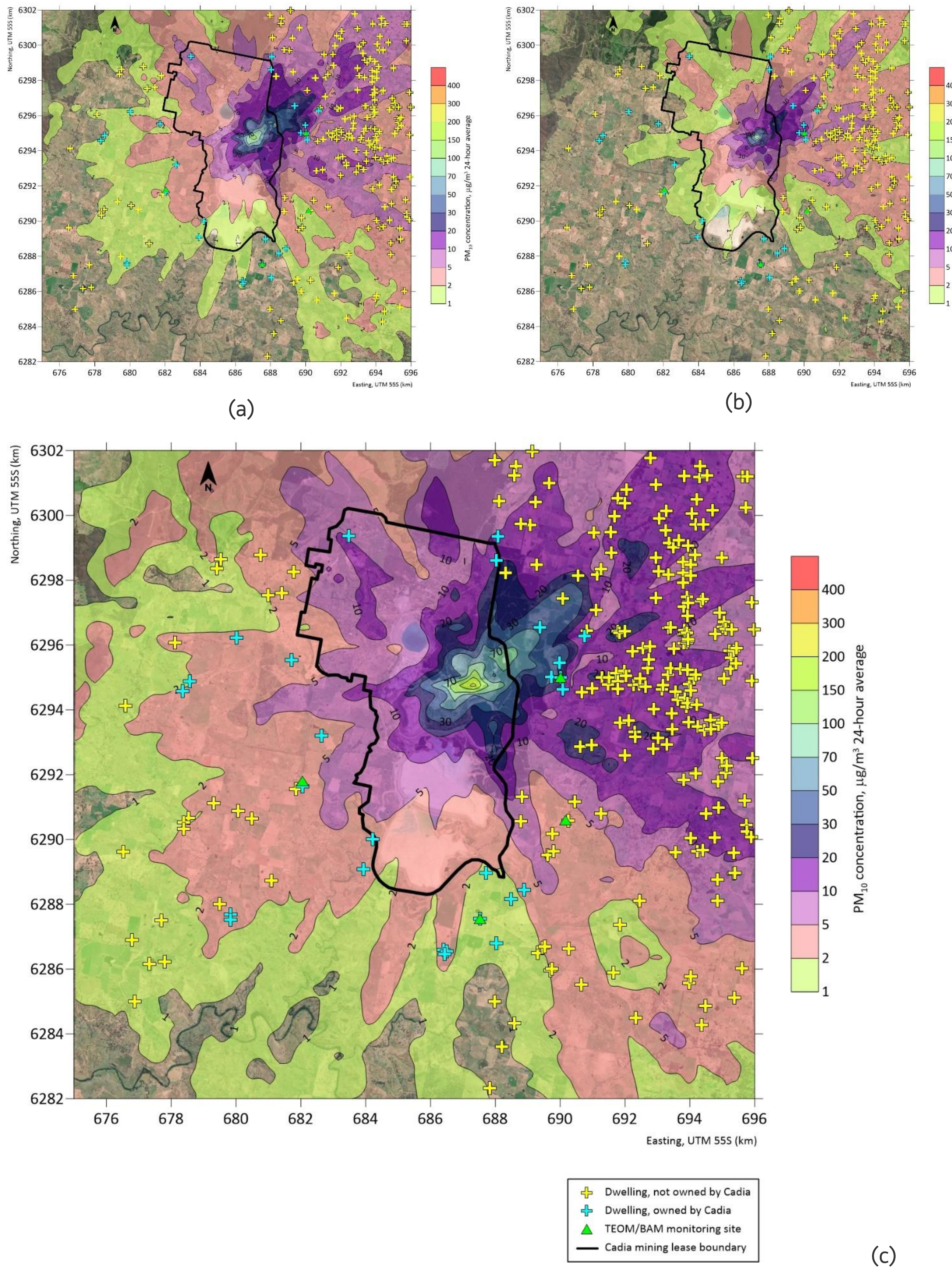

Figure Q-3: 24-hour average concentrations of PM_{10} due only to vent emissions, Option 3.
(a) VR3A, VR5 and VR7 (b) VR8 (c) All vents combined

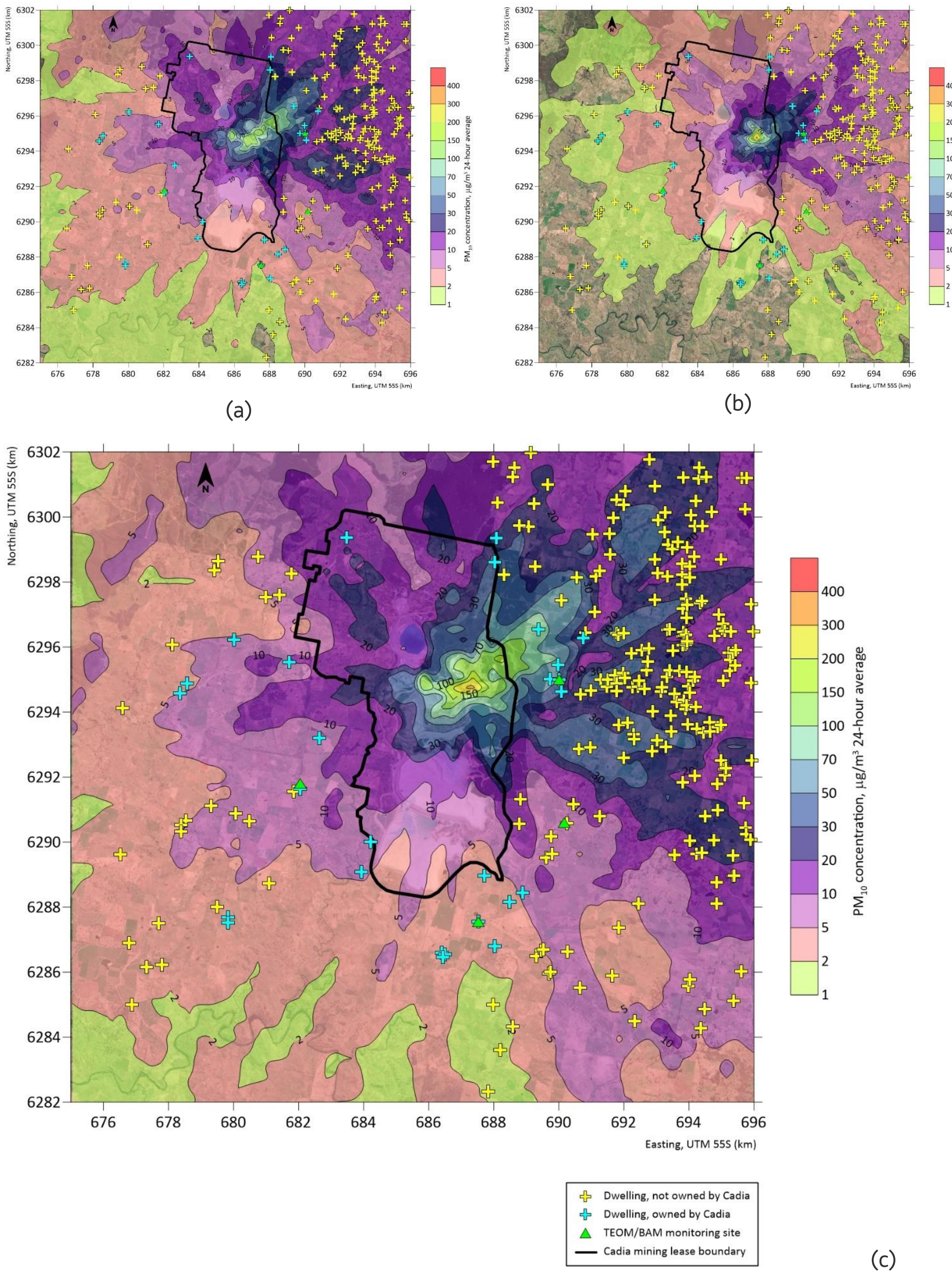

Figure Q-4: 24-hour average concentrations of PM_{10} due only to vent emissions, Option 4.
(a) VR3A, VR5 and VR7 (b) VR8 (c) All vents combined

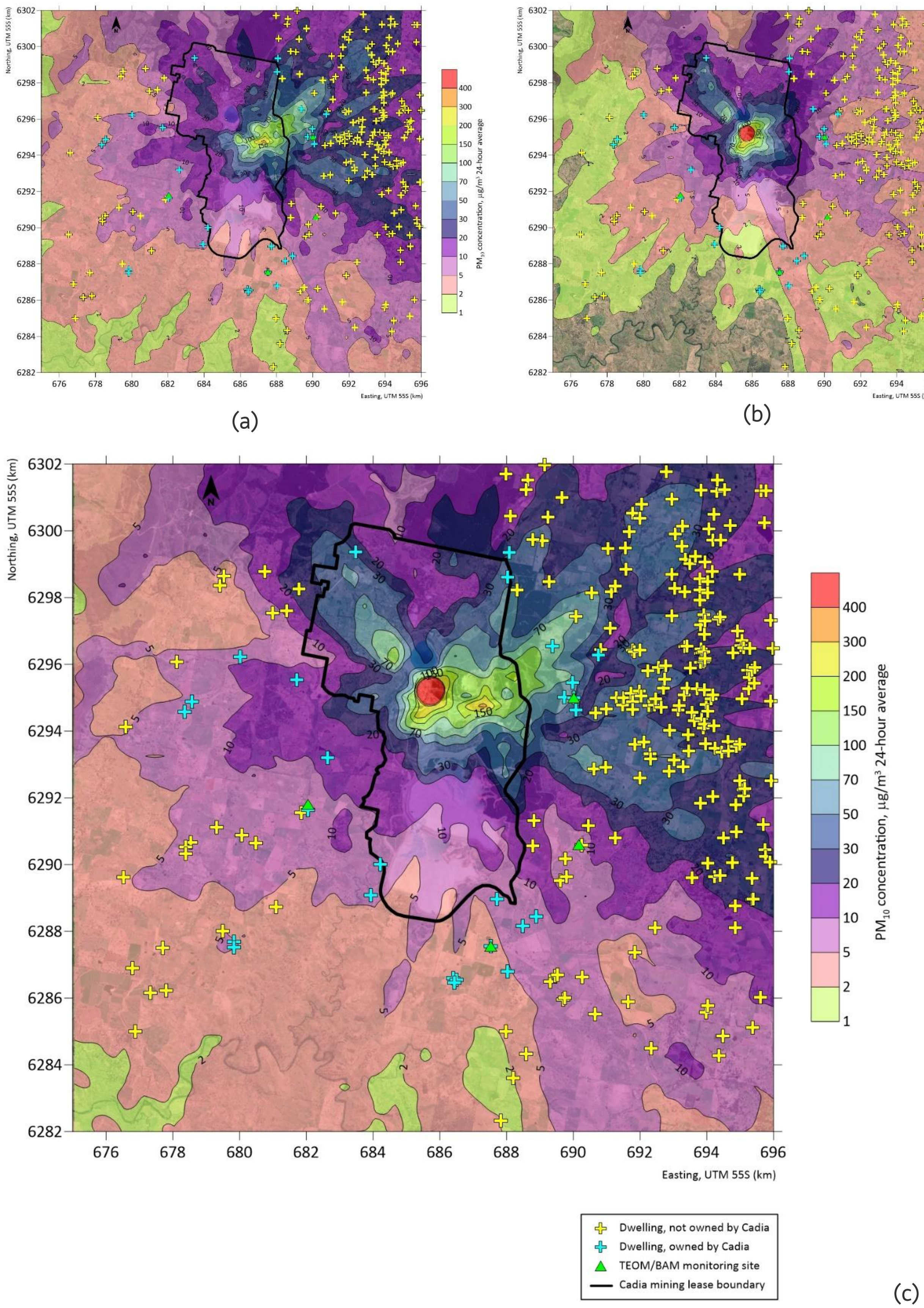

Figure Q-5. 24-hour average concentrations of PM$_{10}$ due only to vent emissions, Option 5.
(a) VR3A, VR5, VR7 and VR8 (b) VR11, R-VR4,and R-VR6 (c) All vents combined

Appendix R. Model Results for Jacobs' Cumulative Emission Model Options

Appendix R. Model Results for Jacobs' Cumulative Emission Model Options

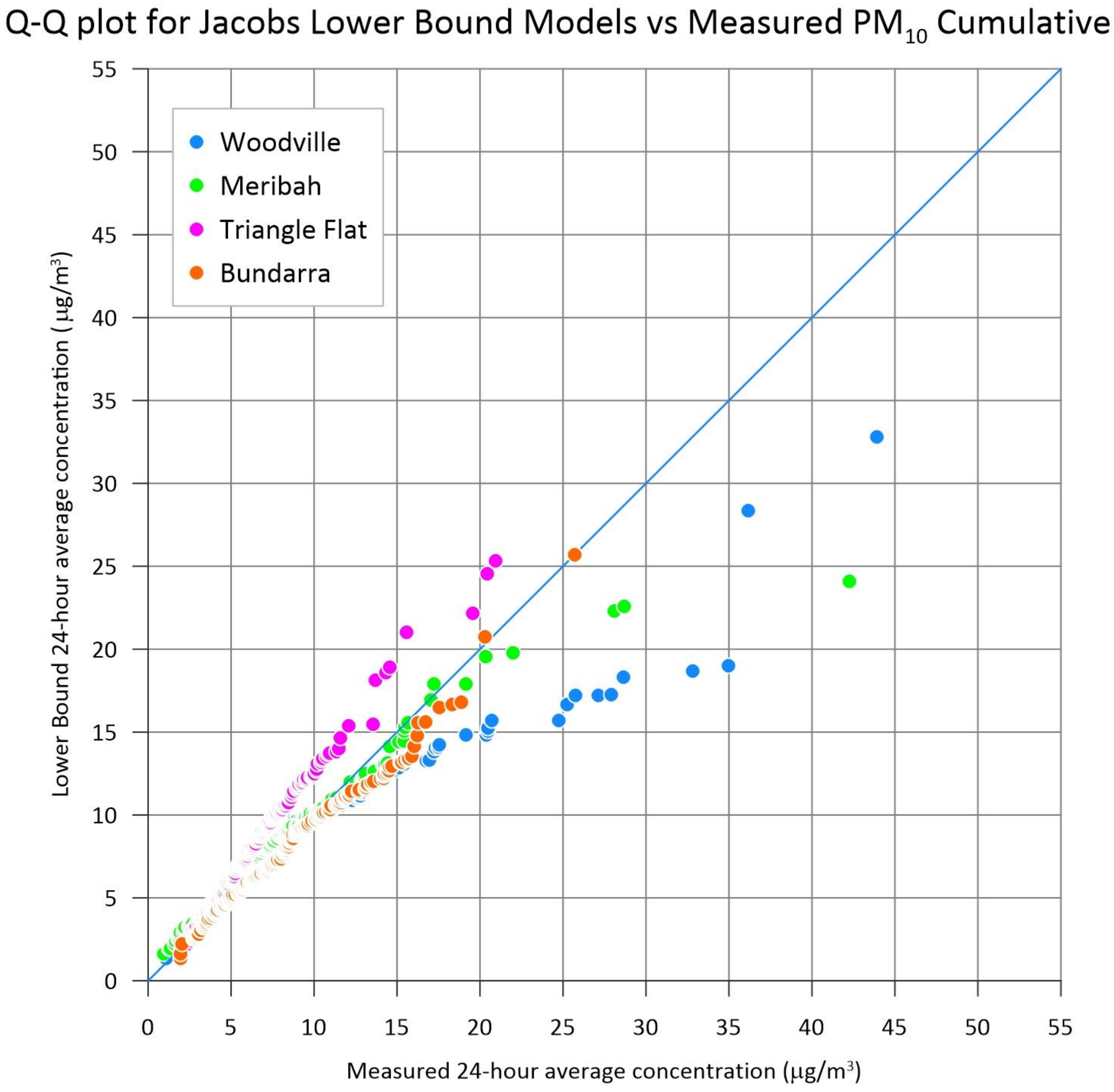

Figure R-1. Q-Q plot for Lower Bound cumulative emission model option for PM_{10}, 24-hour average.

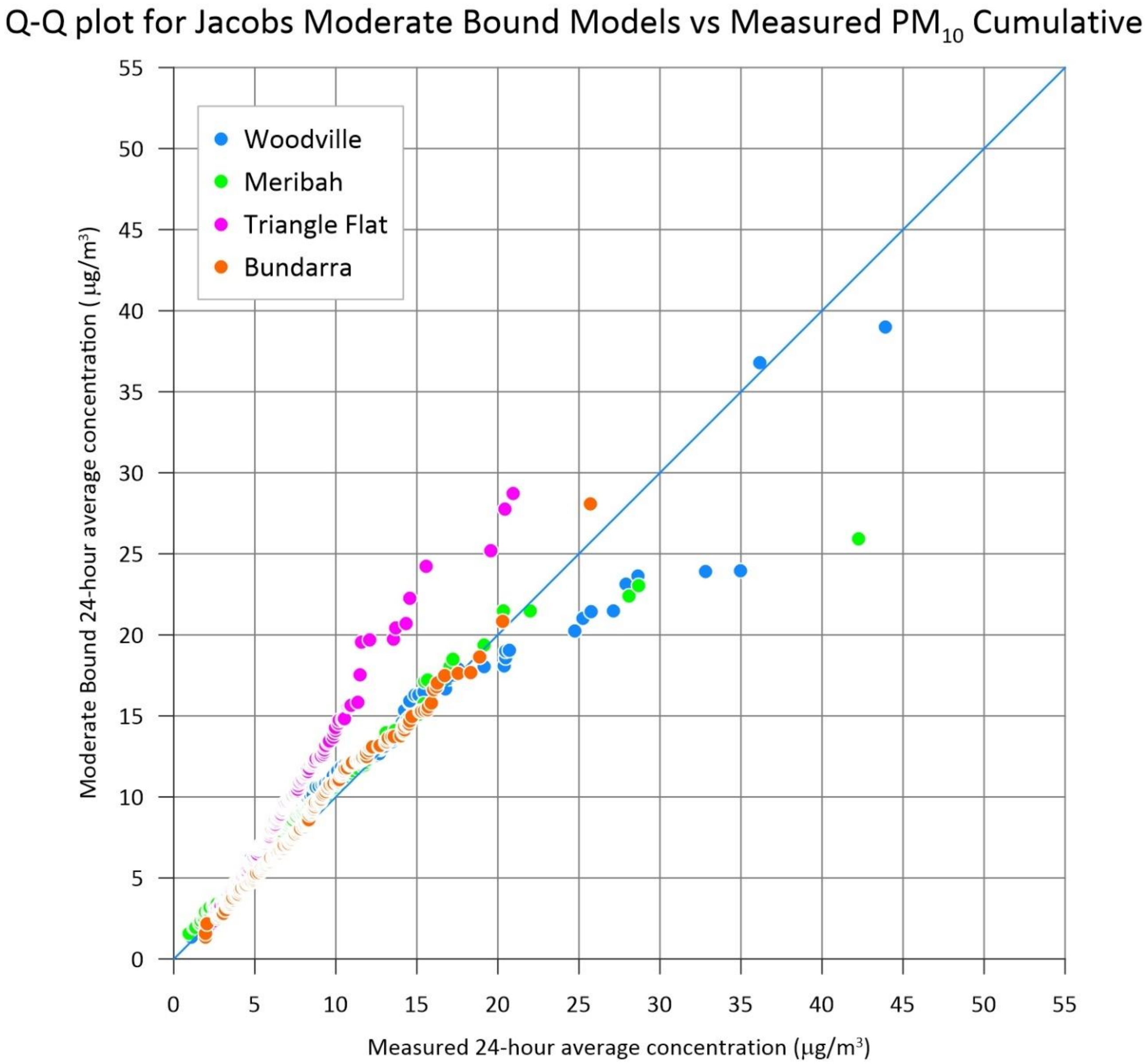

Figure R-2. Q-Q plot for Moderate Bound cumulative emission model option for PM_{10}, 24-hour average.

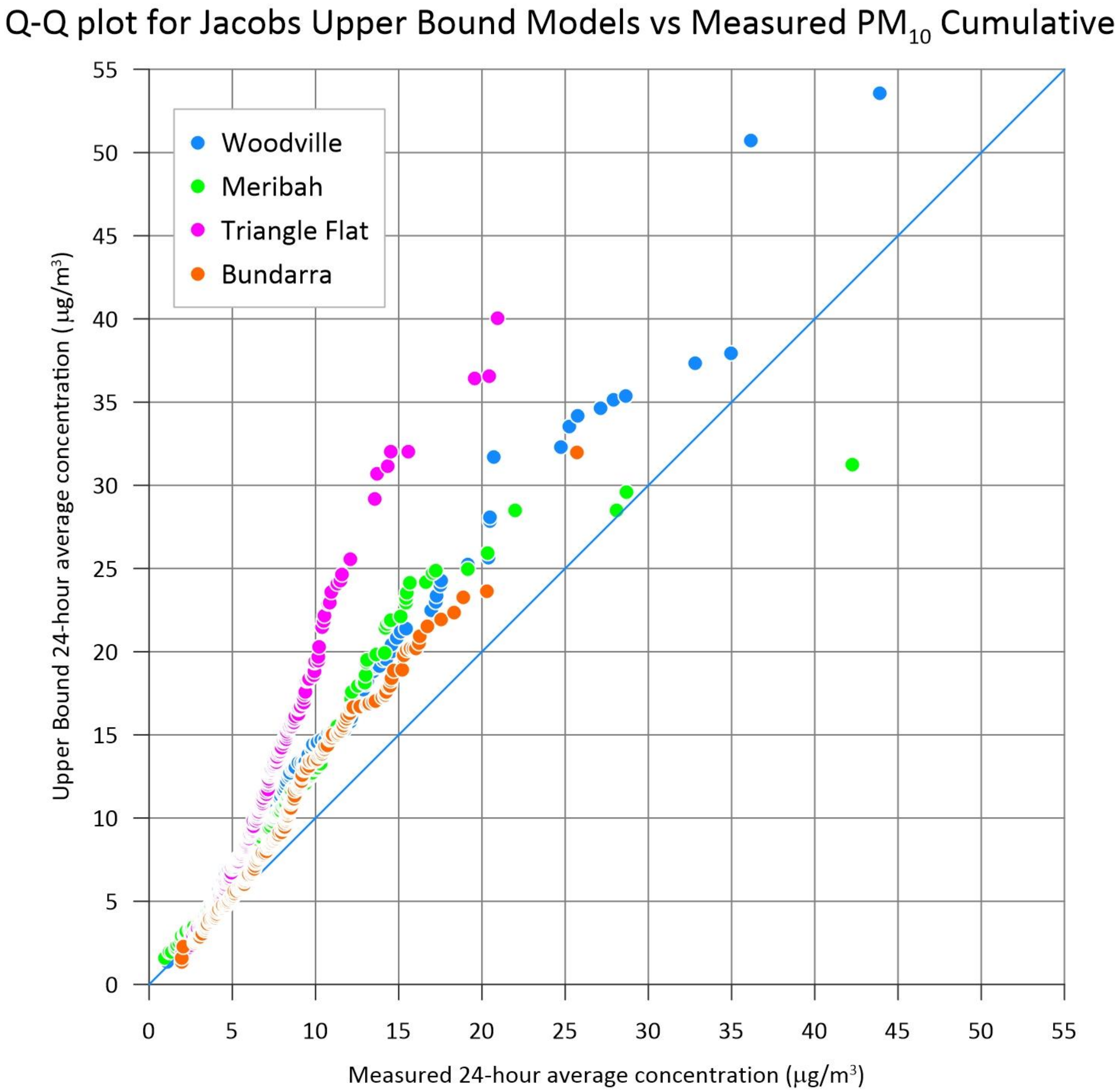

Figure R-3. Q-Q plot for Upper Bound cumulative emission model option for PM_{10}, 24-hour average.

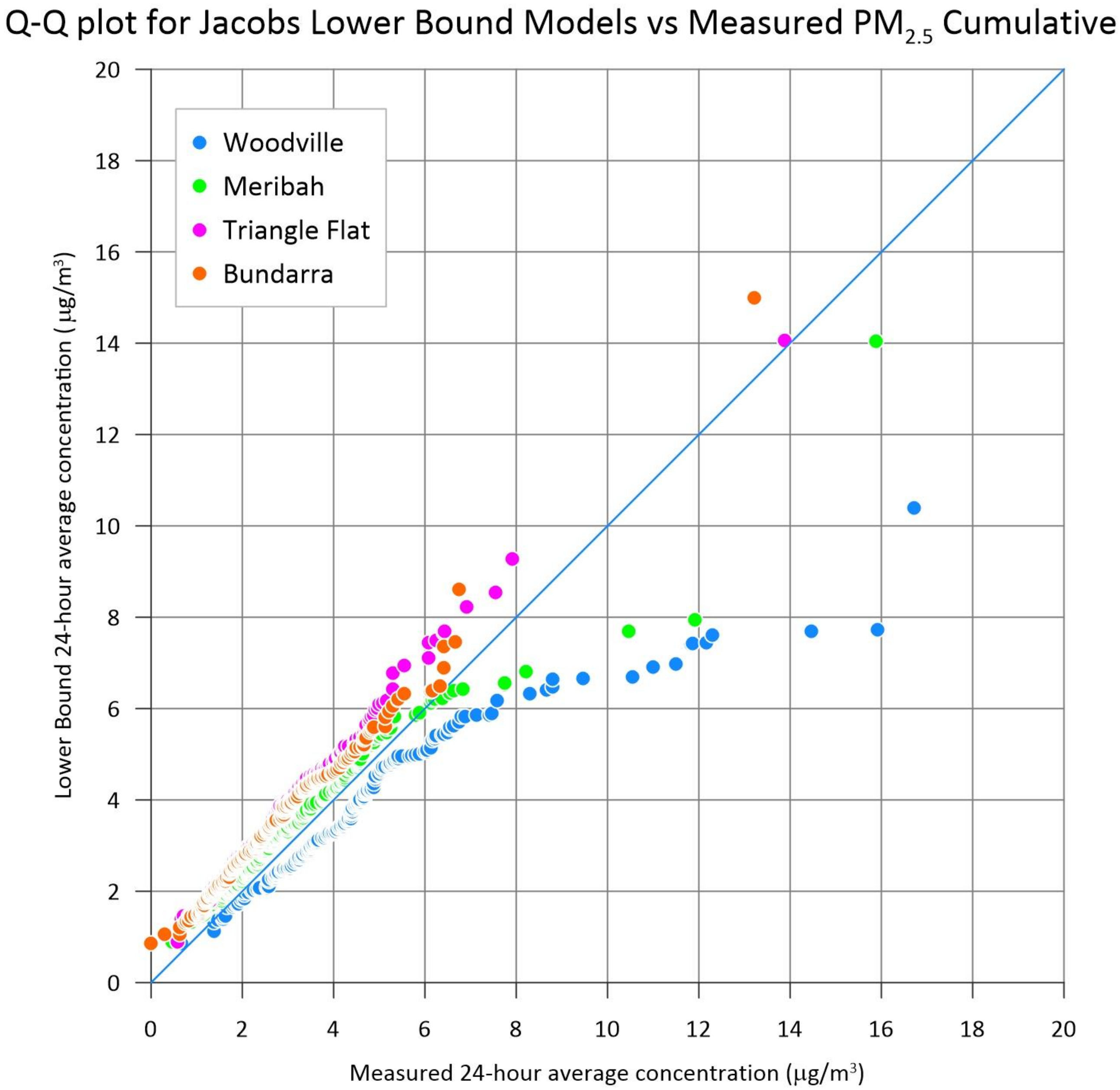

Figure R-4. Q-Q plot for Lower Bound cumulative emission model option for $PM_{2.5}$, 24-hour average.

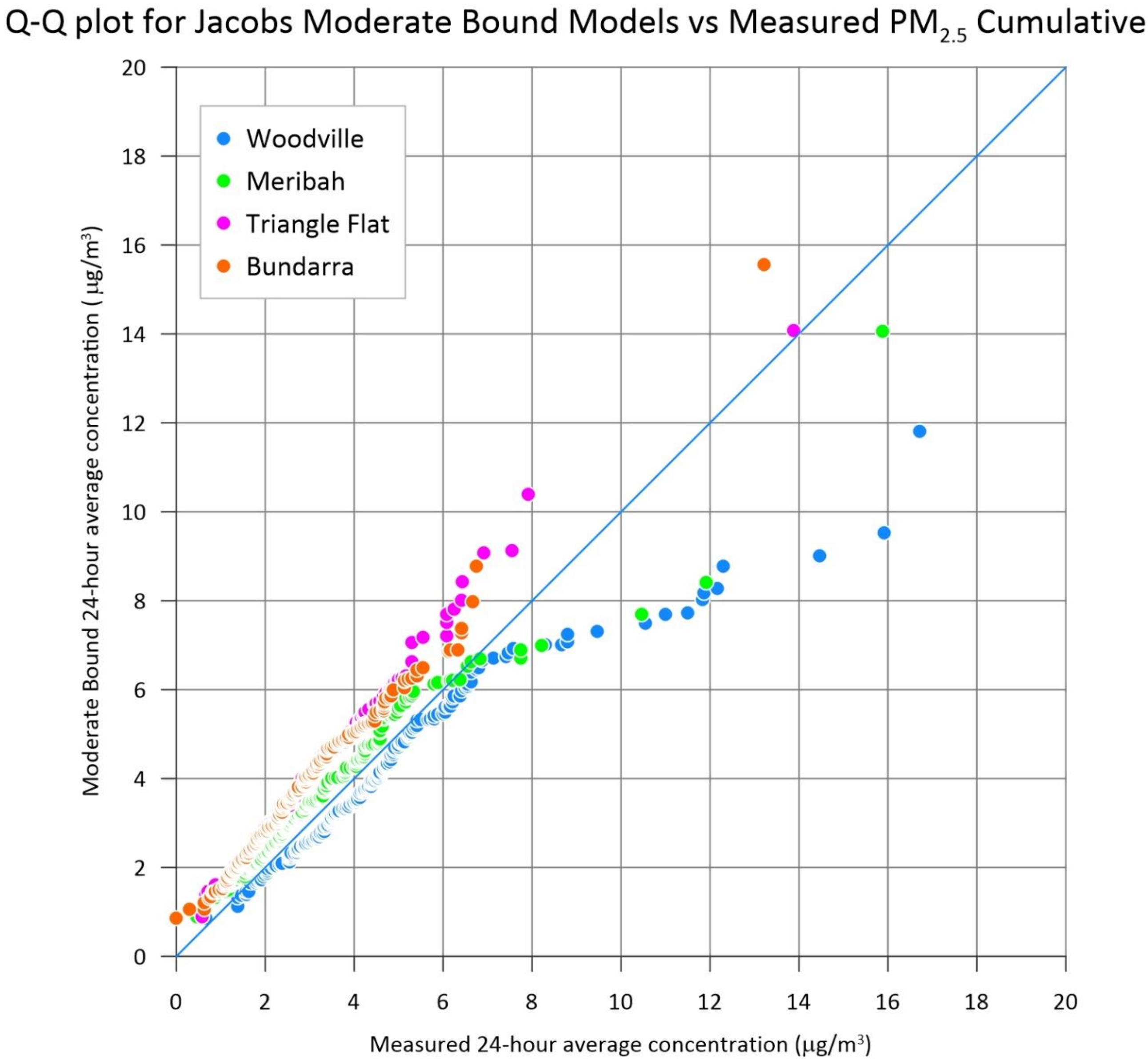

Figure R-5. Q-Q plot for Moderate Bound cumulative emission model option for $PM_{2.5}$, 24-hour average.

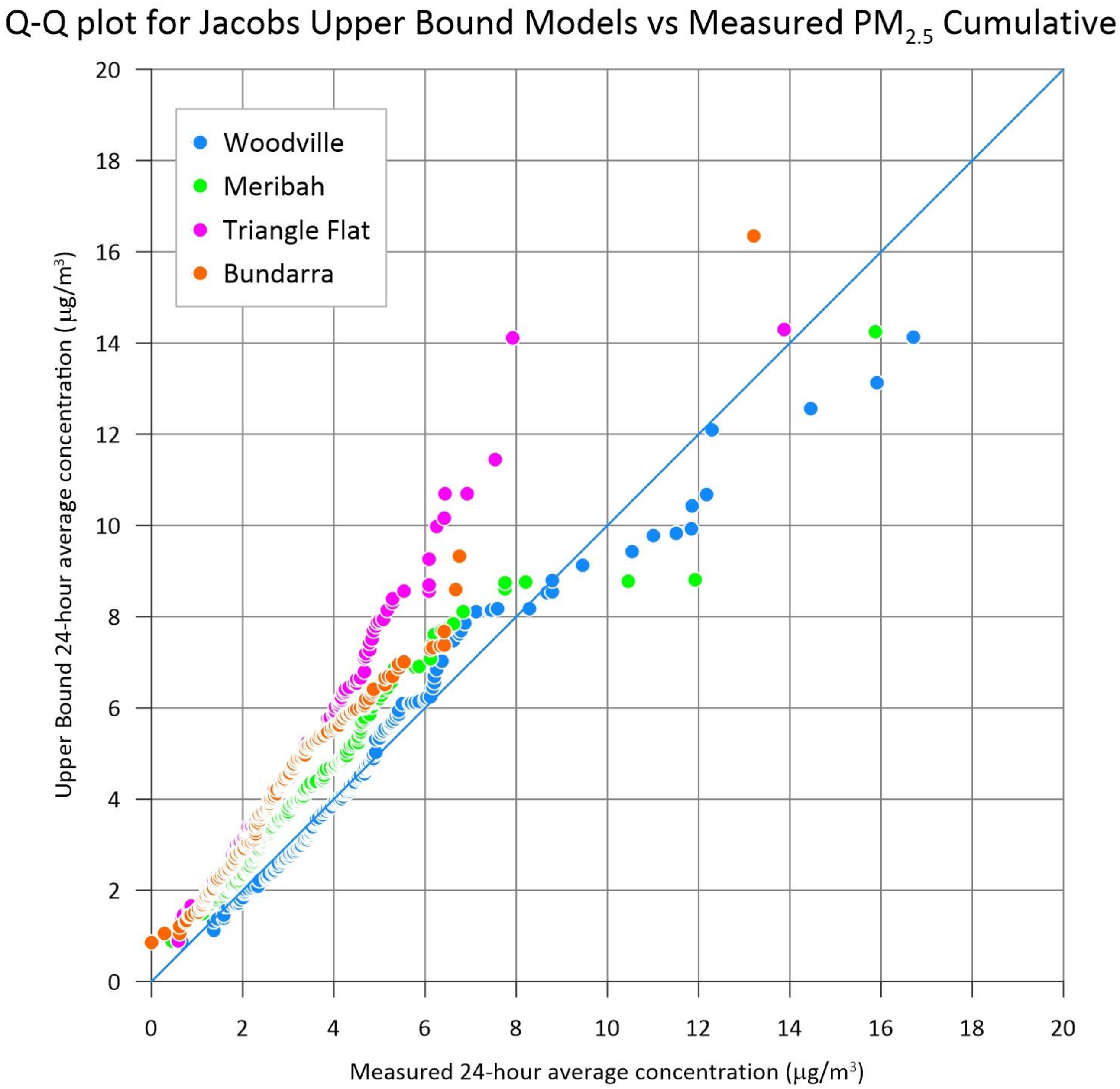

Figure R-6. Q-Q plot for Upper Bound cumulative emission model option for $PM_{2.5}$, 24-hour average.

Appendix S. Model Results for Jacobs' Recommended Model

Appendix S. Model Results for Jacobs' Recommended Model

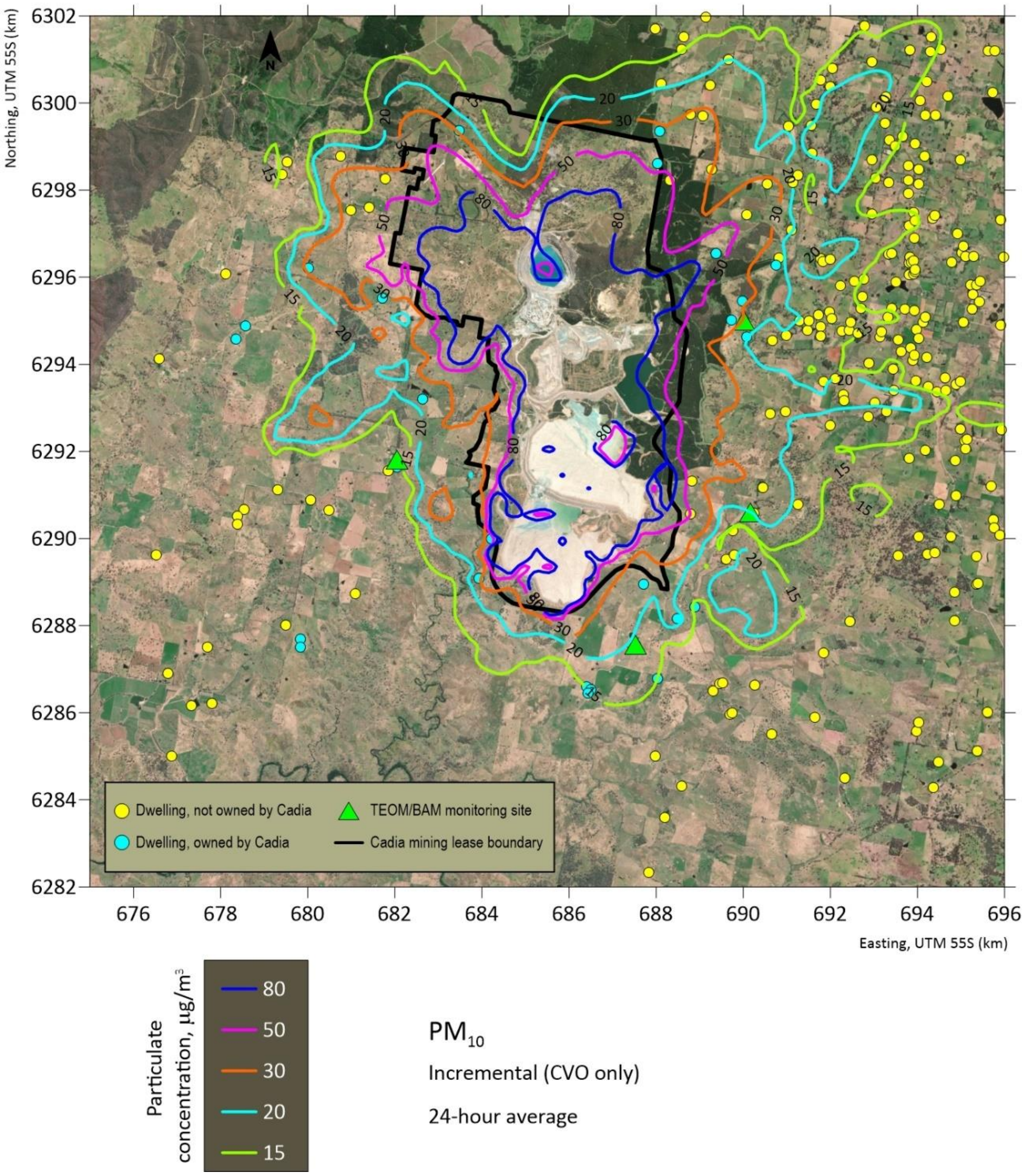

Figure S-1. Jacobs' Recommended Model, incremental 24-hour average PM_{10}.

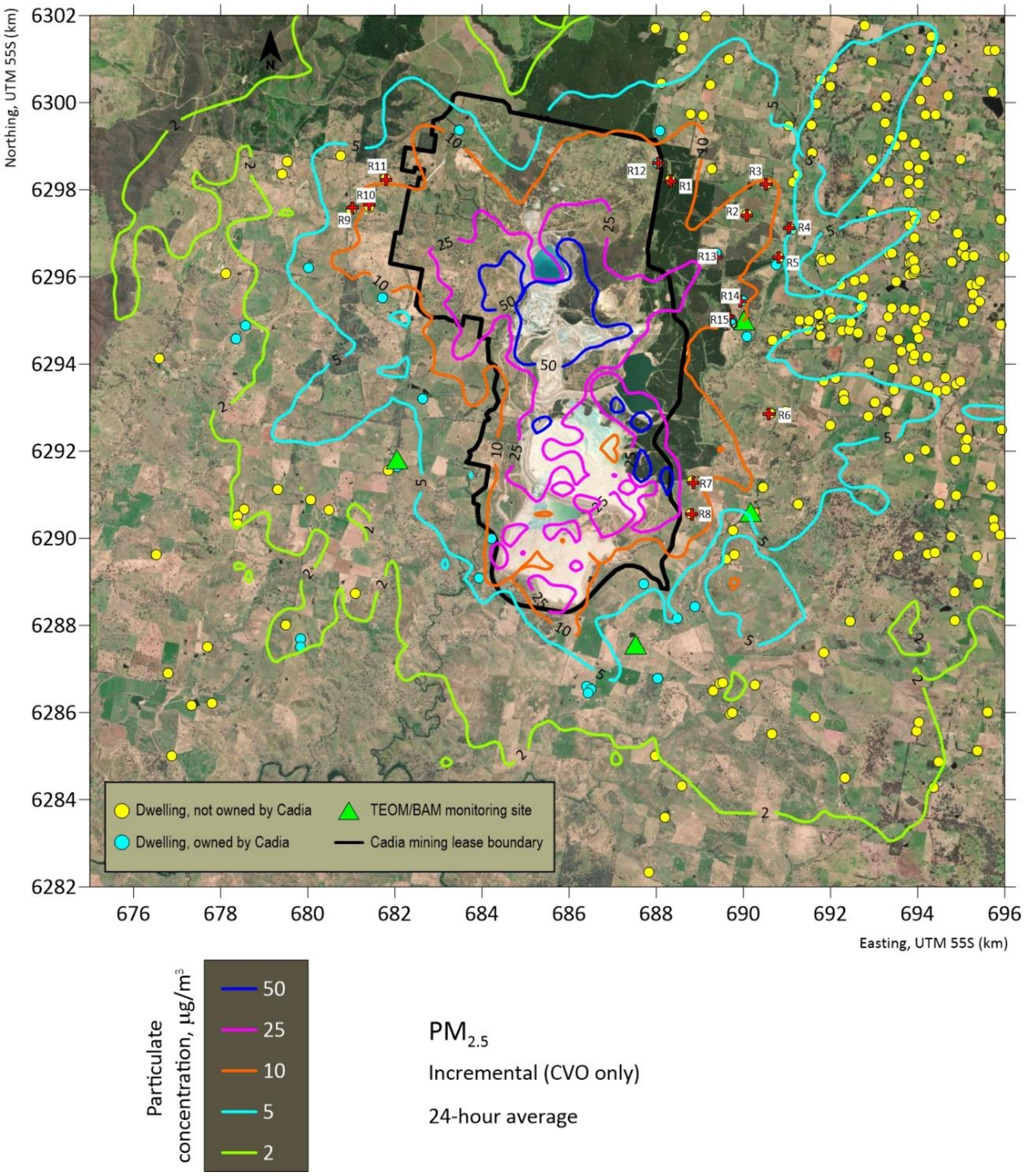

Figure S-2. Jacobs' Recommended Model, incremental 24-hour average $PM_{2.5}$.

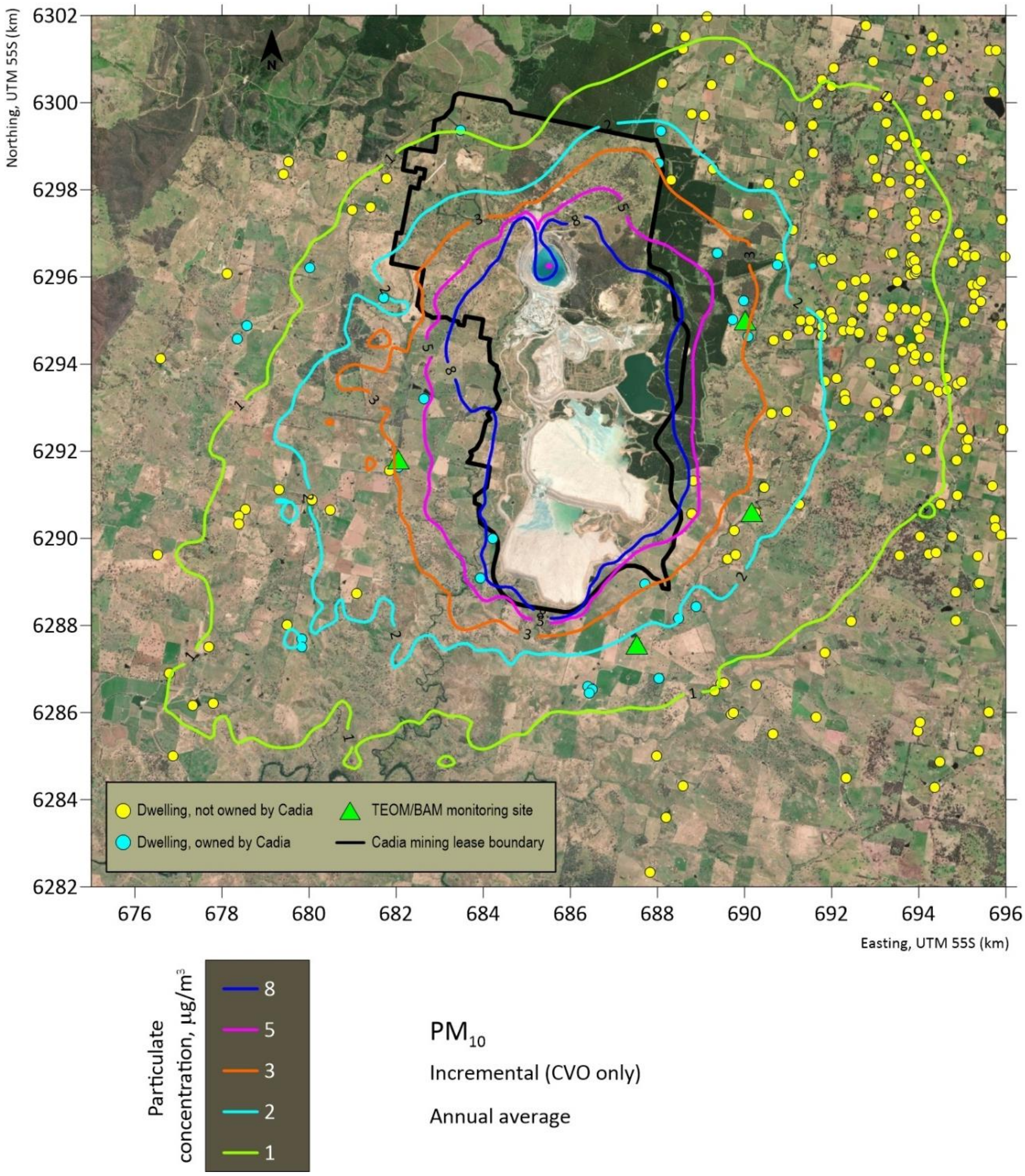

Figure S-3. Jacobs' Recommended Model, incremental annual average PM_{10}.

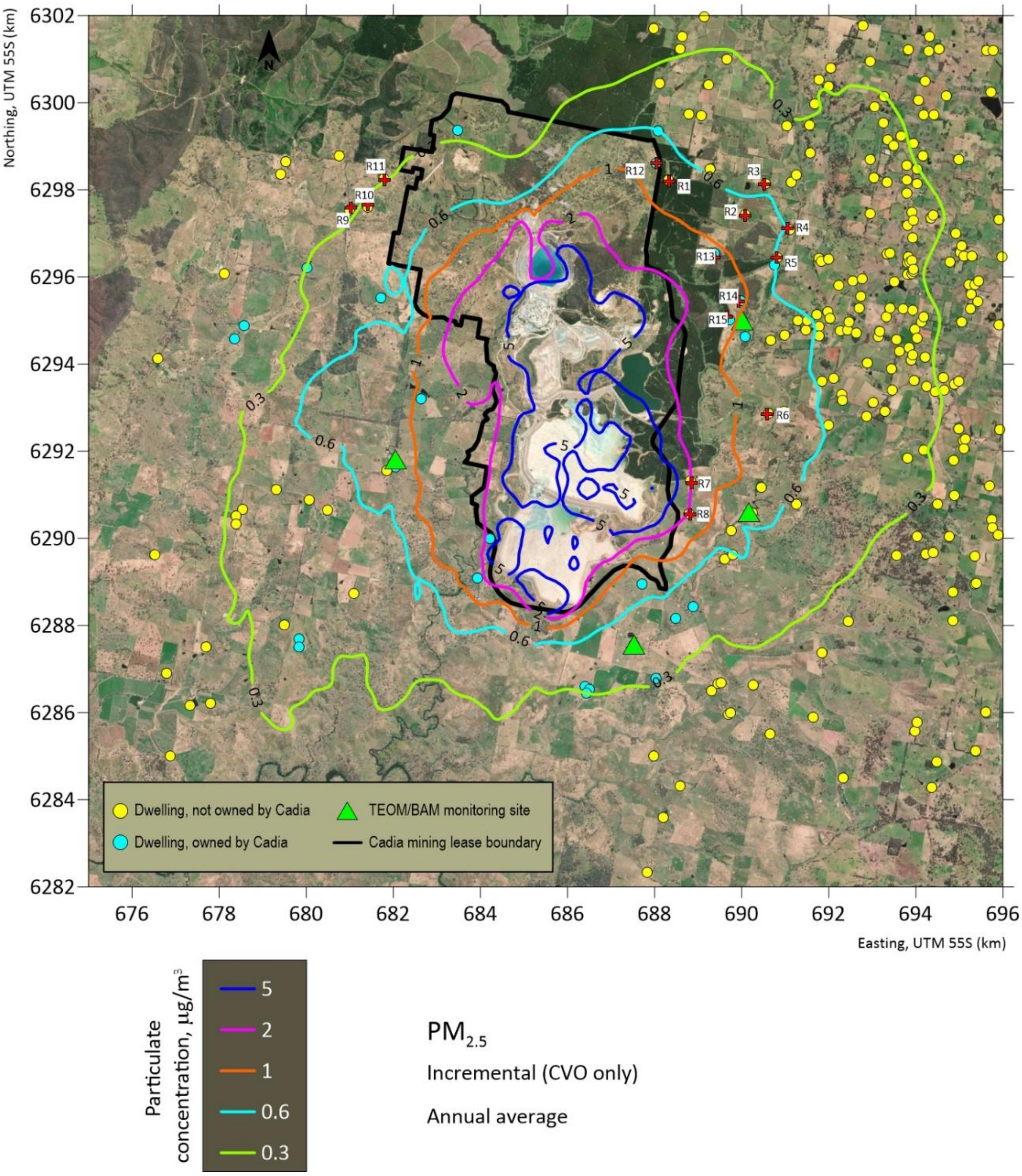

Figure S-4. Jacobs' Recommended Model, incremental annual average $PM_{2.5}$.

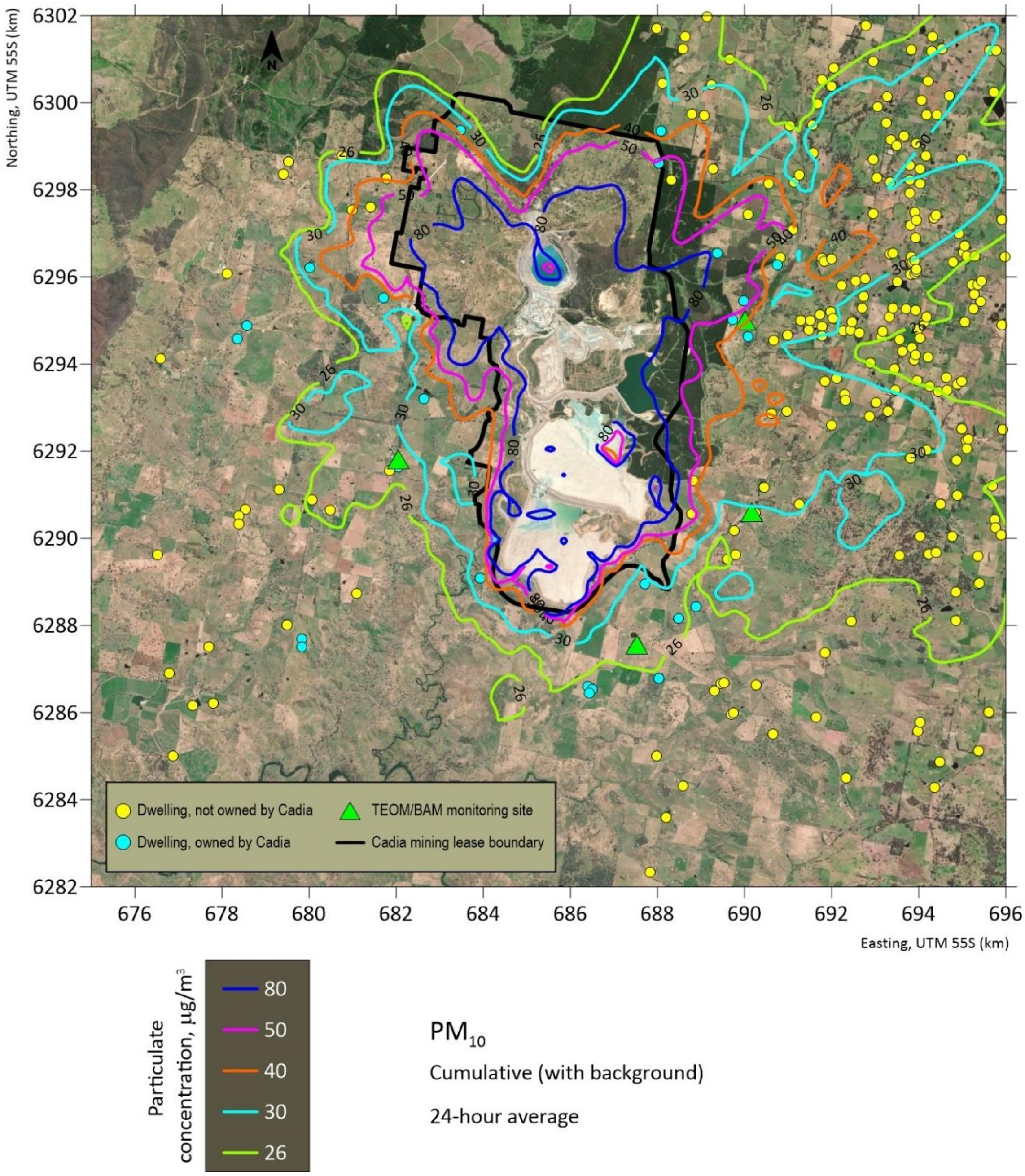

Figure S-5. Jacobs' Recommended Model, cumulative 24-hour average PM_{10}.

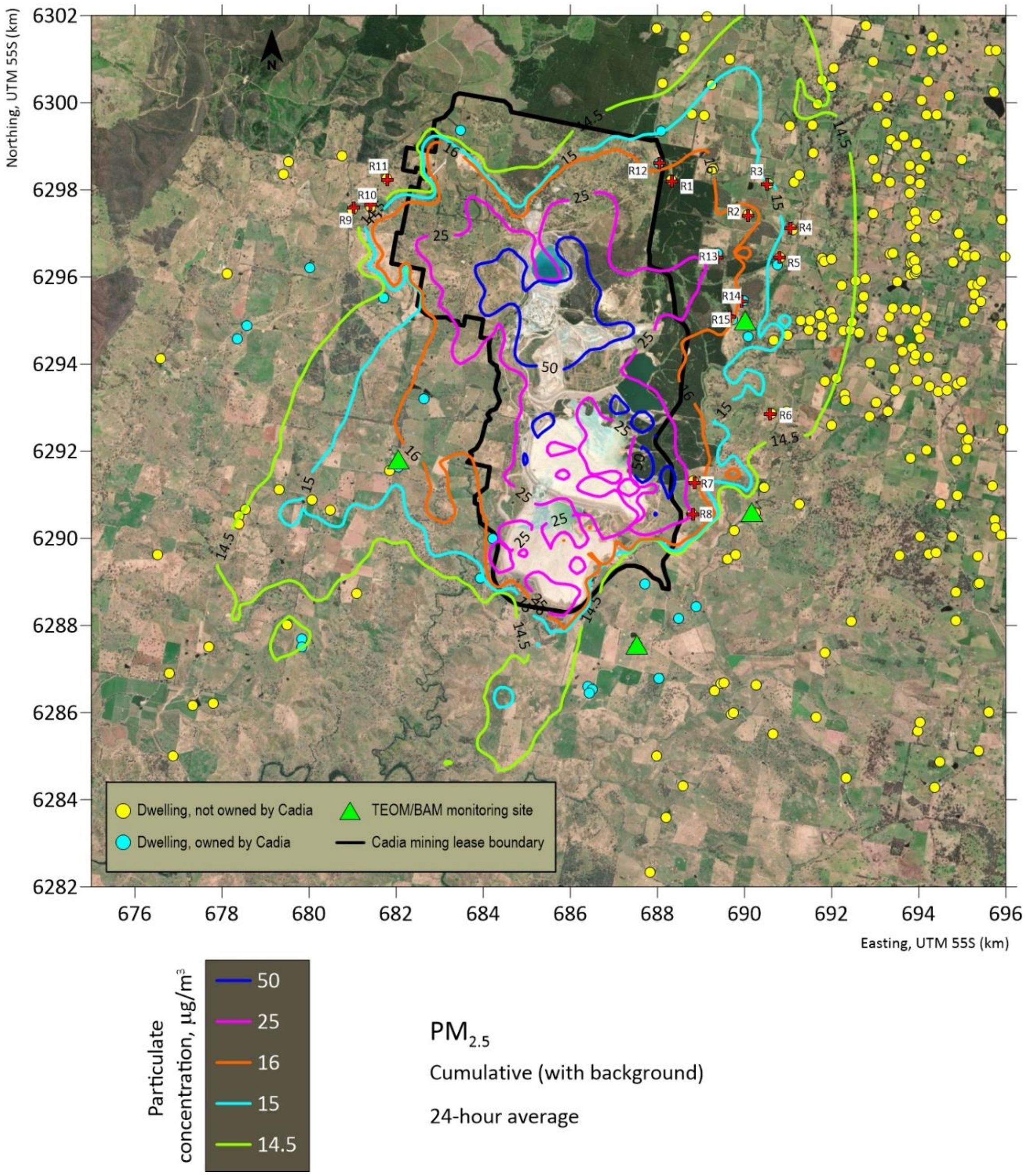

Figure S-6. Jacobs' Recommended Model, cumulative 24-hour average $PM_{2.5}$.

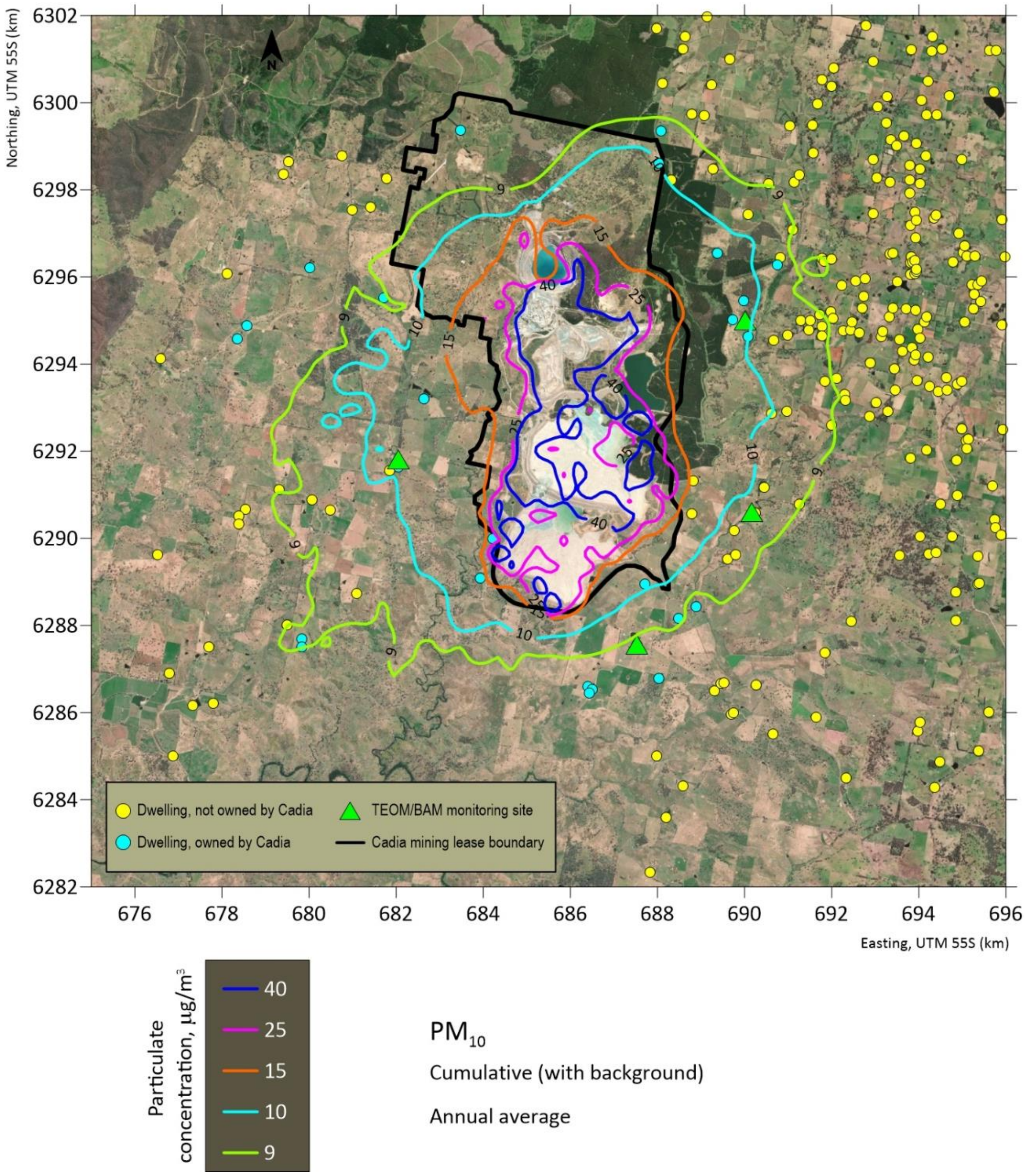

Figure S-7. Jacobs' Recommended Model, cumulative annual average PM_{10}.

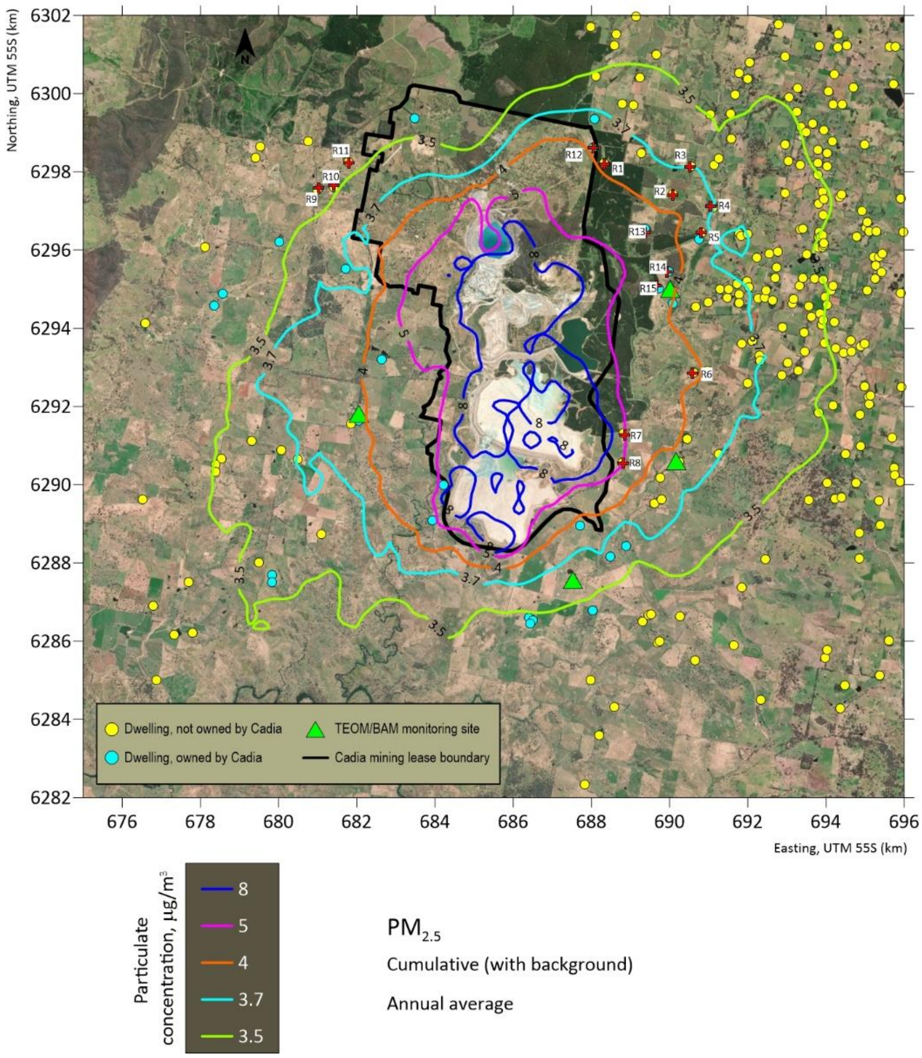

Figure S-8. Jacobs' Recommended Model, cumulative annual average $PM_{2.5}$.

Appendix T. Model Results for Cumulative Vent Models

Appendix T. Model Results for Cumulative Vent Models

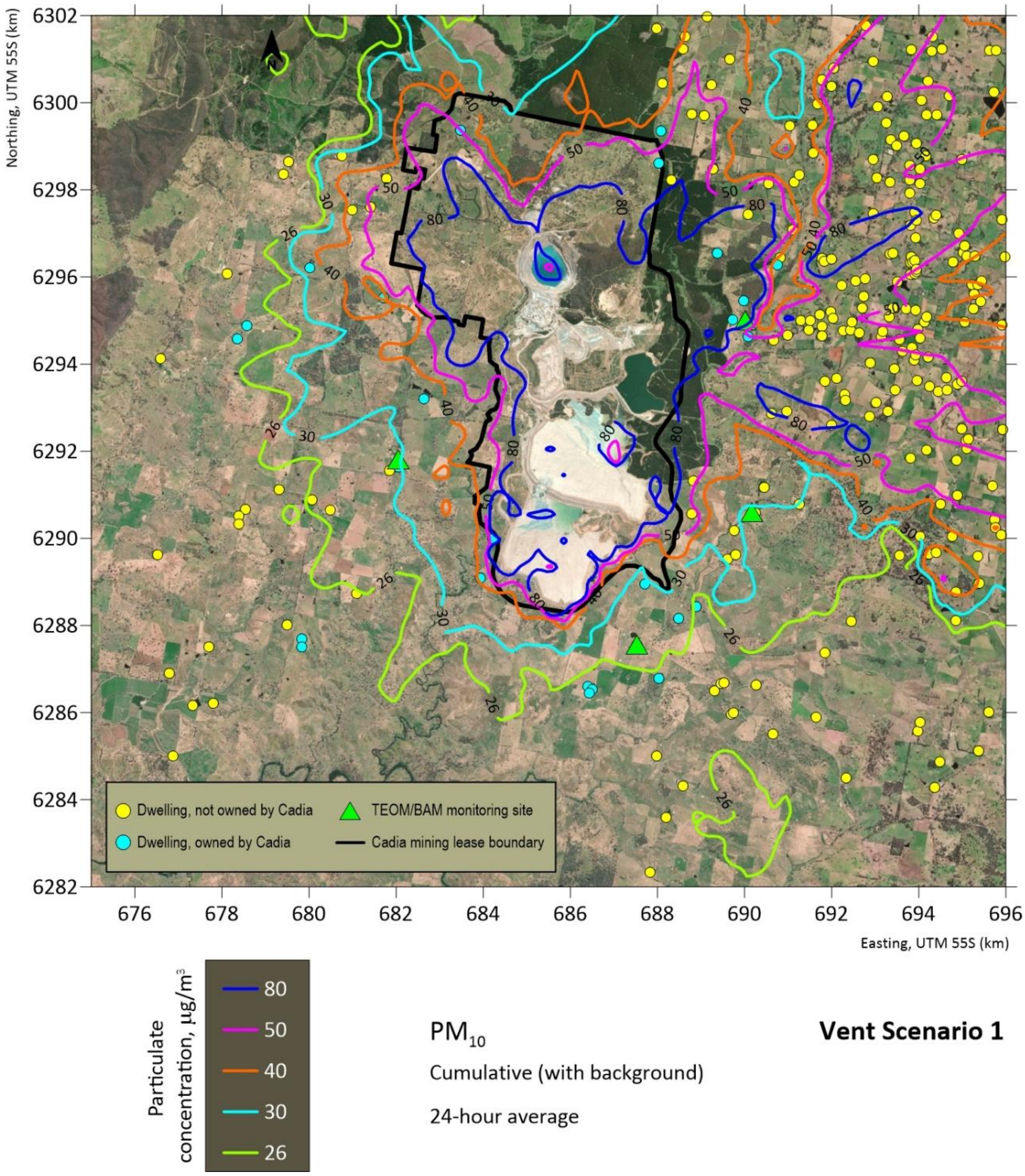

Figure T-1. Cumulative model results for vent emission Scenario 1, 24-hour average PM_{10}.

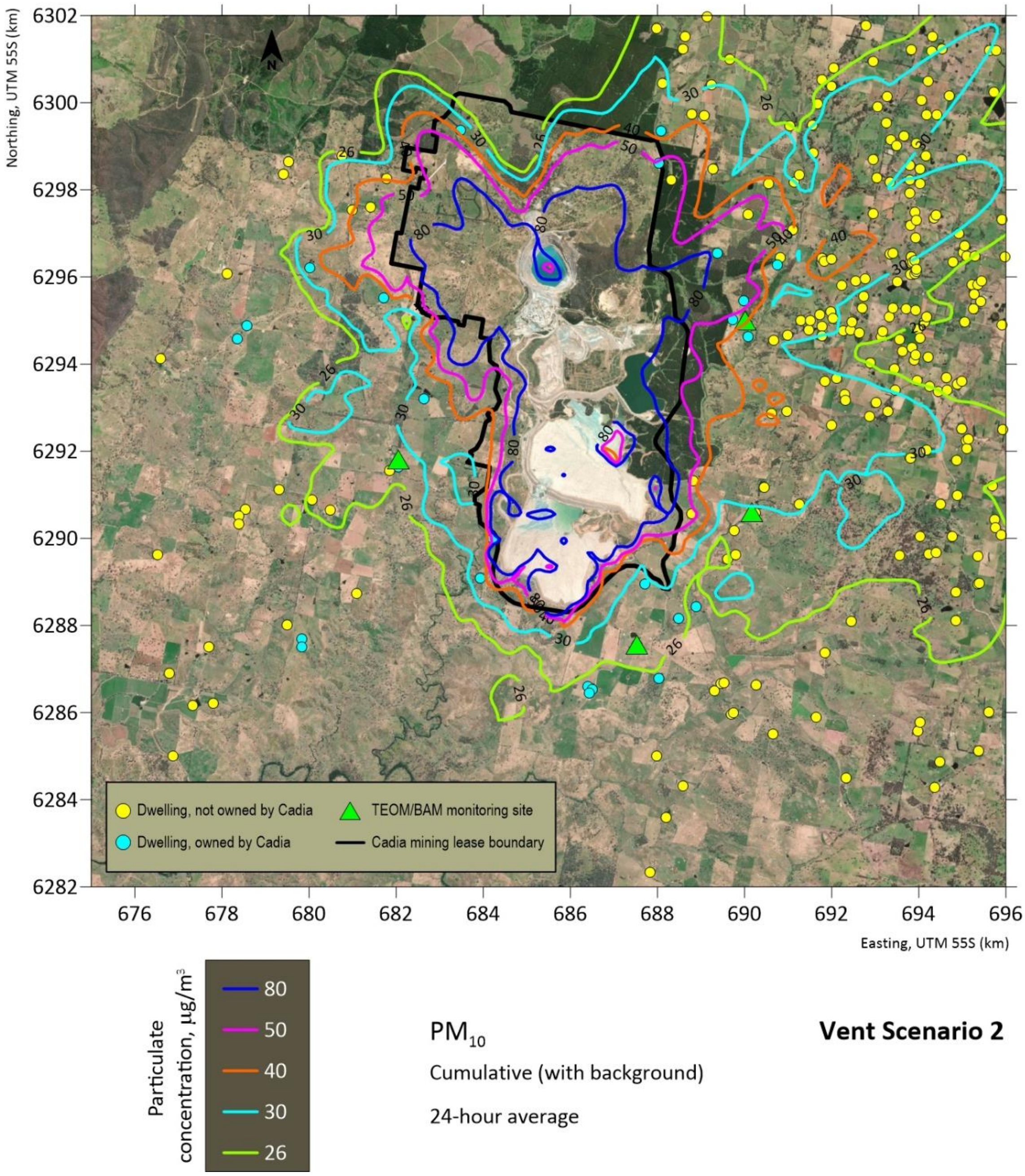

Figure T-2. Cumulative model results for vent emission Scenario 2, 24-hour average PM_{10}.

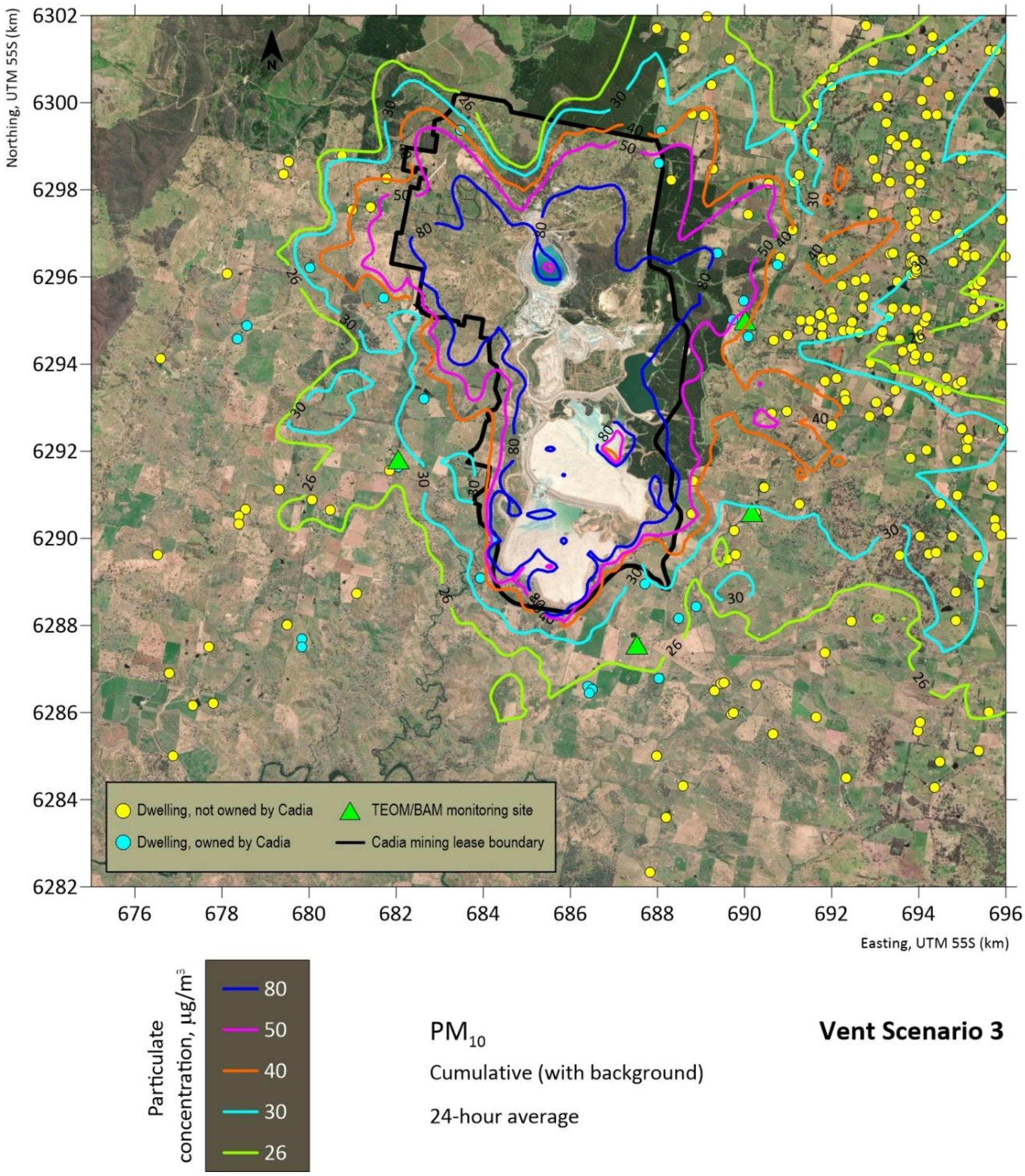

Figure T-3. Cumulative model results for vent emission Scenario 3, 24-hour average PM_{10}.

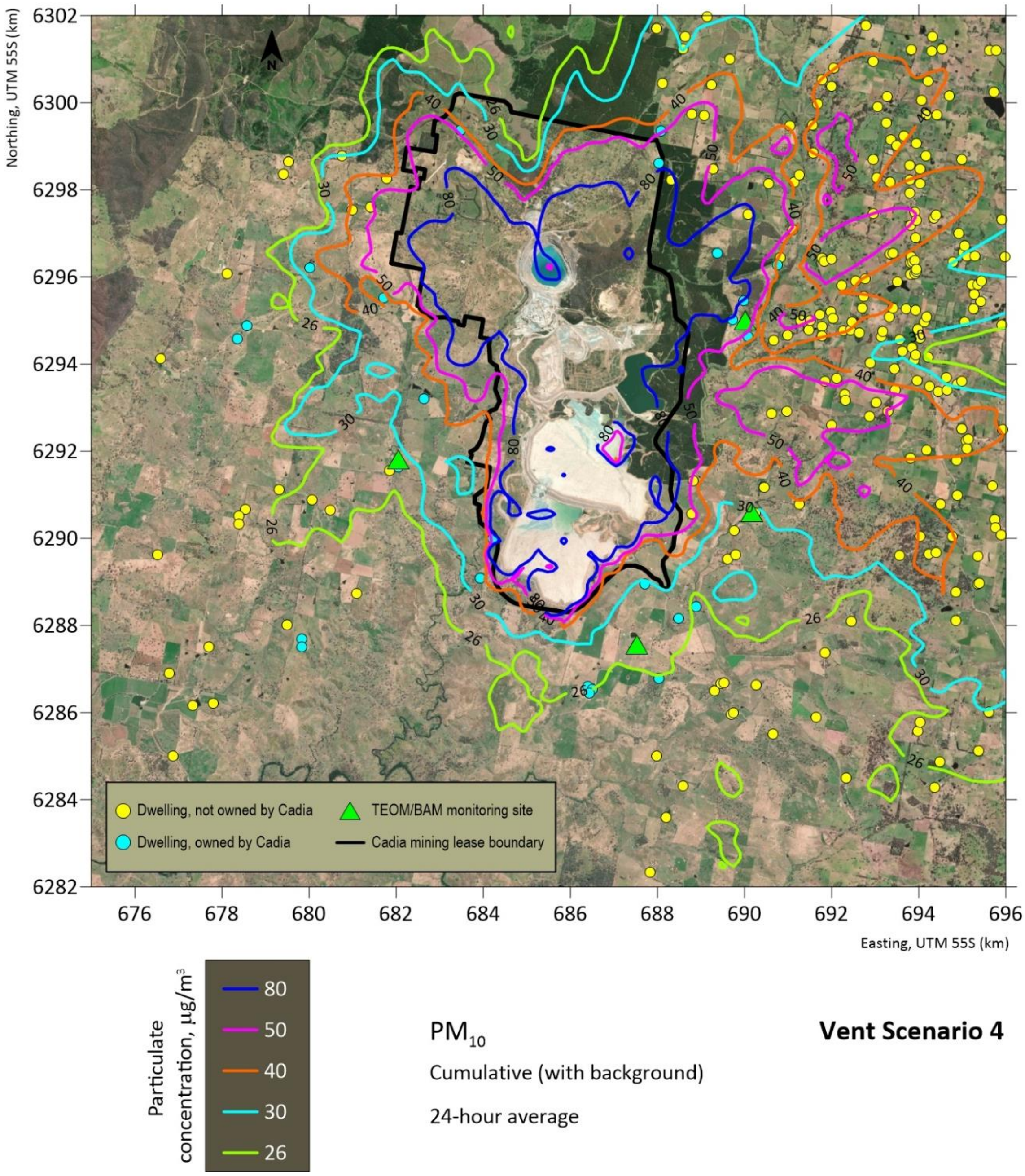

Figure T-4. Cumulative model results for vent emission Scenario 4, 24-hour average PM_{10}.

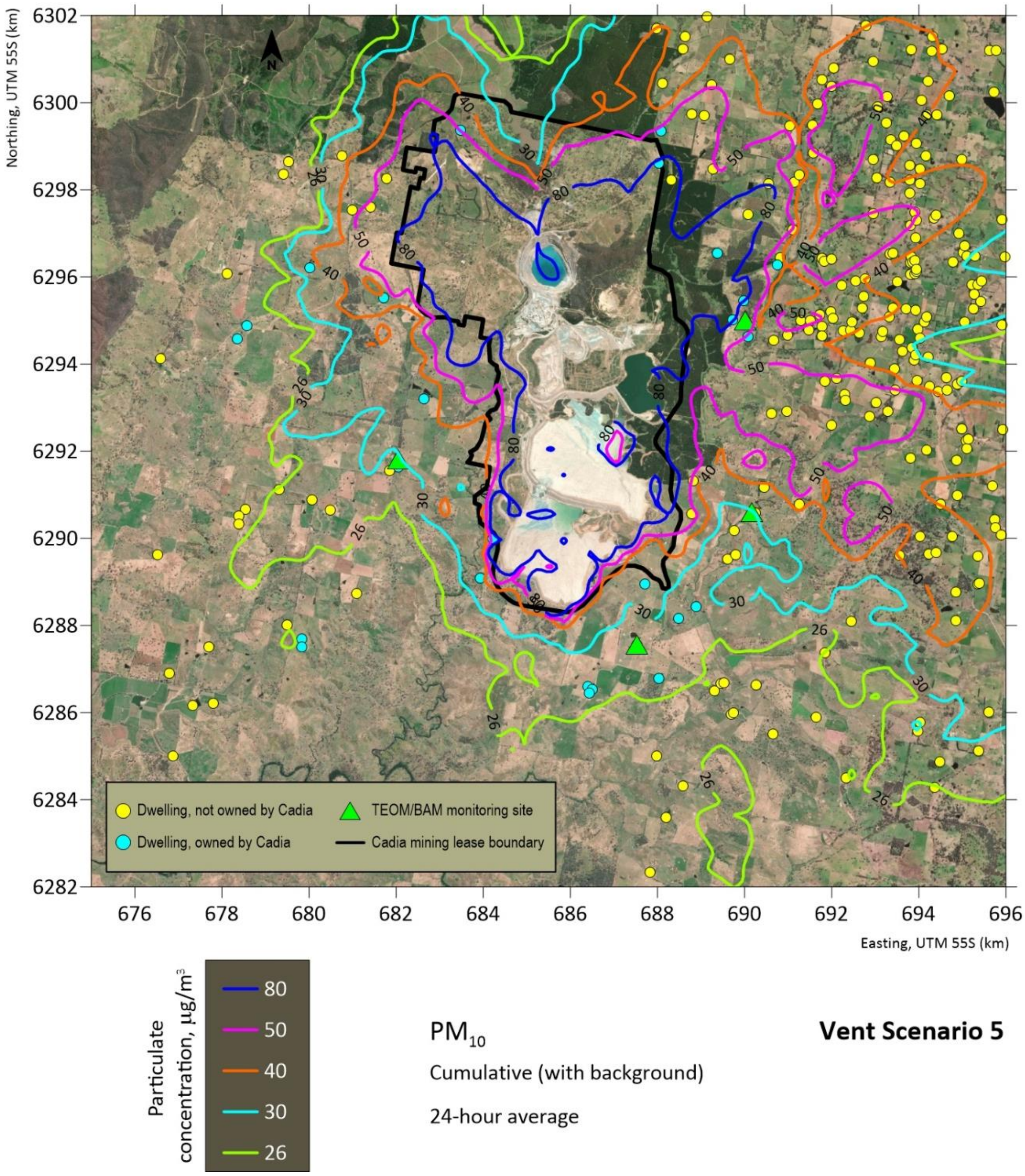

Figure T-5. Cumulative model results for vent emission Scenario 5, 24-hour average PM_{10}.

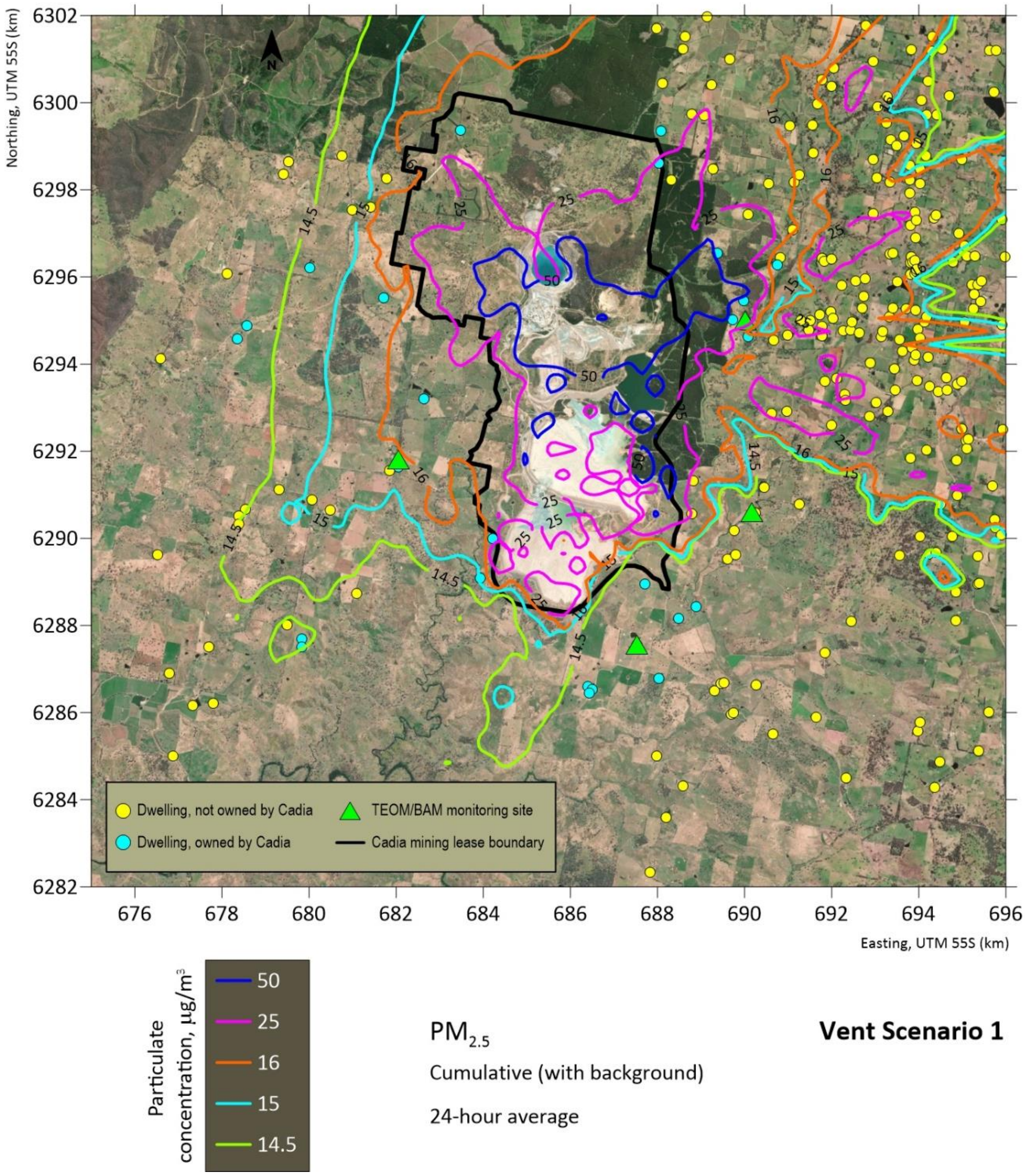

Figure T-6. Cumulative model results for vent emission Scenario 1, 24-hour average $PM_{2.5}$.

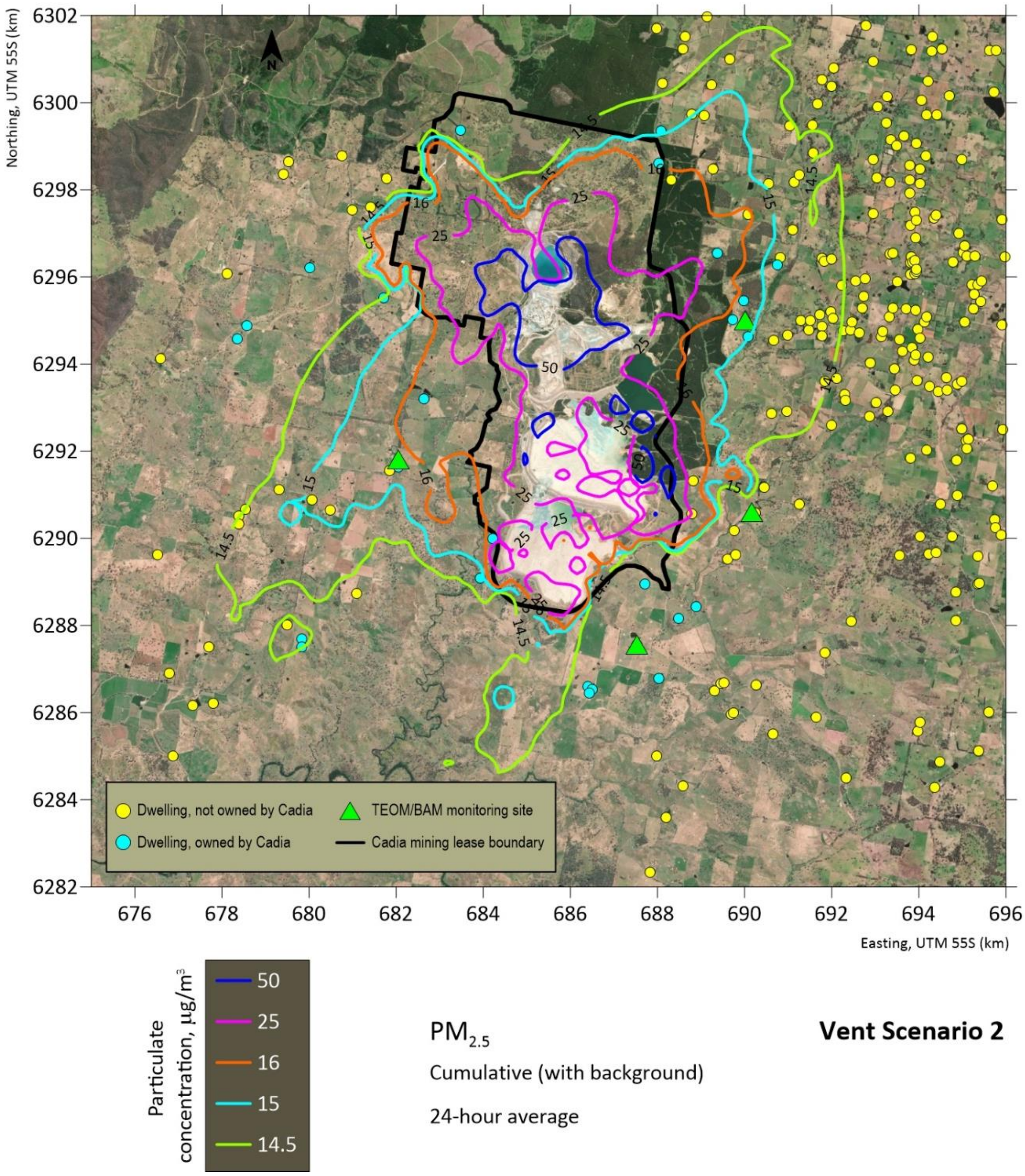

Figure T-7. Cumulative model results for vent emission Scenario 2, 24-hour average $PM_{2.5}$.

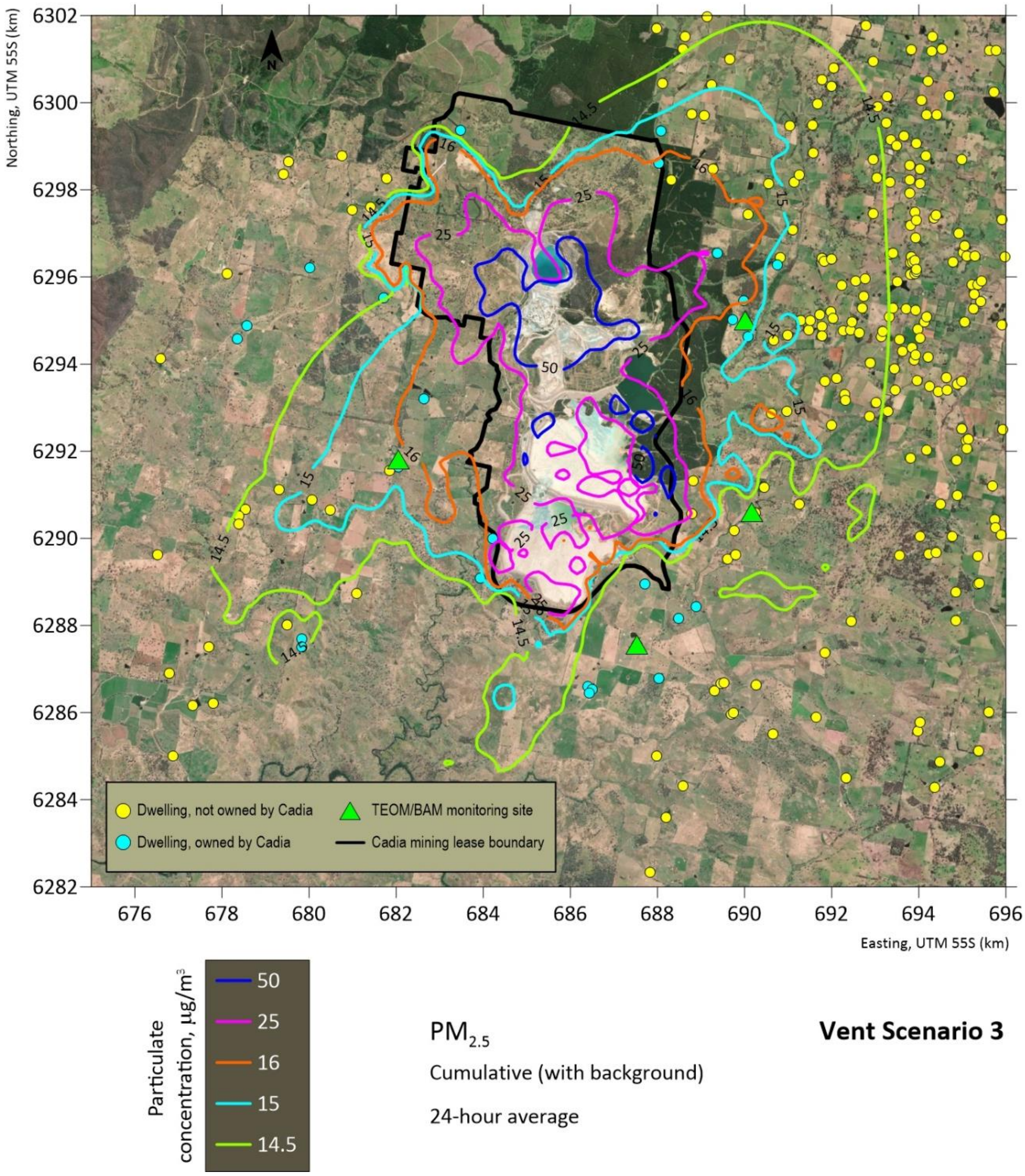

Figure T-8. Cumulative model results for vent emission Scenario 3, 24-hour average $PM_{2.5}$.

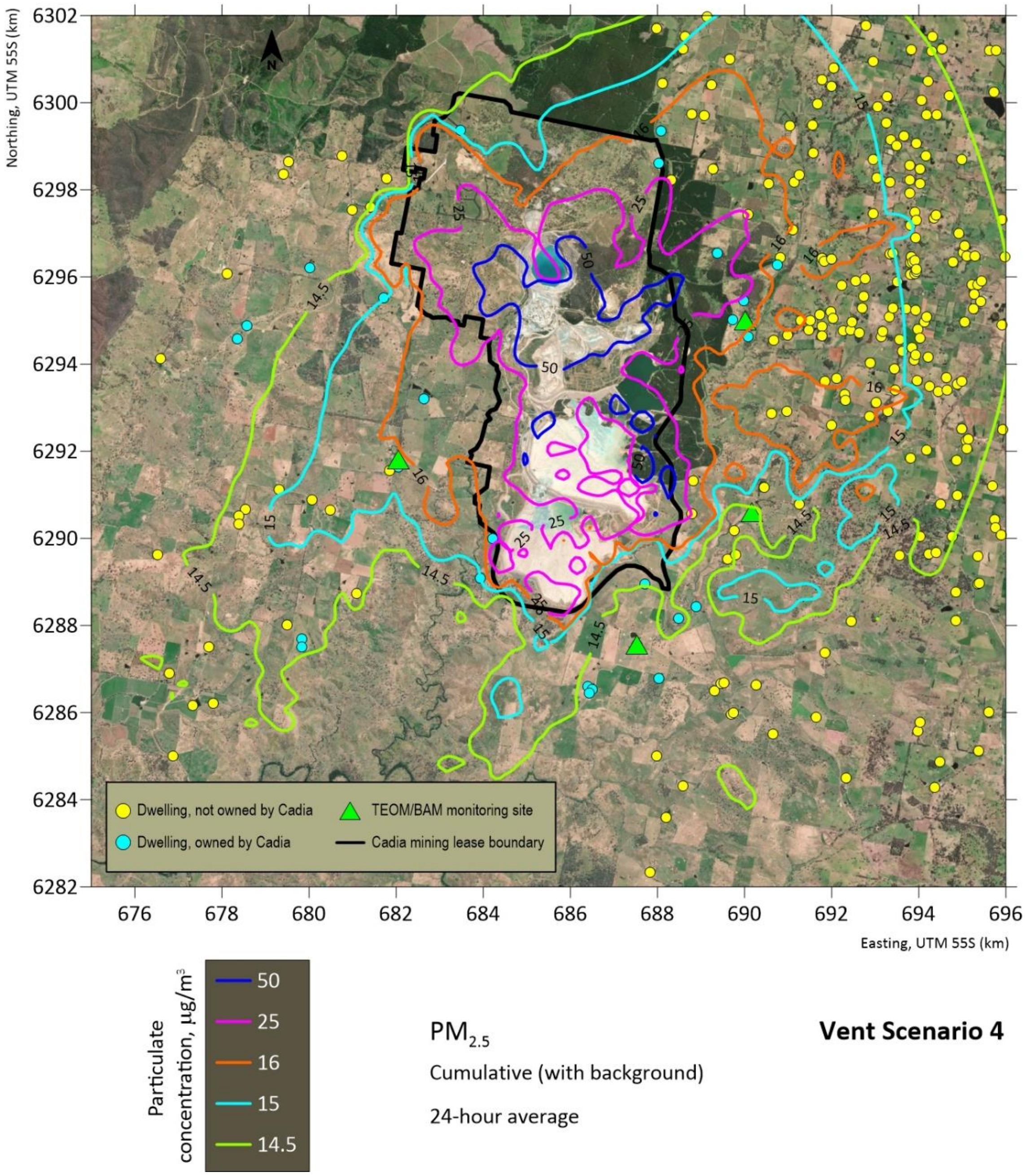

Figure T-9. Cumulative model results for vent emission Scenario 4, 24-hour average $PM_{2.5}$.

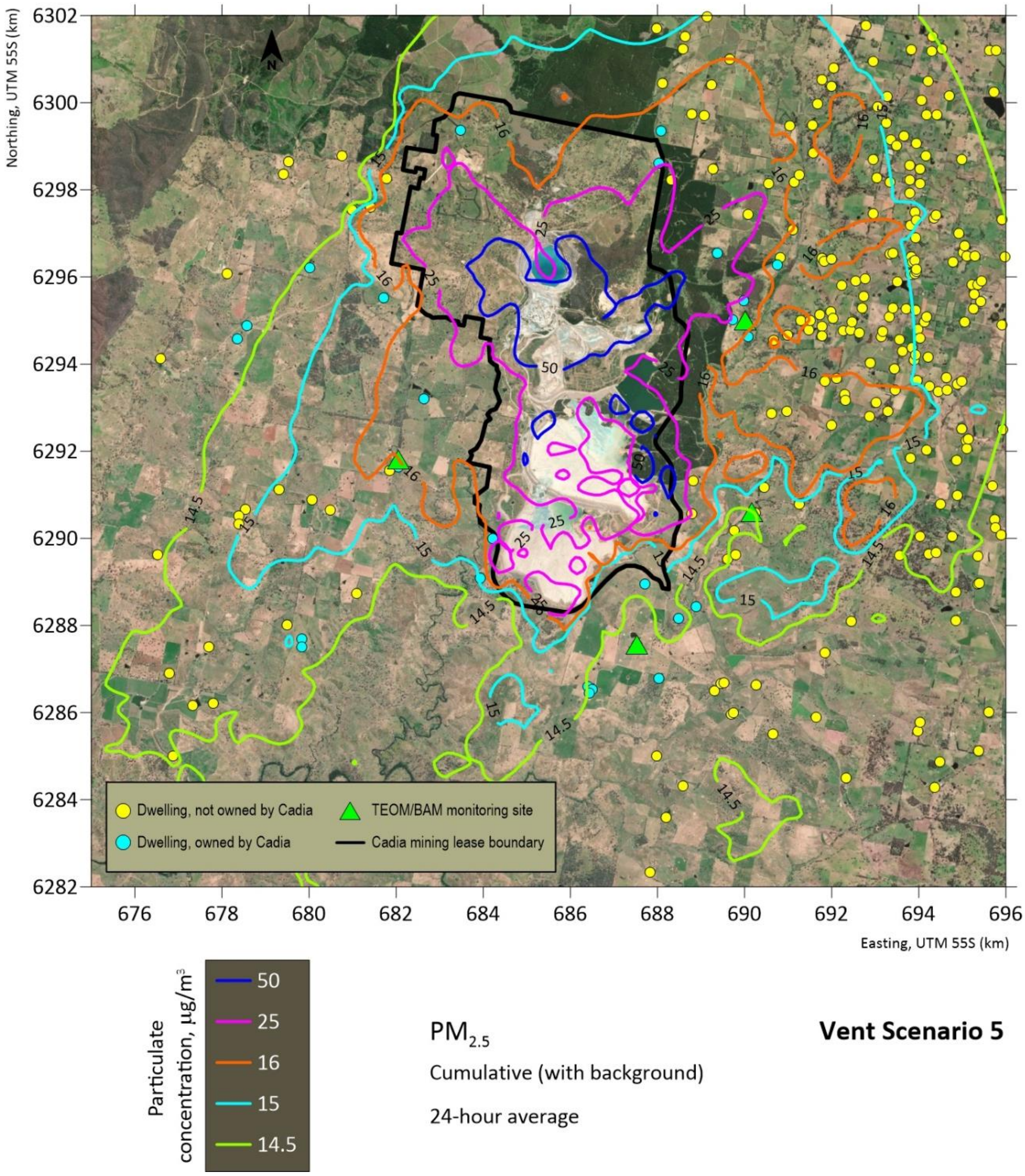

Figure T-10. Cumulative model results for vent emission Scenario 5, 24-hour average $PM_{2.5}$.

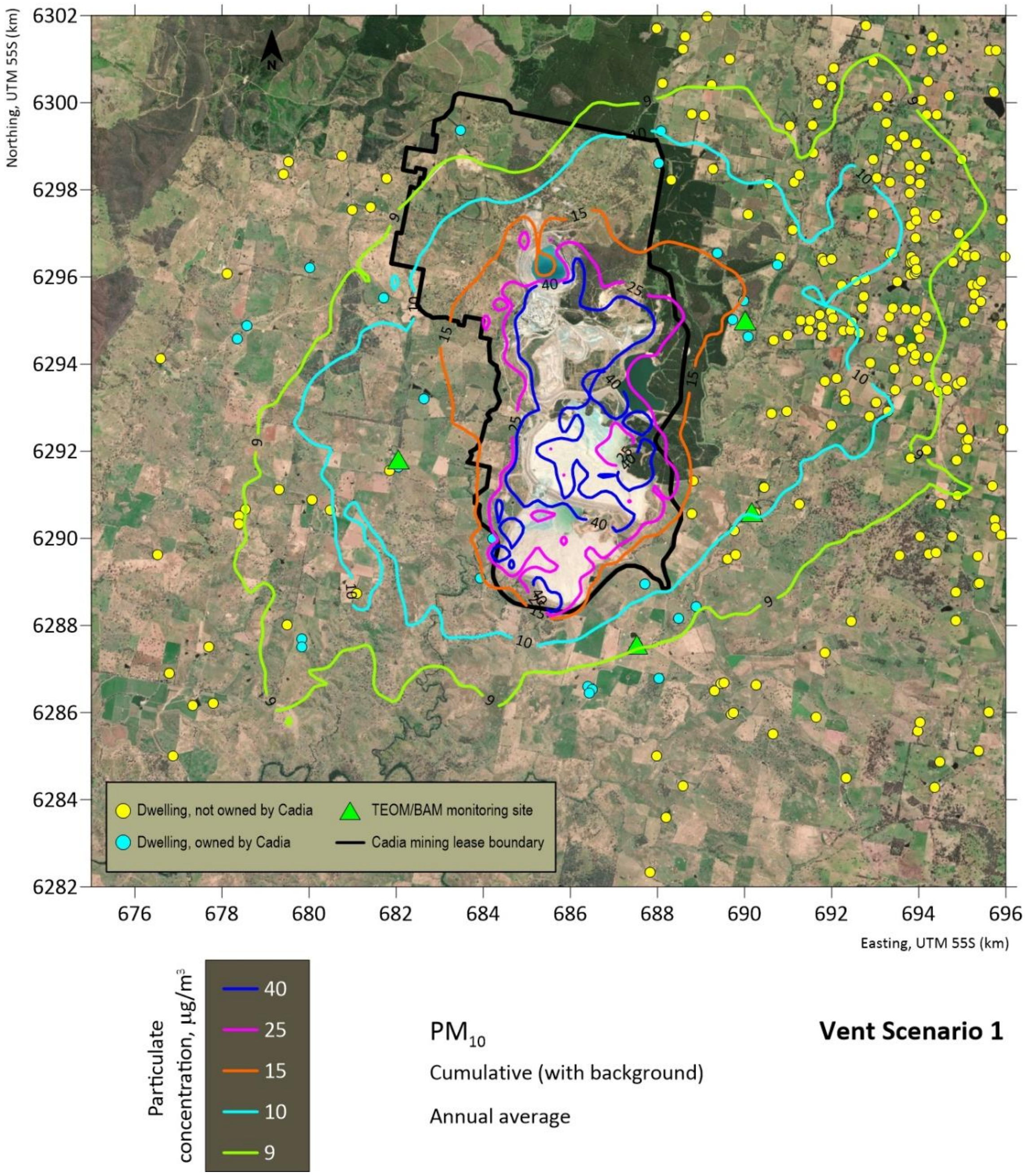

Figure T-11. Cumulative model results for vent emission Scenario 1, annual average PM_{10}.

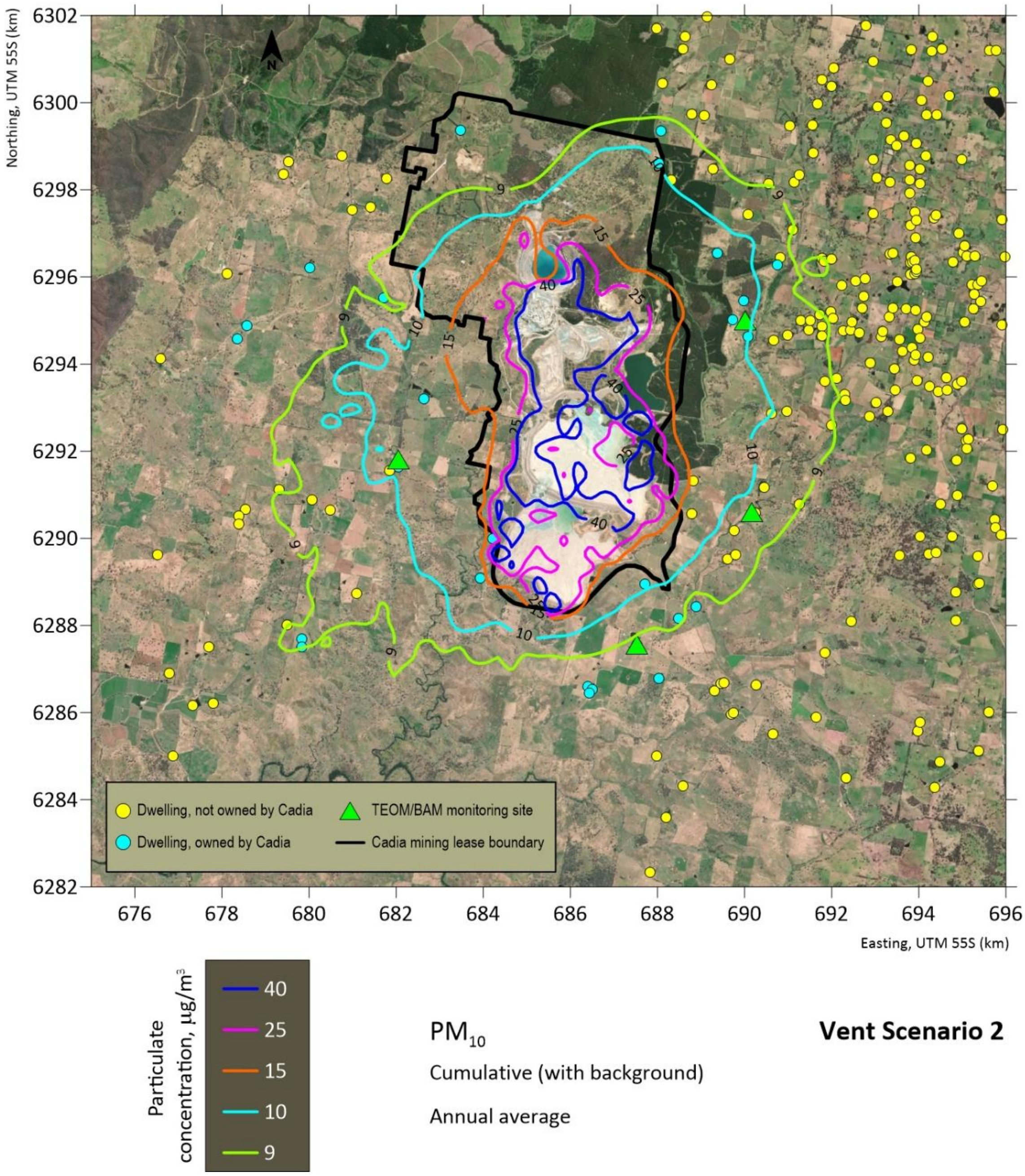

Figure T-12. Cumulative model results for vent emission Scenario 2, annual average PM_{10}.

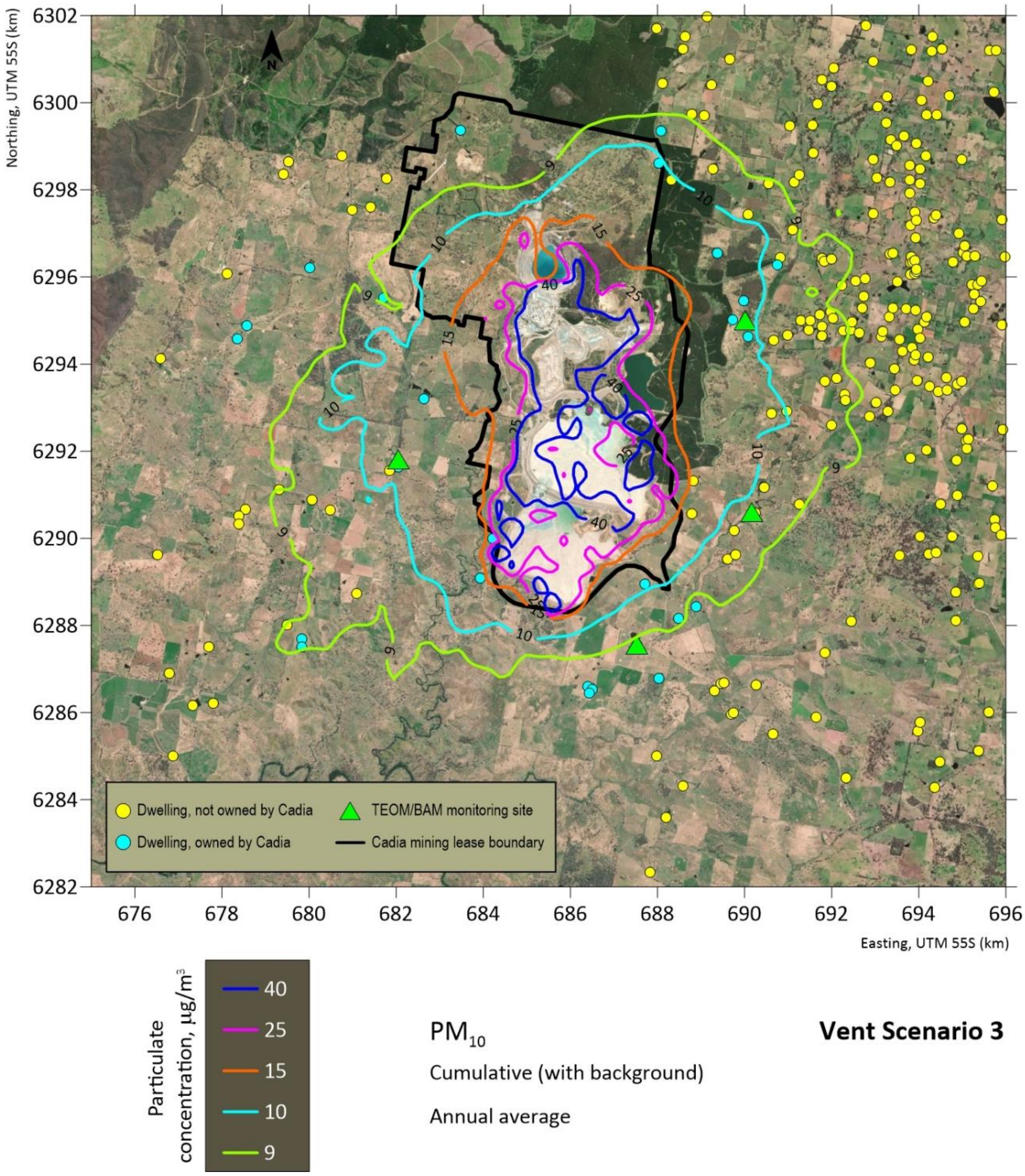

Figure T-13. Cumulative model results for vent emission Scenario 3, annual average PM_{10}.

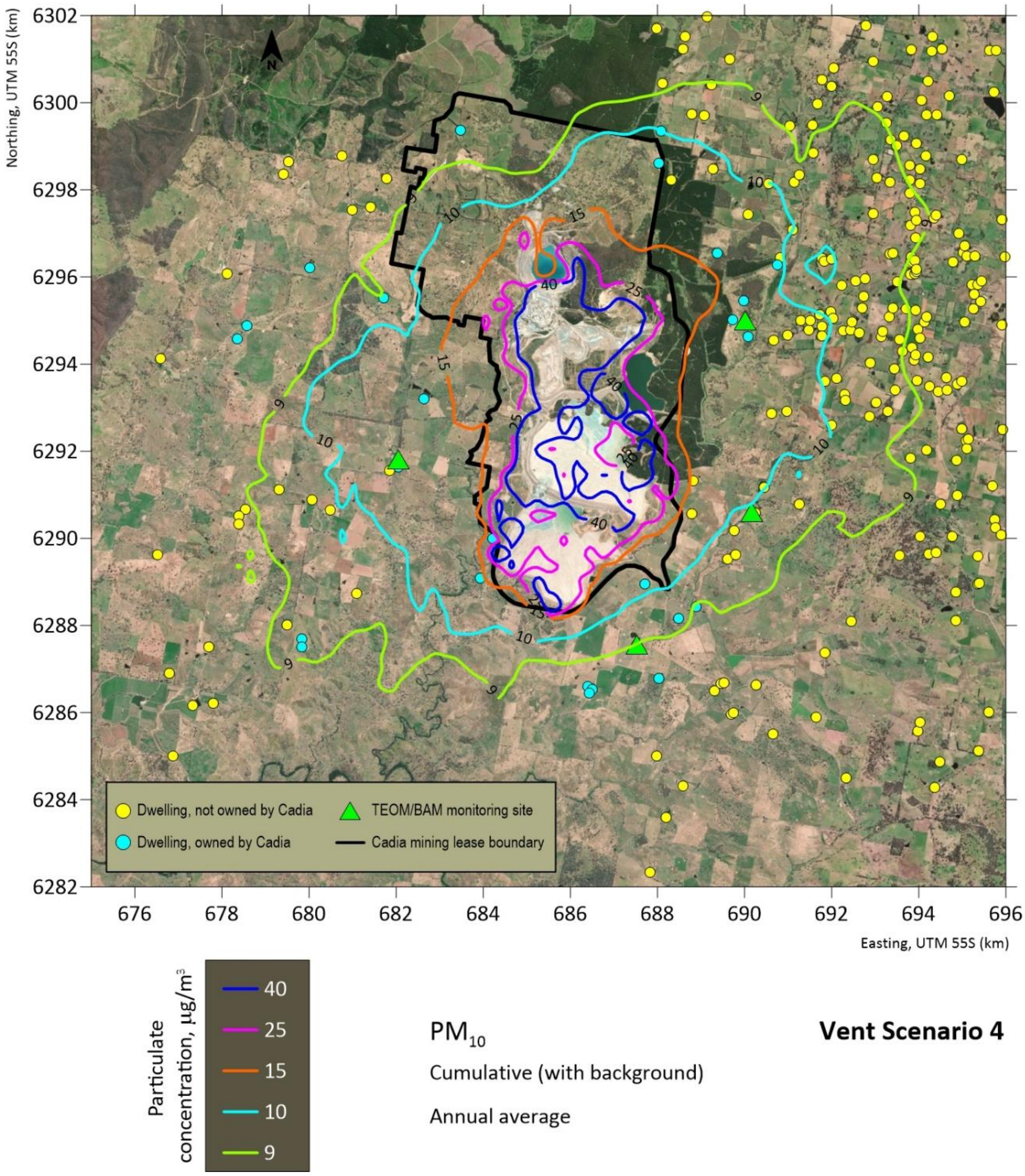

Figure T-14. Cumulative model results for vent emission Scenario 4, annual average PM_{10}.

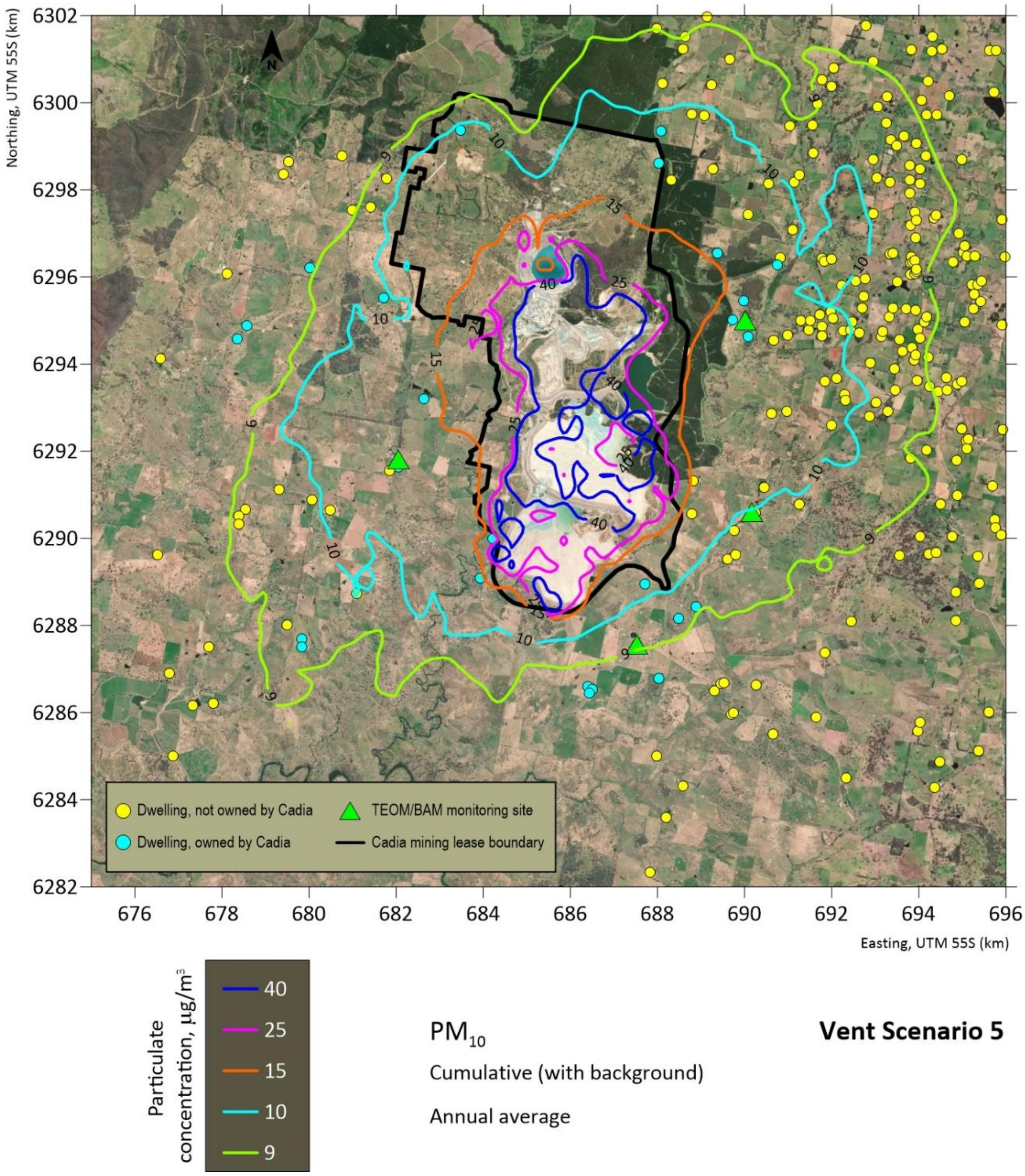

Figure T-15. Cumulative model results for vent emission Scenario 5, annual average PM_{10}.

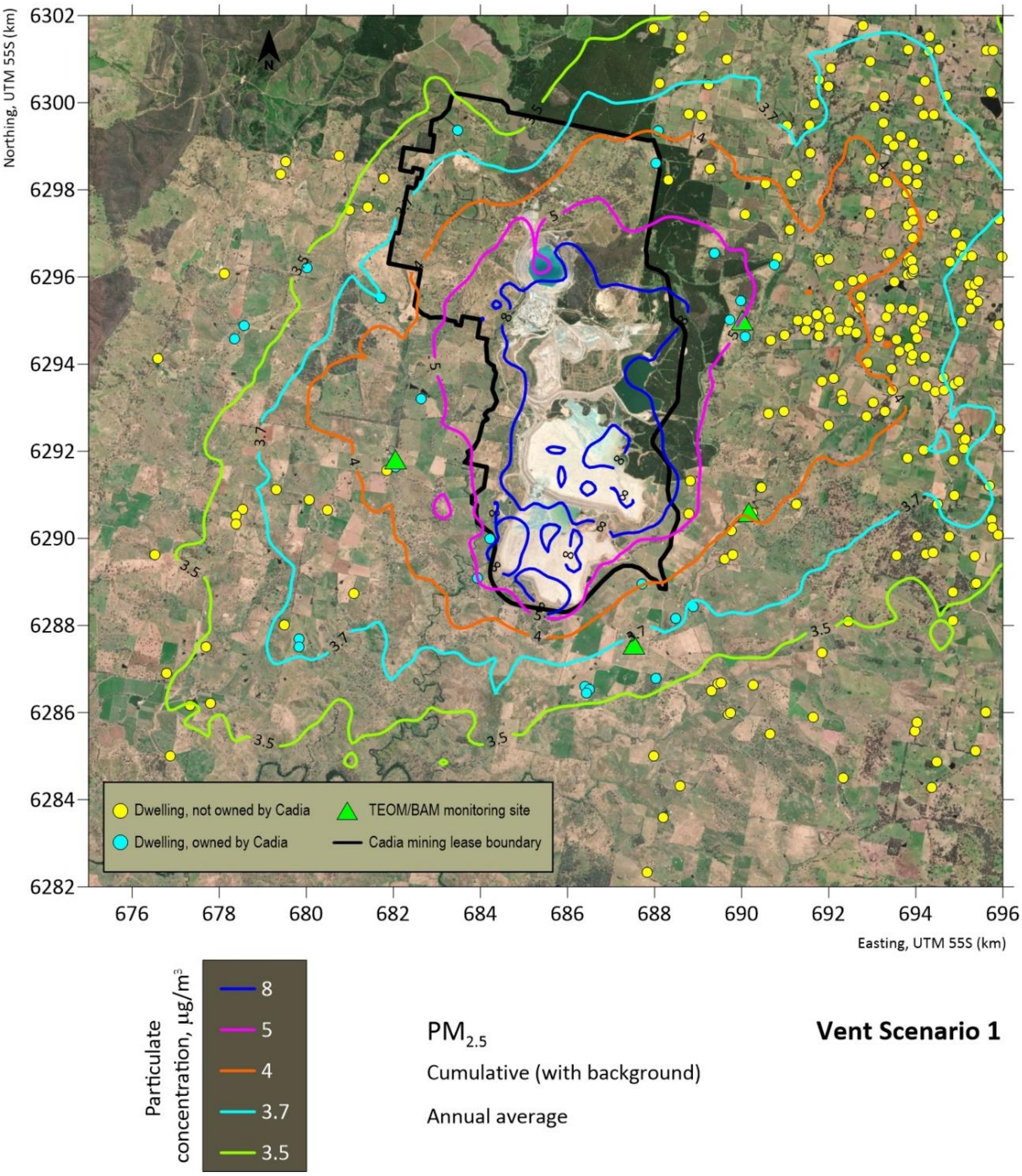

Figure T-16. Cumulative model results for vent emission Scenario 1, annual average $PM_{2.5}$.

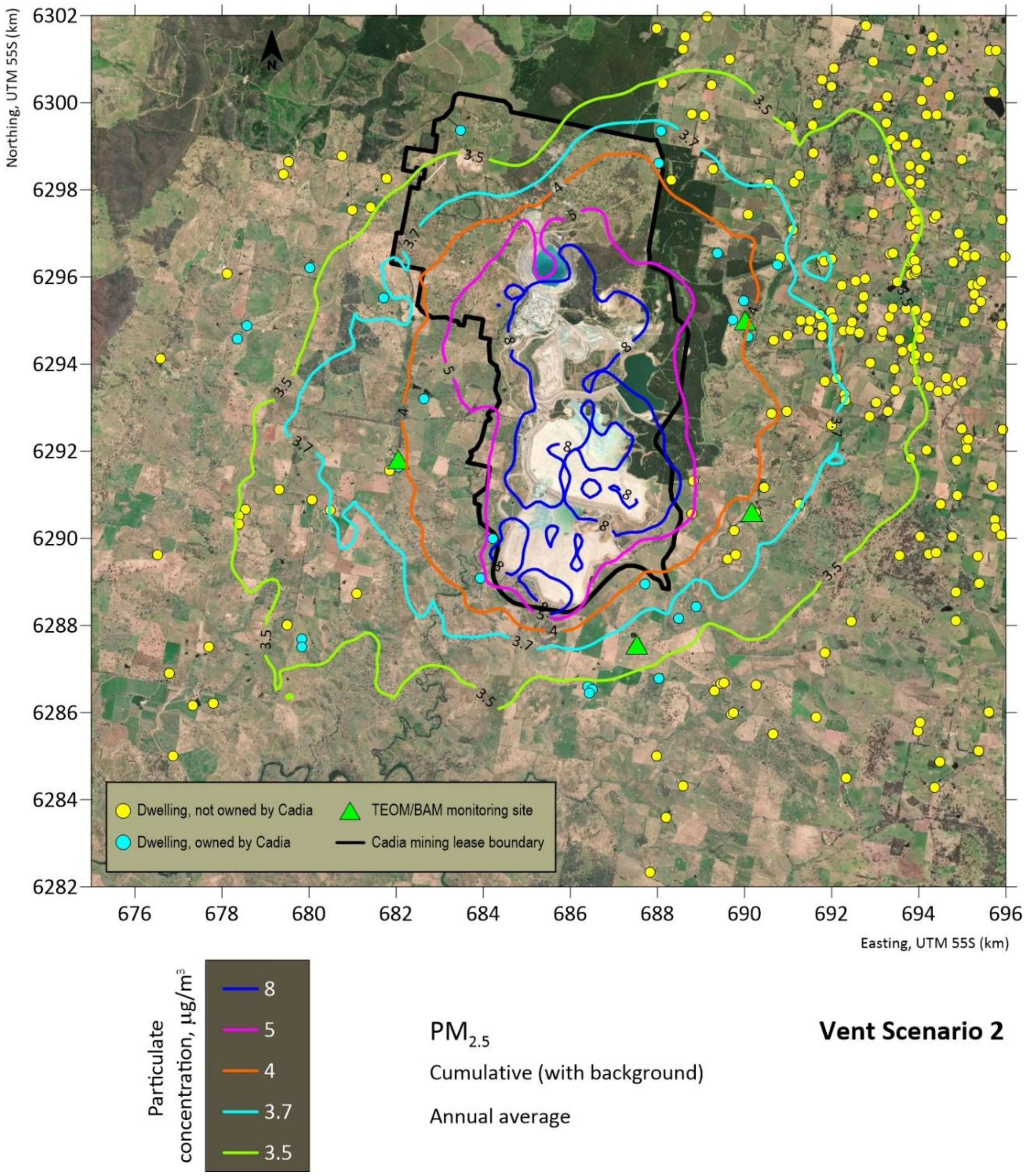

Figure T-17. Cumulative model results for vent emission Scenario 2, annual average $PM_{2.5}$.

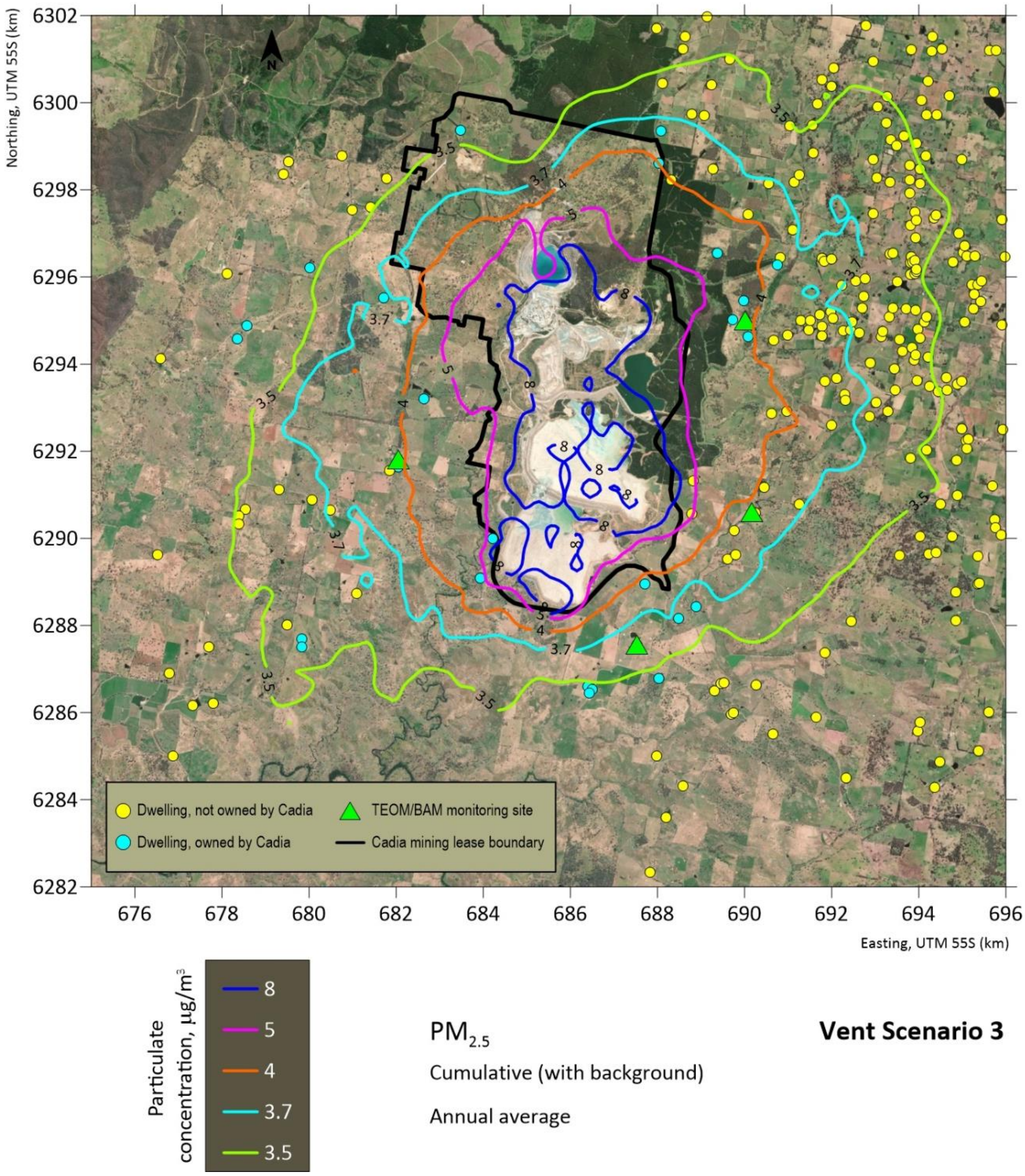

Figure T-18. Cumulative model results for vent emission Scenario 3, annual average $PM_{2.5}$.

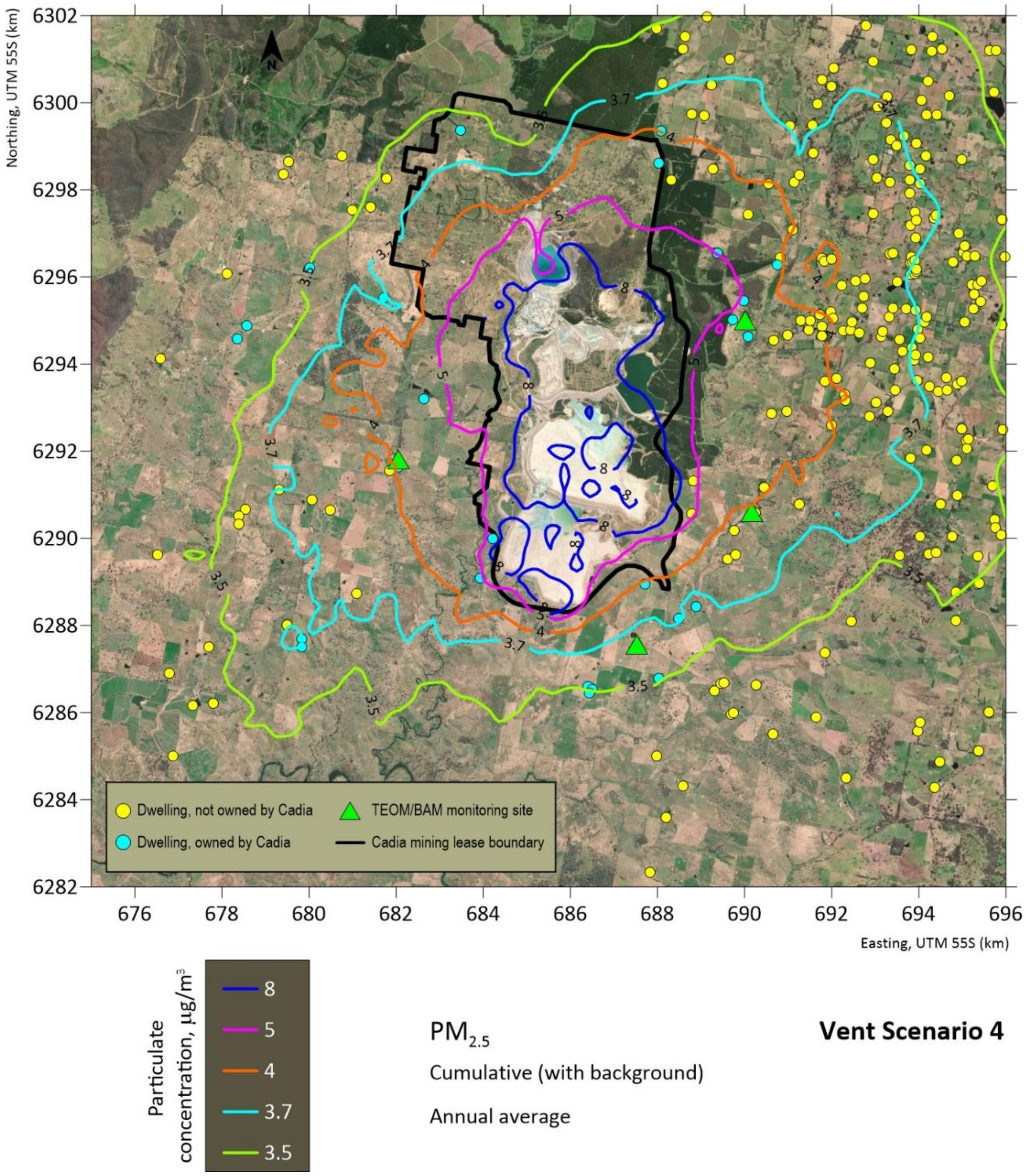

Figure T-19. Cumulative model results for vent emission Scenario 4, annual average $PM_{2.5}$.

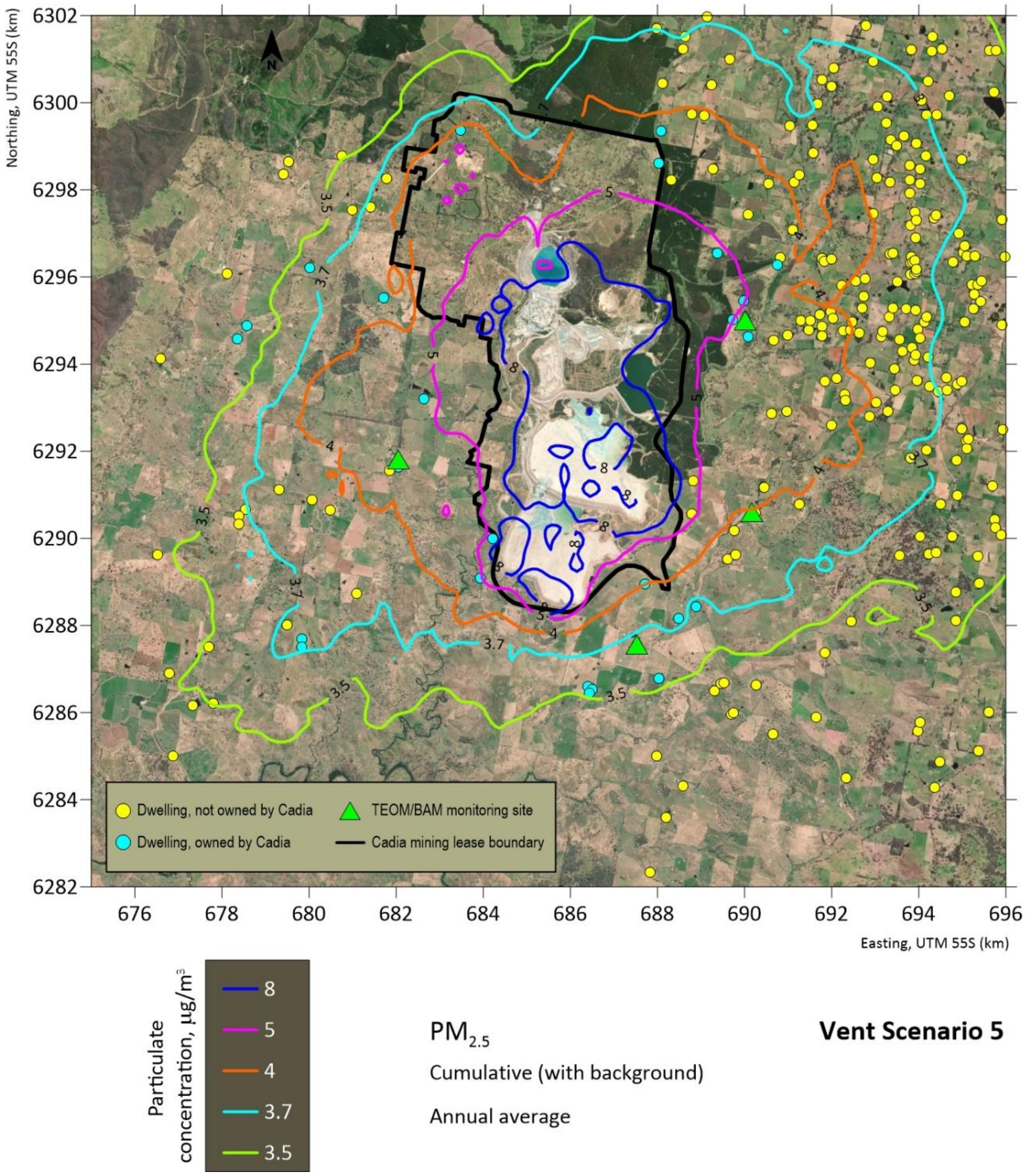

Figure T-20. Cumulative model results for vent emission Scenario 5, annual average $PM_{2.5}$.